

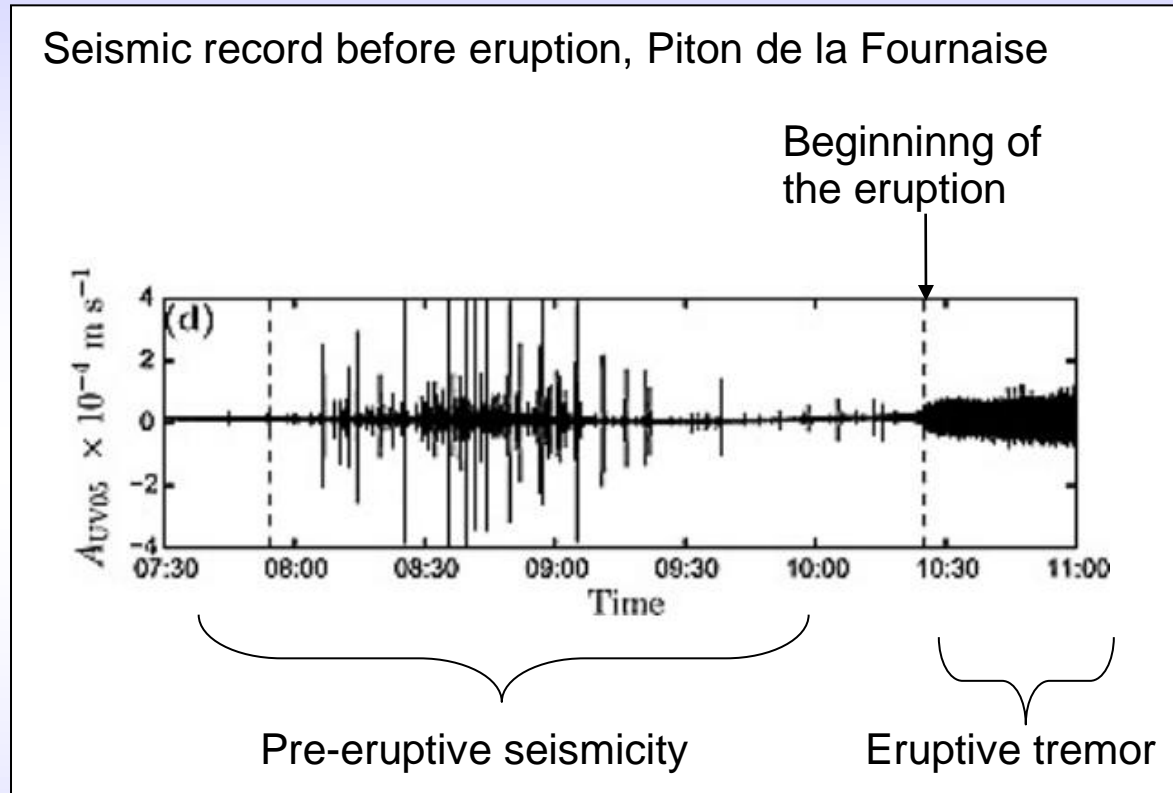
# MT inversion of volcanic sources: difficulties and ways around

Ivan Lokmer

[ivan.lokmer@ucd.ie](mailto:ivan.lokmer@ucd.ie)

Geophysics Group, School of Geological Sciences, University College  
Dublin, Ireland

# Why we are interested in volcano seismicity?

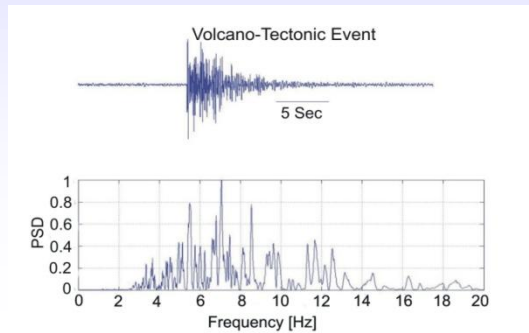


- Seismicity: → useful for assessing the state of volcano  
→ promising tool for forecasting eruptions

# Types of volcanic seismicity (simplified)

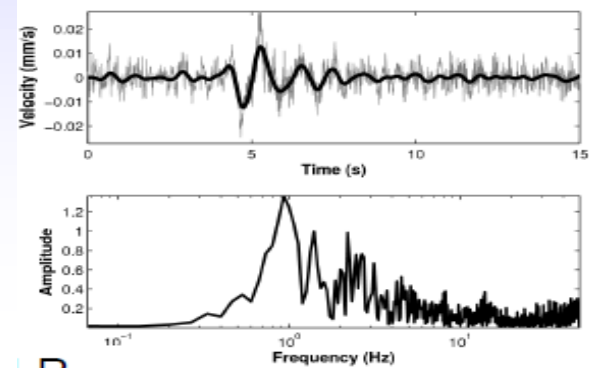
## *Volcano-tectonic events*

- brittle fracture induced by magma movement
- broad spectrum
- usually deeper (several km)



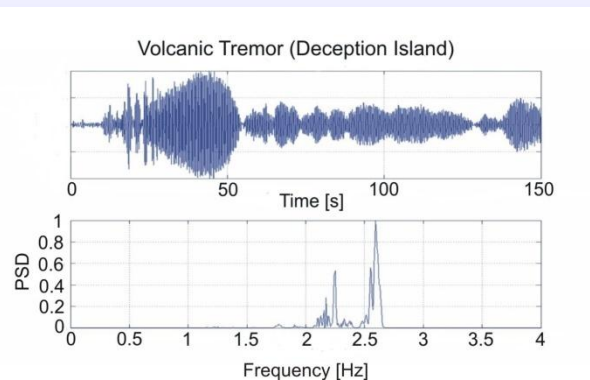
## *Long period (LP) events ( $T = 0.5 - 5$ s)*

- oscillations of the fluid-filled cracks and conduits triggered by the pressure disturbances within magmatic system (e.g. rapid gas injection/discharge)
- shallow (200- 1000 m), often occurring in swarms



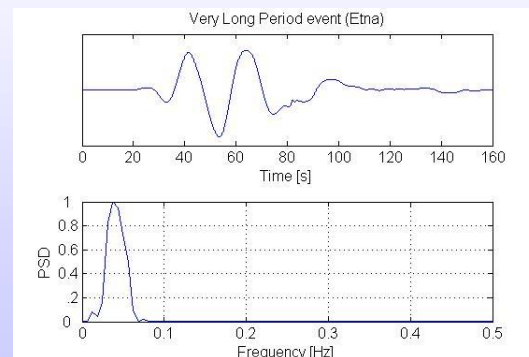
## *Volcanic tremor*

- it can last from minutes to months
- non-stationary flow of magma/gas through cracks with restrictions



## *Very long period (VLP) events ( $T = 10 - 100$ s)*

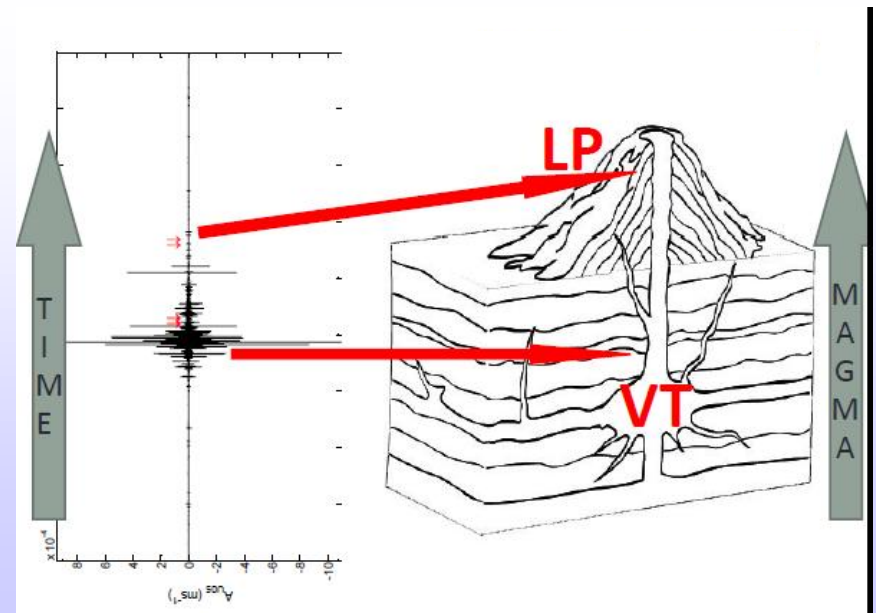
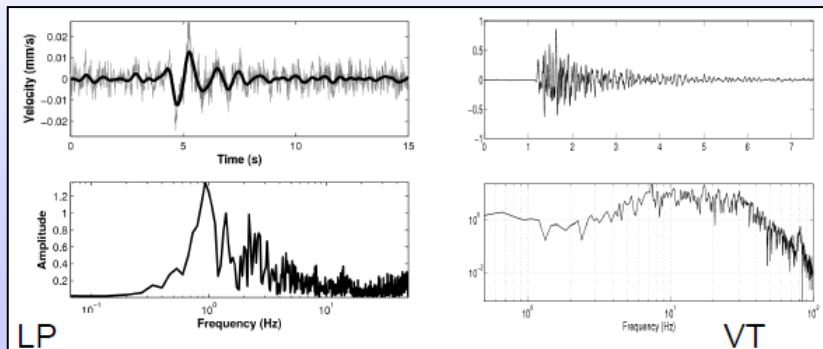
- mass transport of magma and/or gas under volcanoes (e.g. gas slug ascent)



# Why LP events?

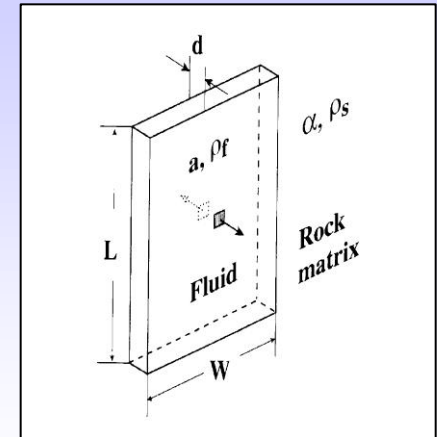
- High quality LP datasets (recorded by BB instruments) have been available only recently (last 20 years)
- LP events appear to be precursors of eruptions (not always) and linked to the fluid dynamics inside a volcano (magma, gas, hydrothermal system)
- Most demanding of all types of volcano-seismic events in terms of moment tensor inversion

Pre-eruptive sequence  
on Piton de la Fournaise

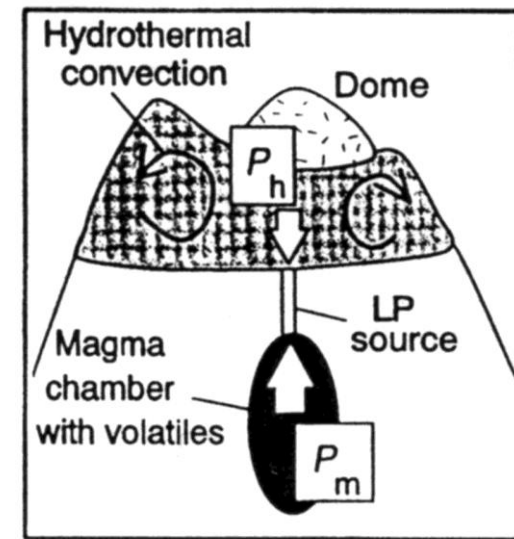
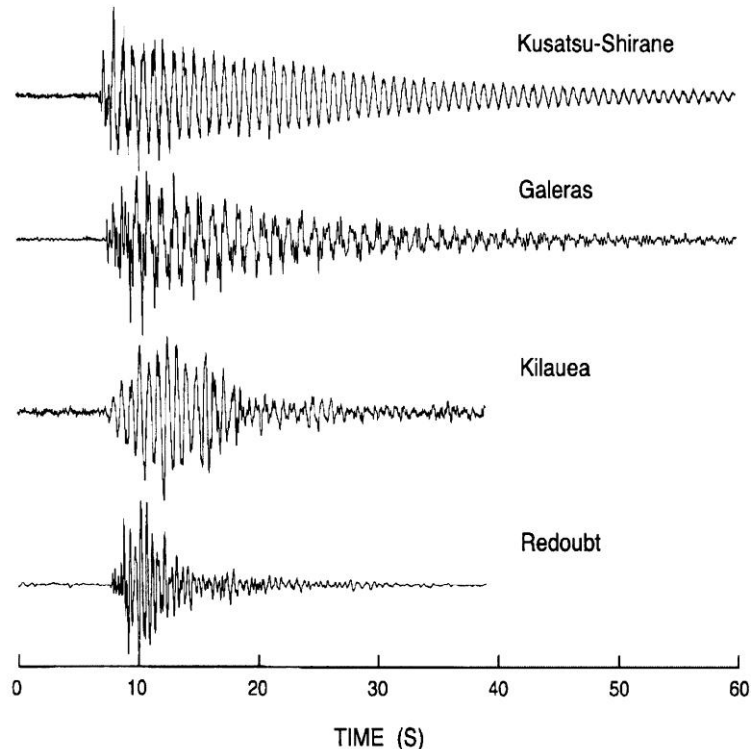


# Existing LP source models

- resonating fluid-filled cracks and conduits triggered by pressure disturbances (Chouet, 1985, 1986; Neuberg, 2000)
- trigger + resonator (different triggers proposed)
- slow waves generated at fluid-solid boundaries → low-frequencies generated by a small source (Ferazzini and Aki, 1987)



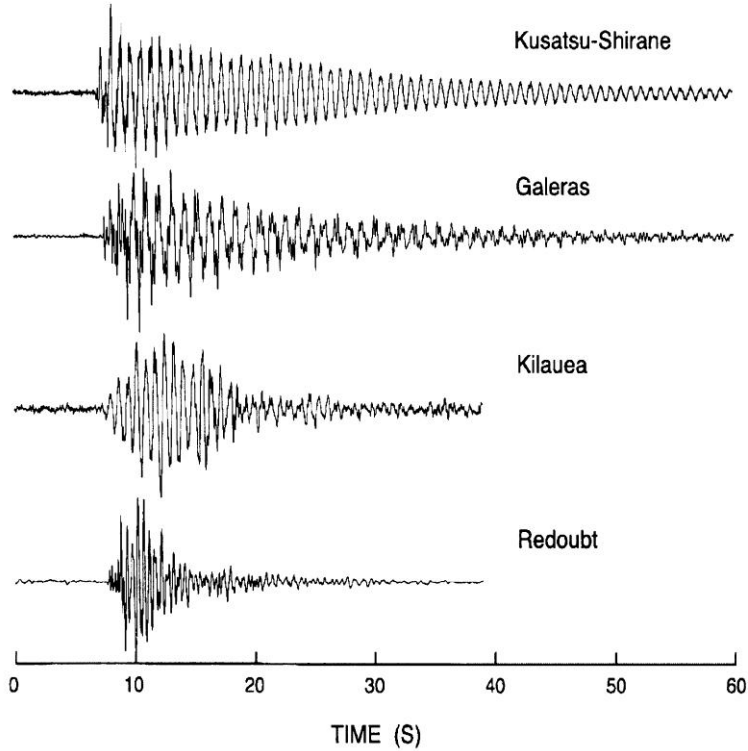
Typical long period (LP) signals (after Chouet, 1996)



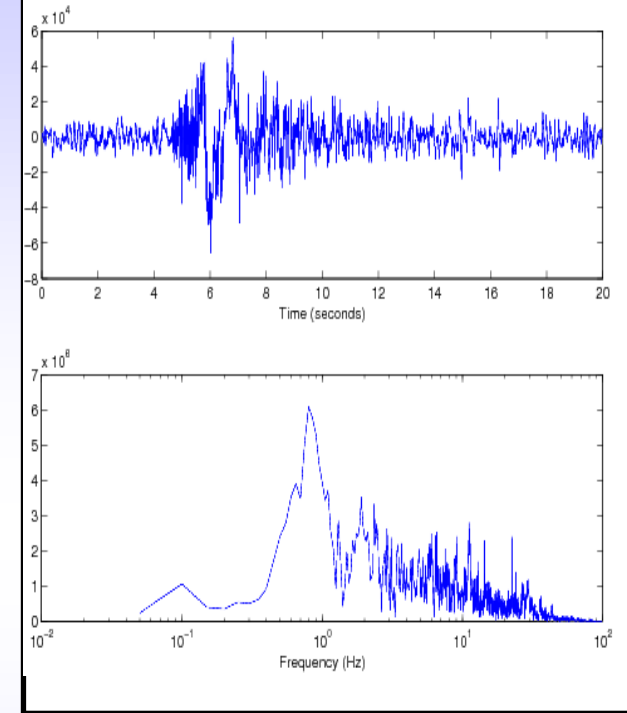
Pre-eruptive process at Redoubt Volcano, Alaska, on 13-14 December 1989 (after Chouet, 1996)

# More examples of LP events

Typical long period (LP) signals (after Chouet, 1996)

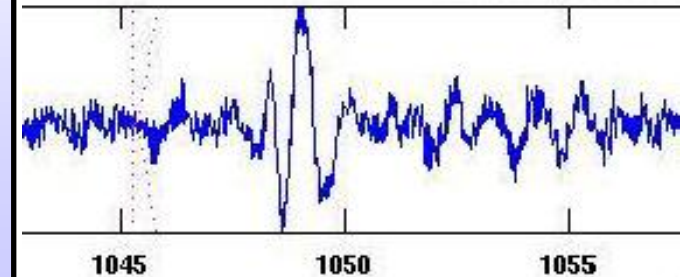


LP on Etna 2008



LP on Turrialba 2011

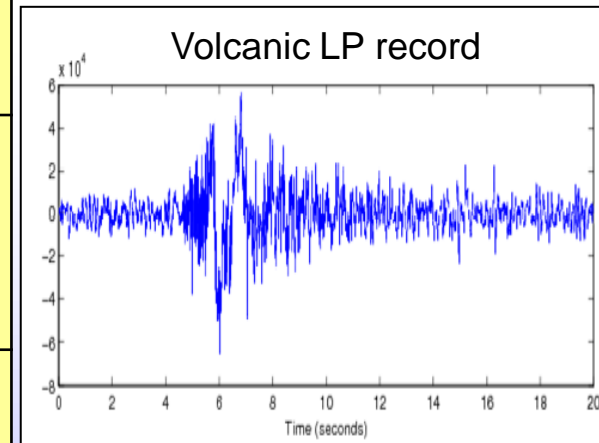
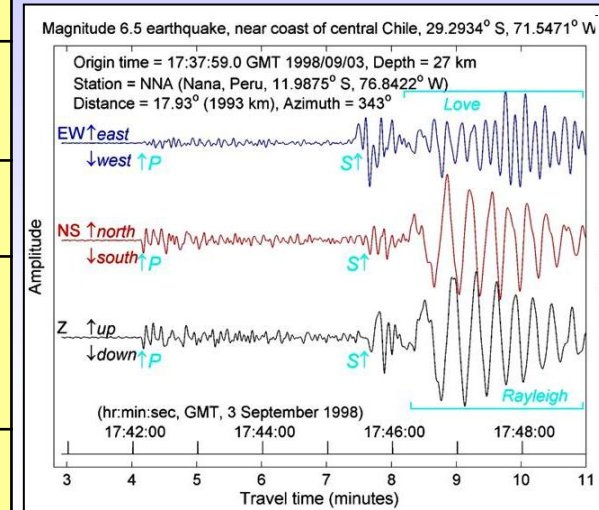
UCD45 09/03/2011



Recorded a few hundred metres from the source

# Tectonic earthquakes vs. volcanic LP events

	<b>Tectonic Earthquakes</b>	<b>Volcanic LP Events</b>
<i>Frequency content</i>	Broad spectrum	Dominant frequency 0.2 – 2 Hz
<i>Size range</i>	M < 9.5	M < 1.5 → small signal to noise ratio
<i>Depth</i>	5 – 700 km	200-1000 m → observed in the near-field (no far-field approximations possible in inversions)
<i>Waveform characteristics</i>	sharp onset, separated phases	emergent onset, intertwined phases → difficulties with locating events, different phases cannot be used separately in source inversions
<i>Propagation effect</i>	medium can be assumed to be layered halfspace or sphere (analytical solution, 2D simulations for Green's functions)	highly heterogeneous medium with topography → no analytical solution, 3D simulations have to be used
<i>Source mechanism</i>	Shear faulting ( <i>a priori</i> information)	Several candidates → no unique <i>a priori</i> constraints can be used for source inversions
<i>Source time function</i>	Ramp function ( <i>a priori</i> information)	Unknown → no <i>a priori</i> source-time history can be used in source inversions



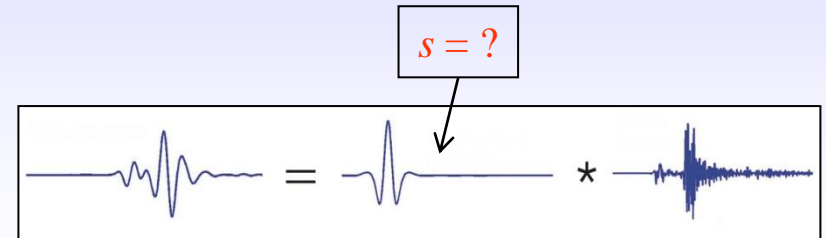
# Source inversion - concept

A recorded seismogram can be viewed as an output of a sequence of linear filters representing excitation (source), propagation (Green's functions), and transfer function of the recording instrumentation:

$$u(t) = s(t) * g(t) * i(t) \quad \leftarrow \text{time domain}$$

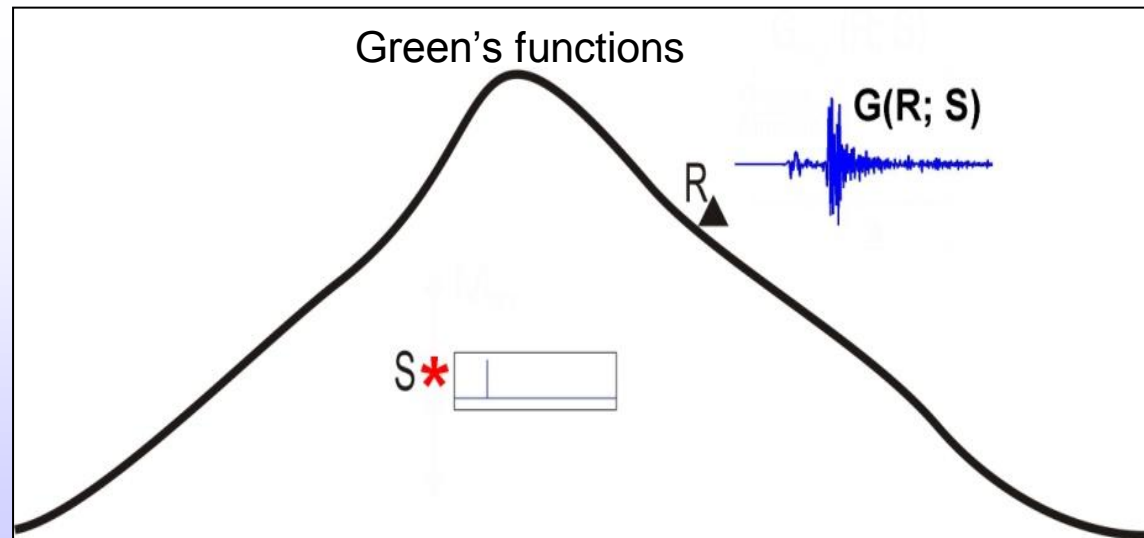
$$U(\omega) = S(\omega) \cdot G(\omega) \cdot I(\omega) \quad \leftarrow \text{frequency domain}$$

$$s = ?$$



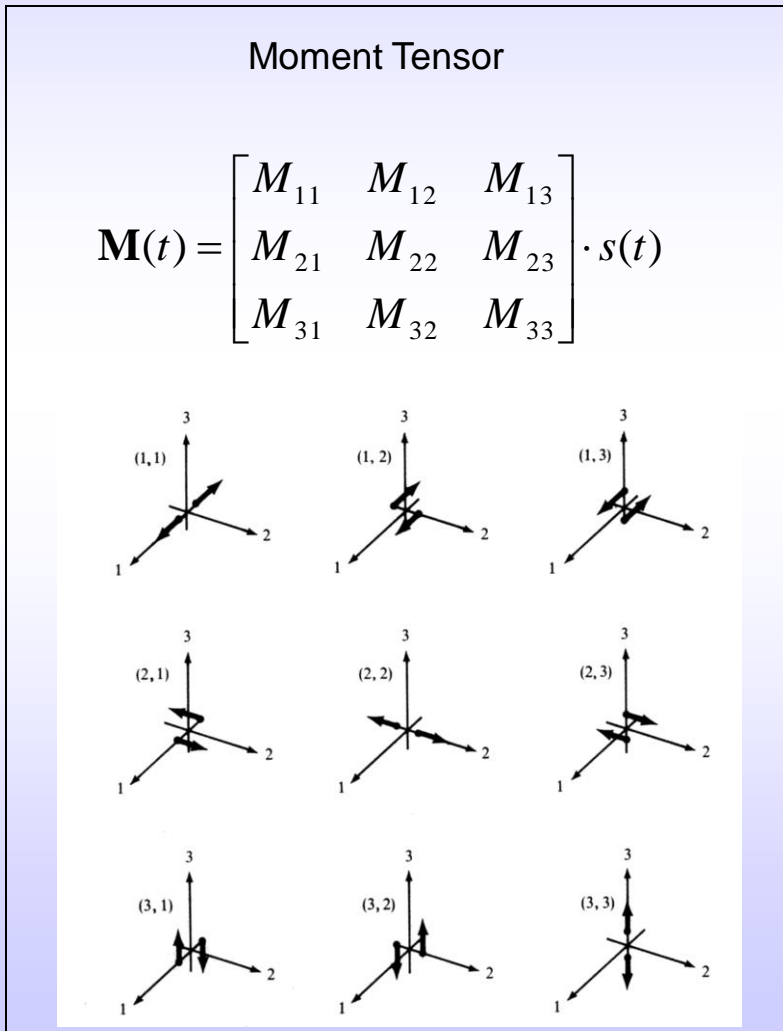
Knowing how propagation through the medium affects the seismic wavefield, the source mechanism can be obtained from the recorded seismograms.

The accuracy of the retrieved source mechanism is limited by the accuracy of the calculated propagation effects (Green's functions).

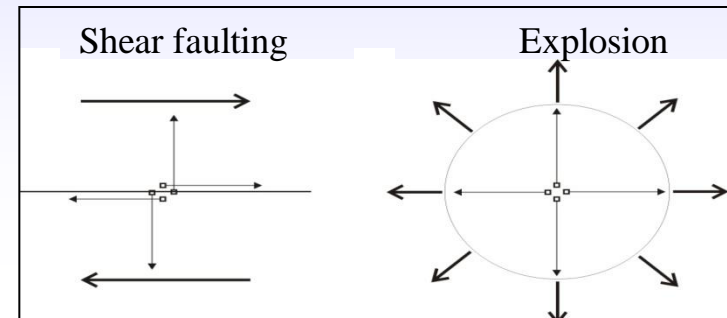


# Source description by moment tensor (MT)

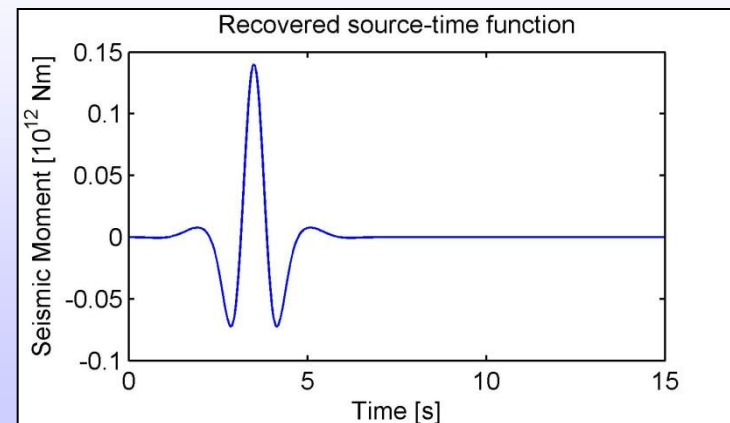
Full time-dependent moment-tensor gives a time-dependent representation of a seismic source by a combination of force couples and dipoles



## 1) Source mechanism



**2) Source-time function** (can be seen as the time dependence of the effective displacement in the source)



# Moment tensor for tensile earthquakes

Moment tensor for a fault with arbitrary inclination of the slip from the fault plane (Aki and Richard, 2002, eq. ):

$$M_{pq} = S[\lambda u_k n_k \delta_{pq} + \mu(u_p n_q + u_q n_p)]$$

$\lambda, \mu$  – Lamé constants,  $\delta_{pq}$  – Kronecker delta,  
 $S$  – fault area,  $u$  – slip vector,  $n$  – normal of the fault

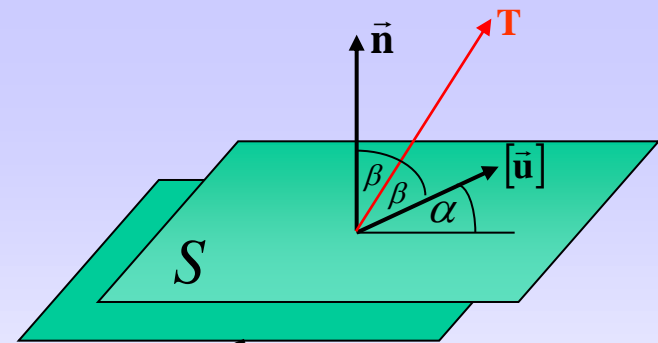
If:

$$\mathbf{n} = [0 \quad 0 \quad 1]^T, \quad \mathbf{u} = u[\cos \alpha \quad 0 \quad \sin \alpha]^T, \quad u = \|\mathbf{u}\|$$

Then:

$$\mathbf{M} = Su \begin{bmatrix} \lambda \sin \alpha & 0 & \mu \cos \alpha \\ 0 & \lambda \sin \alpha & 0 \\ \mu \cos \alpha & 0 & (\lambda + 2\mu) \sin \alpha \end{bmatrix}$$

Vavryčuk, 2001



Moment tensor for a horizontal tensile fault/crack ( $\alpha = 90^\circ$ ):

$$\mathbf{M} = \mu \Delta V \begin{bmatrix} \lambda/\mu & 0 & 0 \\ 0 & \lambda/\mu & 0 \\ 0 & 0 & \lambda/\mu + 2 \end{bmatrix}$$

Moment tensor for a vertical cylindrical conduit (pipe):

$$\mathbf{M} = \mu \Delta V \begin{bmatrix} \lambda/\mu + 1 & 0 & 0 \\ 0 & \lambda/\mu + 1 & 0 \\ 0 & 0 & \lambda/\mu \end{bmatrix}$$

derivation in Lokmer 2008

# Moment tensor decomposition

Moment tensor density for a horizontal tensile fault/crack

$$\mathbf{m} = u \begin{bmatrix} \lambda & 0 & 0 \\ 0 & \lambda & 0 \\ 0 & 0 & \lambda + 2\mu \end{bmatrix} = u(\lambda + \frac{2}{3}\mu) \begin{bmatrix} 1 & 0 & 0 \\ 0 & 1 & 0 \\ 0 & 0 & 1 \end{bmatrix} + u \cdot \frac{2}{3}\mu \begin{bmatrix} -1 & 0 & 0 \\ 0 & -1 & 0 \\ 0 & 0 & 2 \end{bmatrix}$$

Moment tensor density for a vertical narrow cylindrical conduit (pipe):

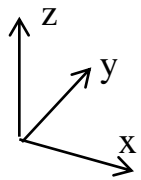
$$\mathbf{m} = u \begin{bmatrix} \lambda + \mu & 0 & 0 \\ 0 & \lambda + \mu & 0 \\ 0 & 0 & \lambda \end{bmatrix} = u(\lambda + \frac{2}{3}\mu) \begin{bmatrix} 1 & 0 & 0 \\ 0 & 1 & 0 \\ 0 & 0 & 1 \end{bmatrix} - u \cdot \frac{1}{3}\mu \begin{bmatrix} -1 & 0 & 0 \\ 0 & -1 & 0 \\ 0 & 0 & 2 \end{bmatrix}$$

# Moment tensor decomposition

volumetric change

deviatoric component

Moment tensor is commonly decomposed into isotropic component, double-couple and CLVD

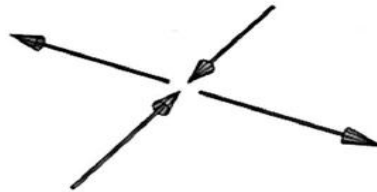
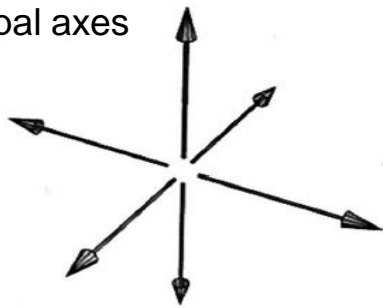


$$\begin{bmatrix} 1 & 0 & 0 \\ 0 & 1 & 0 \\ 0 & 0 & 1 \end{bmatrix}$$

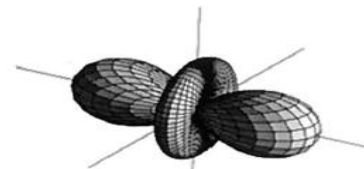
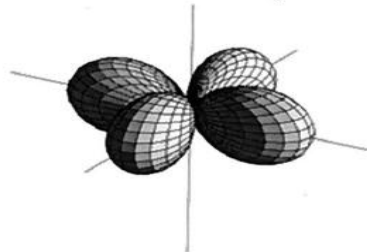
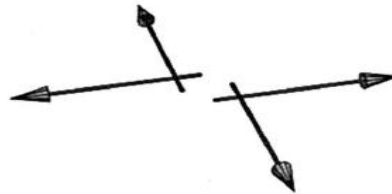
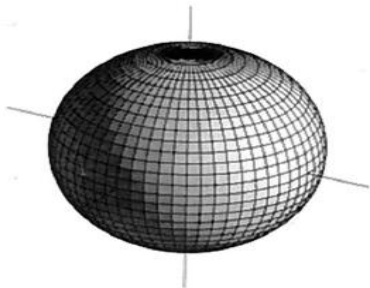
$$\begin{bmatrix} 1 & 0 & 0 \\ 0 & -1 & 0 \\ 0 & 0 & 0 \end{bmatrix}$$

$$\begin{bmatrix} 2 & 0 & 0 \\ 0 & -1 & 0 \\ 0 & 0 & -1 \end{bmatrix}$$

Principal axes



P-wave radiation  
Pattern (far-field)

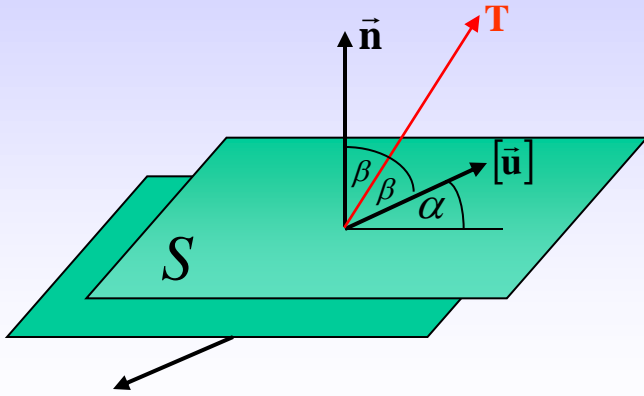


after Julian et al., 1998

non-unique  
decomposition of  
deviatoric component

References for MT  
decomposition: Knopoff  
and Randall, 1970; Jost  
and Hermann, 1989;  
Šileny and Pšenčík,  
1995; Dahm, 1996;  
Julian et al., 1998;  
Vavryčuk, 2001

# Moment tensor for tensile crack: resolution problem



Diagonal form of MT for tensile earthquakes

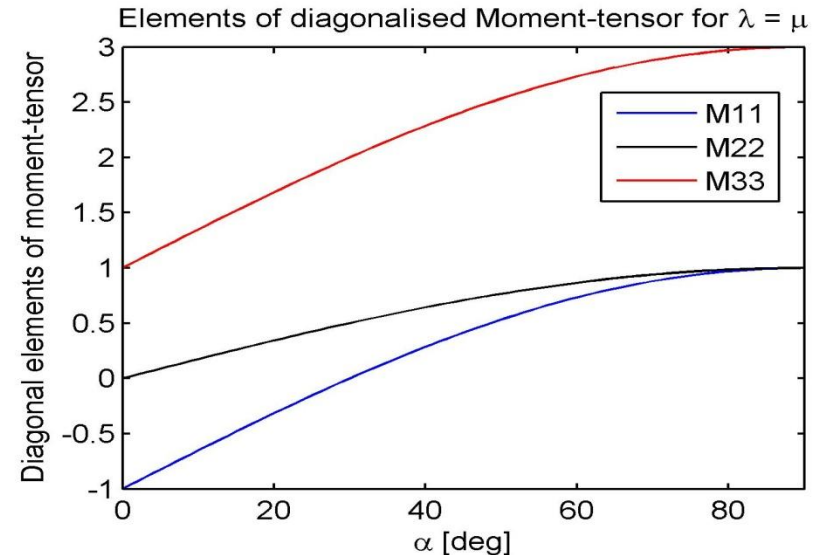
$$\mathbf{M} = \mu S u \begin{bmatrix} (\lambda/\mu + 1)\sin \alpha - 1 & 0 & 0 \\ 0 & \lambda/\mu \sin \alpha & 0 \\ 0 & 0 & (\lambda/\mu + 1)\sin \alpha + 1 \end{bmatrix}$$

Ratio of the eigenvalues of moment tensor varies slowly for steep angles of crack opening ( $\alpha > 65^\circ$ )

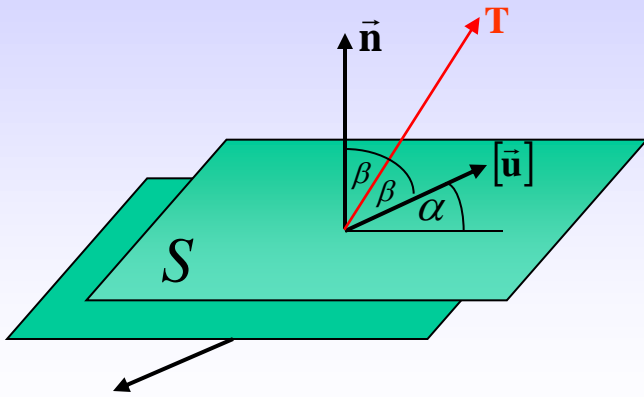
→ In practice, it is very difficult to accurately resolve the contribution of double-couple (slip inclination angle) in the source mechanism from our noisy solutions

→ Fortunately, the trace of moment tensor ( $\sim$  volumetric change) stays rather constant, so we can determine volumetric change (limiting factor is our knowledge of the shear modulus)

Problem 1:



# Moment tensor for tensile earthquakes: uncertainty in Poisson's ratio



Diagonal form of MT for tensile earthquakes

$$\mathbf{M} = \mu S u \begin{bmatrix} (\lambda/\mu + 1)\sin \alpha - 1 & 0 & 0 \\ 0 & \lambda/\mu \sin \alpha & 0 \\ 0 & 0 & (\lambda/\mu + 1)\sin \alpha + 1 \end{bmatrix}$$

For different values of Poisson's ratio, tensile cracks with different mechanisms have very similar moment tensors

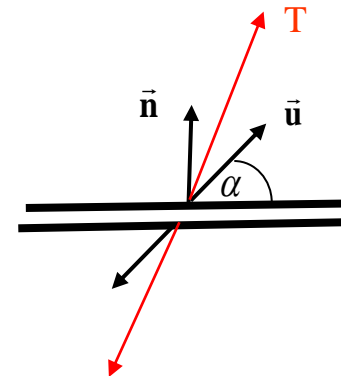
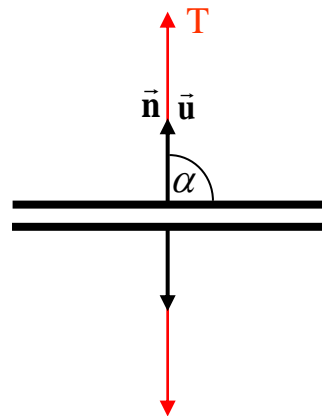
→  $\lambda/\mu$  in the source zone can be significantly different to  $\lambda/\mu$  in the intact medium (and is unknown)

→ again, deviatoric part of the moment tensor is a problem, while the isotropic part is rather stable

Problem 2:

$$\lambda/\mu = 2, \alpha = 90^\circ \Rightarrow (1:1:2)$$

$$\lambda/\mu = 3.2, \alpha = 45^\circ \Rightarrow (1:1.1:2)$$



# Moment tensor (MT) inversion

The  $n$ -th component of displacement (recorded at the station  $s$ ), due to a moment tensor  $\mathbf{M} = [M_{pq}(\omega)]$  applied at a point source (frequency domain):

$$u_n^s(\omega) = \sum_{p,q} M_{pq}(\omega) \cdot G_{np,q}^s(\omega) + F_p(\omega) \cdot G_{np}^s(\omega)$$

As volcanic sources may involve mass transport (gas and/or liquid), a single force term (SF) is usually added to the standard equations used for the inversion (e.g. Takei and Kumazawa, 1994; Nakano et al., 2003)

For each frequency, we have to solve the following system:

$$\mathbf{u} = \mathbf{Gm}$$

$(n_u \times 1) = (n_u \times n_m) (n_m \times 1)$   
 $n_u$  - the total number of seismograms  
 $n_m$  - the number of MT (+ SF) components

Observed  
seismograms

Synthetic  
seismograms

$\mathbf{u}$  - data;  
 $\mathbf{G}$  - Green's functions;  
 $\mathbf{m}$  - source parameters

$$\text{residual} = \|\text{observed seismograms} - \text{synthetic seismograms}\|^2 \rightarrow \min$$

$$\mathbf{m}^{est} = (\mathbf{G}^T \mathbf{G})^{-1} \mathbf{G}^T \mathbf{u} \quad \leftarrow \text{The least squares solution}$$

$$R = \sum_{\omega} \frac{\|\mathbf{u} - \mathbf{Gm}\|_2^2}{\|\mathbf{u}\|_2^2} = \sum_{\omega} \frac{(\mathbf{u} - \mathbf{Gm})^T (\mathbf{u} - \mathbf{Gm})}{\mathbf{u}^T \mathbf{u}} \quad \leftarrow \text{Residual (misfit function)}$$

Residual originates from:

- (i) incorrect Green's functions (topography and heterogeneity),
- (ii) the breakdown of the point-source assumption,
- (iii) the noise contaminating our dataset

# Principal component analysis (PCA)

- PCA is used for determining main factors contributing to a set of observations
- Can the data be explained by a single source-time function?

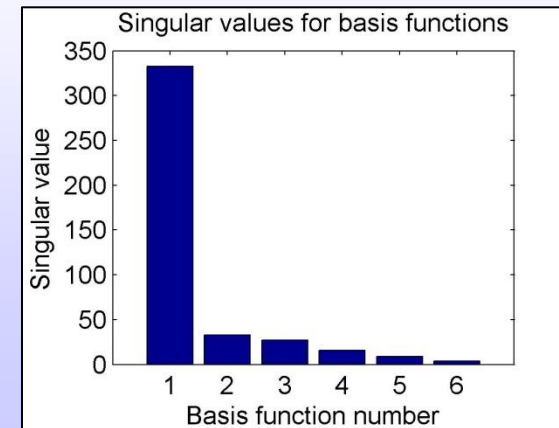
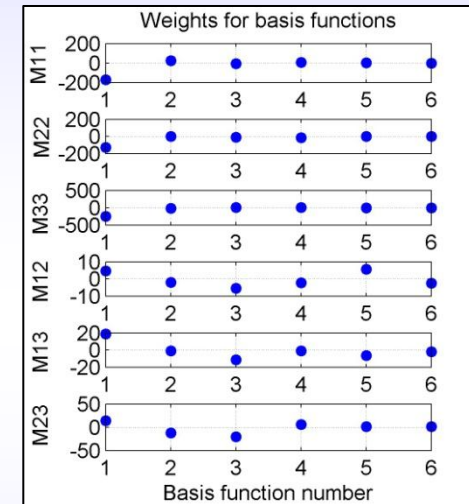
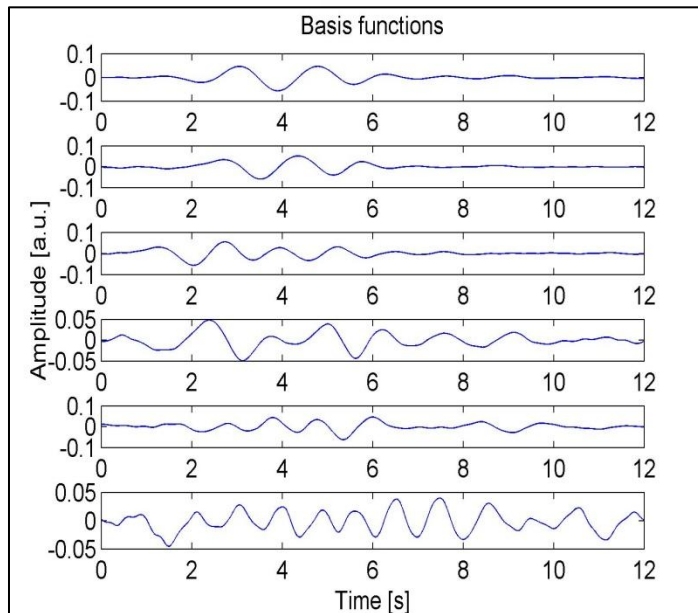
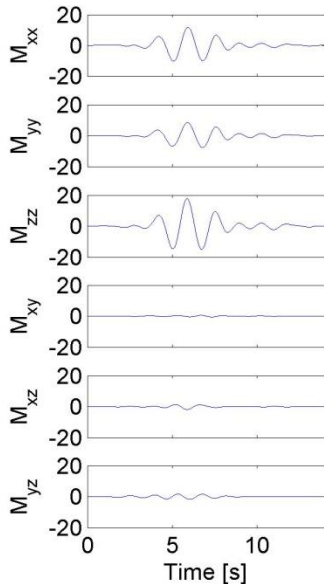
$$\mathbf{M}^T = \mathbf{A}^T \mathbf{V}^T + \mathbf{E}^T$$

**M** – MT source-time functions ( $n \times 6$ )  
 $n$  is the number of time samples  
**V** – basis functions ( $n \times 6$ )  
**A** – basis function weights ( $6 \times 6$ )  
**E** – error matrix ( $n \times 6$ )

Singular value decomposition

$$\mathbf{M}^T = \mathbf{U} \mathbf{S} \mathbf{V}^T$$

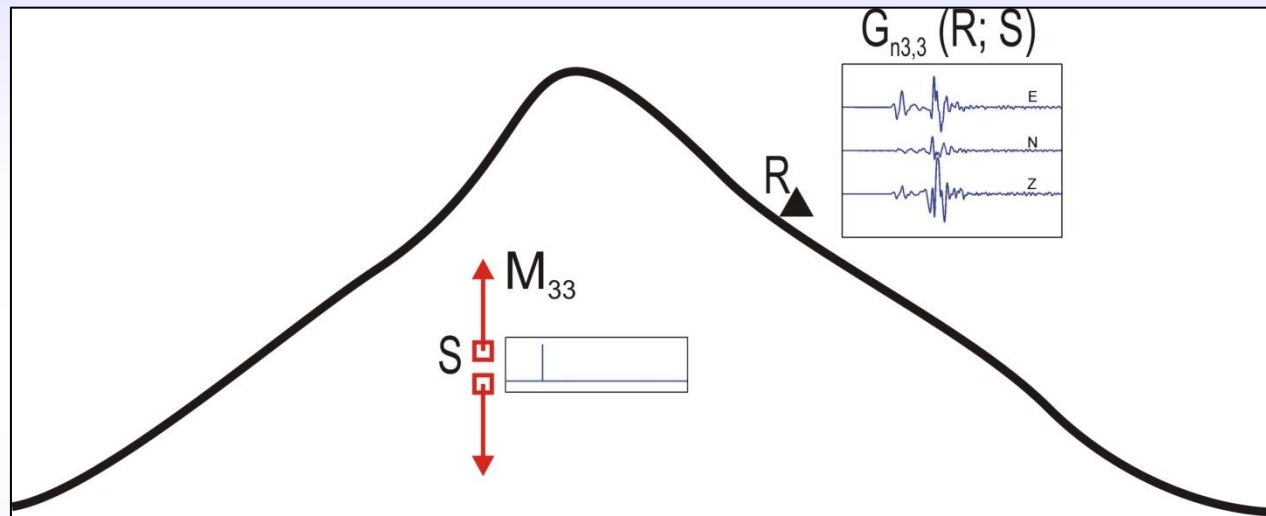
**U**  $\mathbf{S}$  = **A**<sup>T</sup>  
**U** – orthogonal matrix ( $6 \times 6$ )  
**S** – matrix of singular values ( $6 \times 6$ )



Problems related to the modelling of  
propagation effect (Green's functions)  
on volcanoes

# Propagation effect - Green's functions calculation

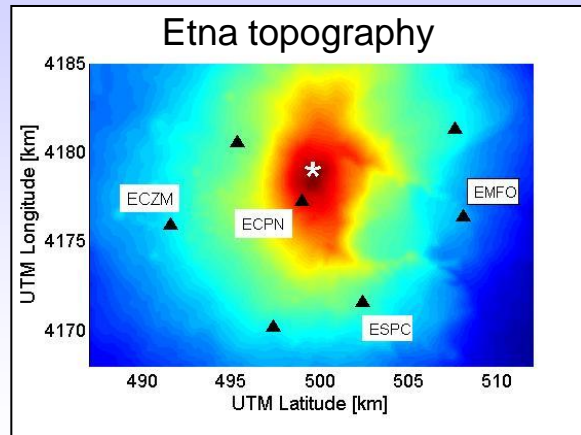
Green's functions – a set of seismograms that representing the medium response to the impulse excitation applied at the source ( if the impulse response of the linear system is known, a response to any given source time function can be constructed)



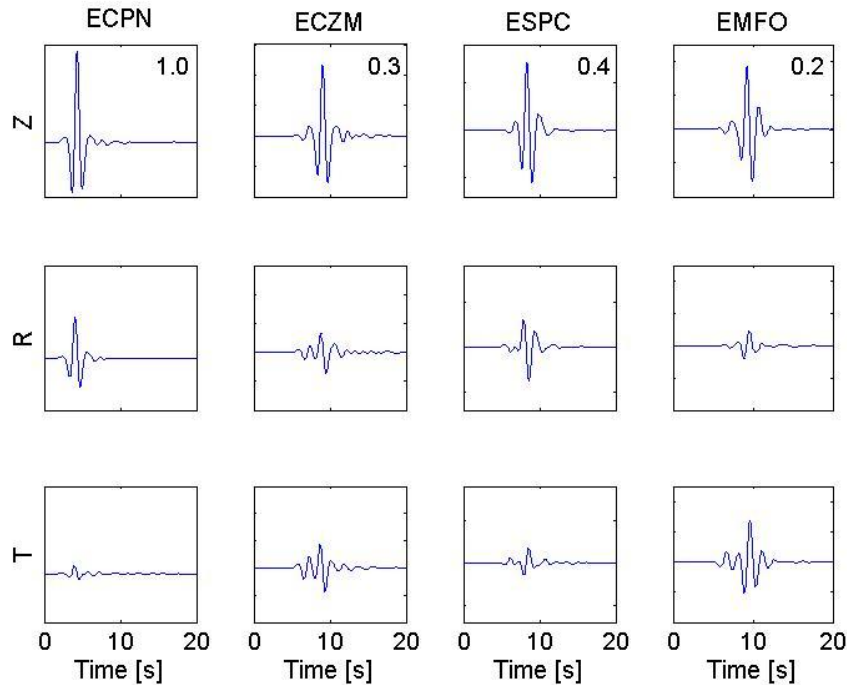
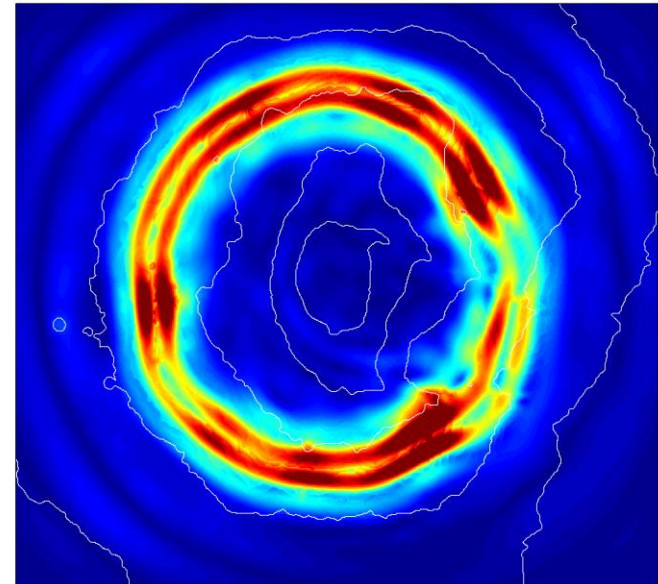
Accuracy of Green's functions critically depends on:

- accurate modelling of topography
  - modelling of near-field wavefield
  - correct shallow velocity model (remember, very shallow sources!)
  - accuracy of source location
- easy to account for (numerical simulations)
- PROBLEM!**

# Topography effect I



Snapshot of the wavefield (wave magnitude)

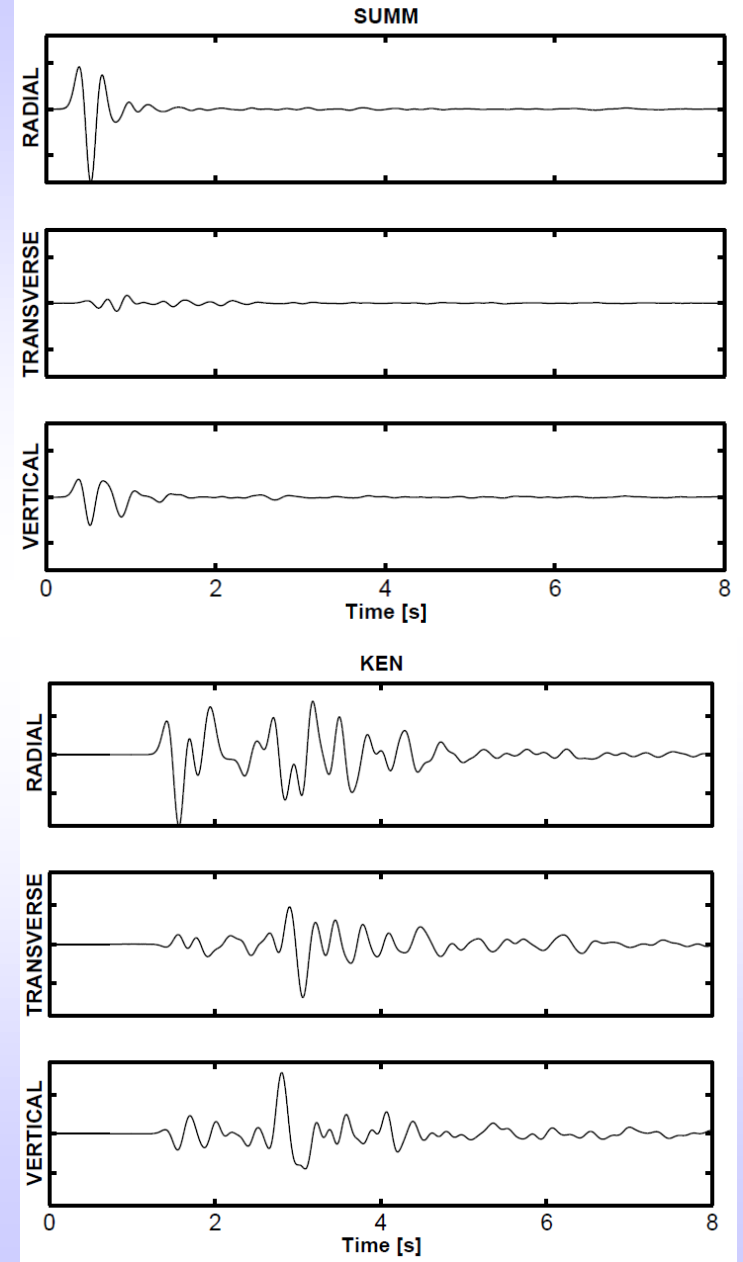
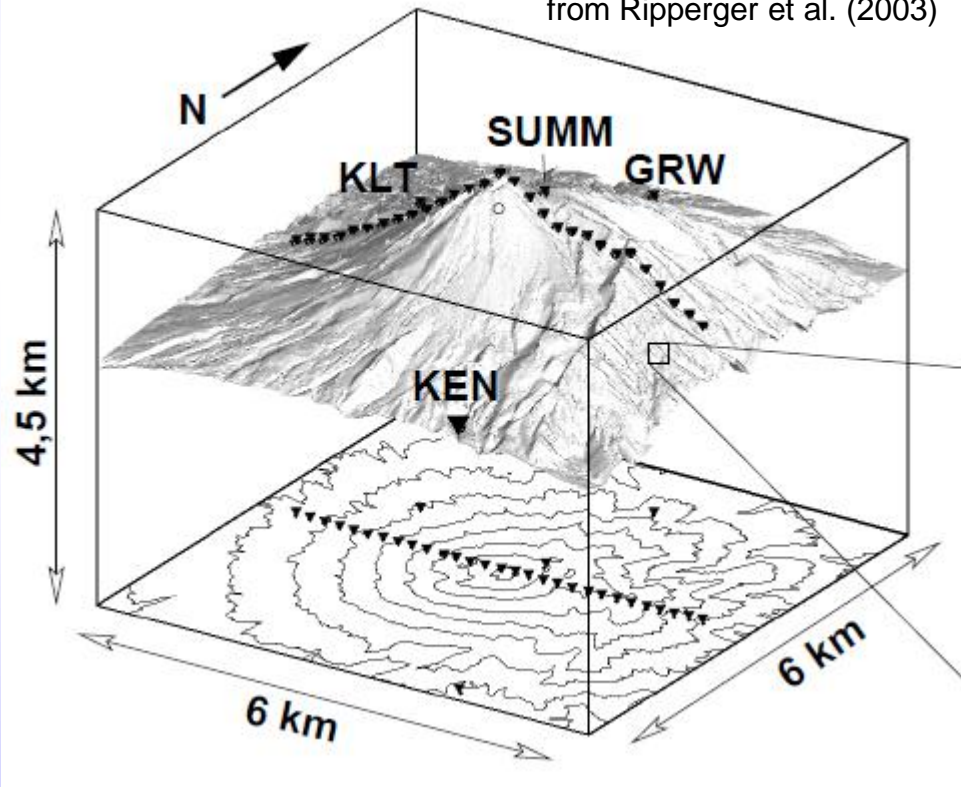


- Vertical force at the 600 m deep source
- Significant amount of transverse motion generated at some stations → importance of topography inclusion to the simulations related to volcanoes
- **3D simulations necessary**

# Topography effect II

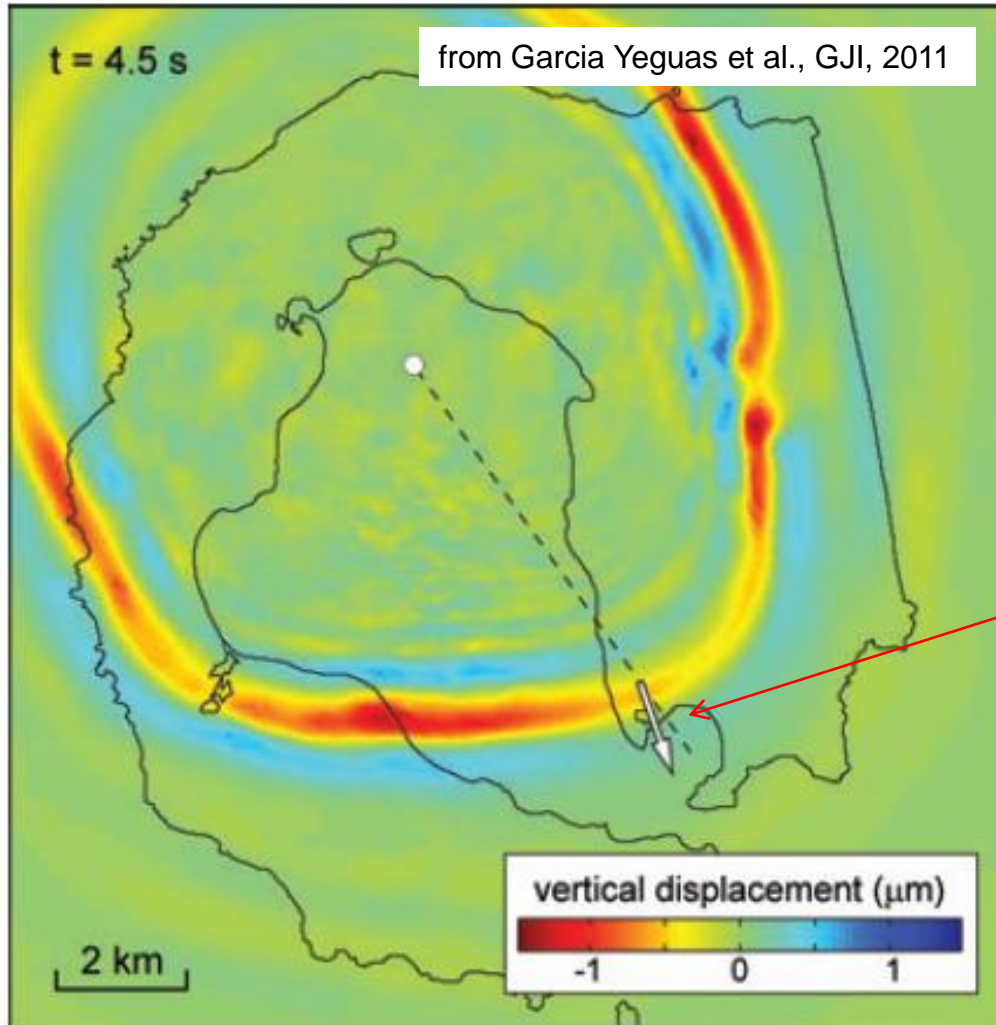
Numerical simulation for Merapi volcano, Indonesia (isotropic source)

from Ripperger et al. (2003)



# Topography effect III

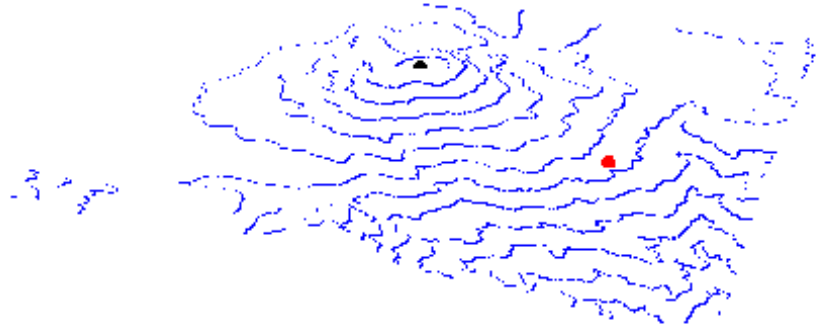
Snapshot of wavefield due to isotropic source  
Deception Island, Antarctica



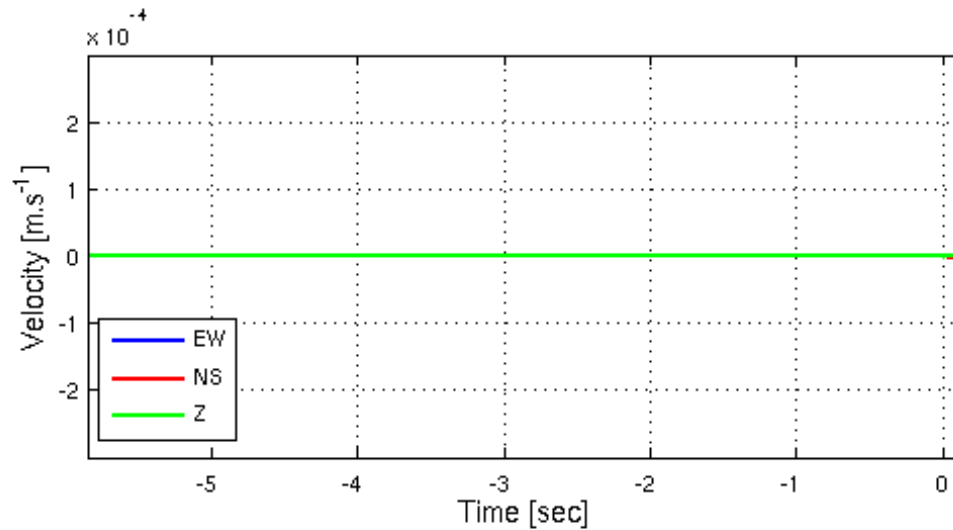
Direction of the apparent  
slowness vector at the array  
site

# Topography effect III

Seismic Wavefield on the Surface



- Homogeneous velocity model used for simulation
- Without topography, recorded waveforms would be simple pulses

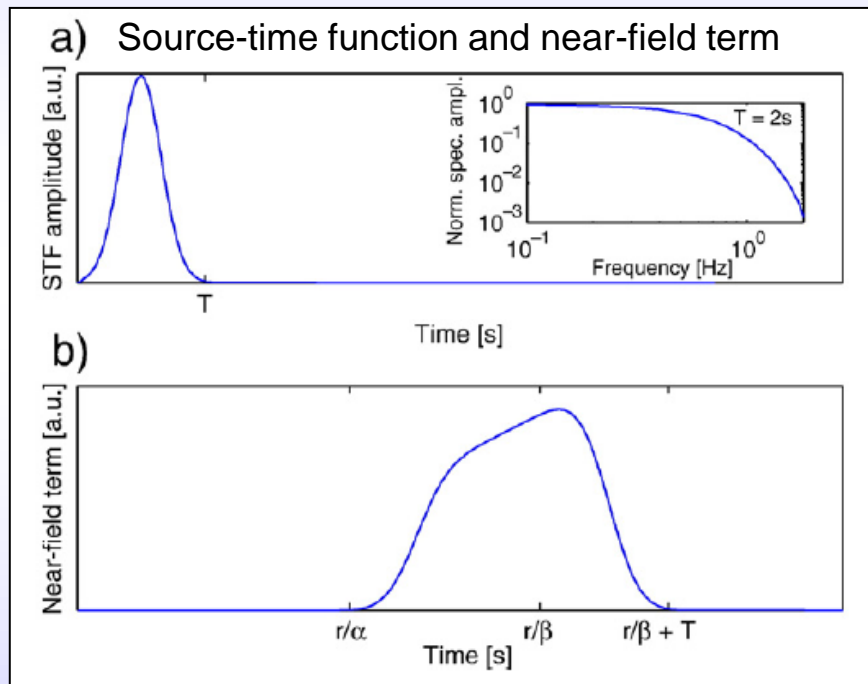


References: Neuberg and Pointer, 2000; Ripperger et al., 2003; Cesca et al., 2008; O'Brien and Bean, 2009; Lee et al., 2009

# Near-field effect I

Displacement  $\mathbf{u}$  in a homogeneous infinite medium at distance  $r$  from a source with the source-time function  $M(t)$  (Aki and Richards, 2002, eq. 4.32):

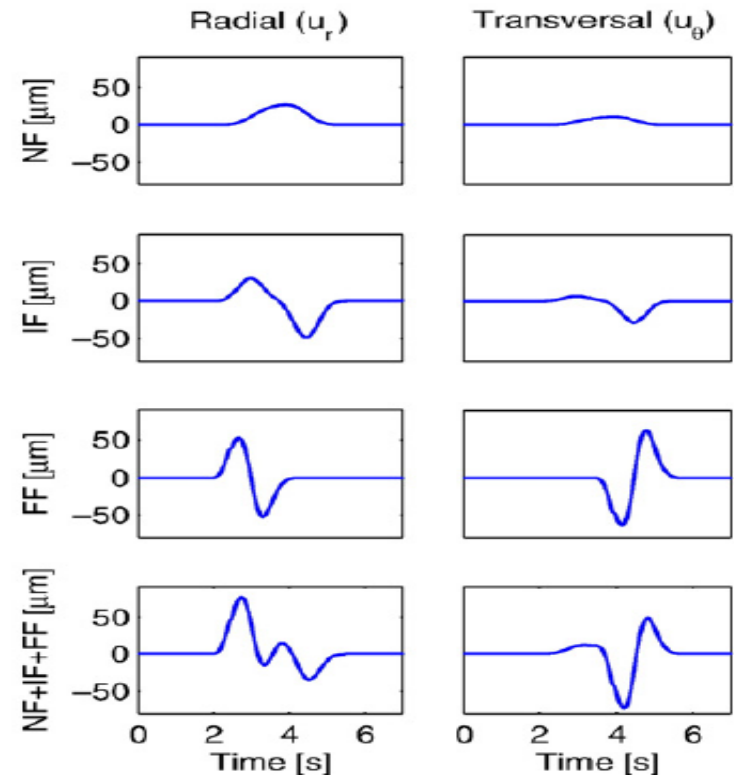
$$\mathbf{u}(\mathbf{r}, t) = \frac{\mathbf{R}^N}{4\pi\rho r^4} \int_{r/\alpha}^{r/\beta} \tau M(t-\tau) d\tau + \frac{\mathbf{R}^{IP}}{4\pi\rho\alpha^2 r^2} M(t-\frac{r}{\alpha}) + \frac{\mathbf{R}^{IS}}{4\pi\rho\beta^2 r^2} M(t-\frac{r}{\beta}) + \frac{\mathbf{R}^{FP}}{4\pi\rho\alpha^3 r} \dot{M}(t-\frac{r}{\alpha}) + \frac{\mathbf{R}^{FS}}{4\pi\rho\beta^3 r} \dot{M}(t-\frac{r}{\beta}),$$



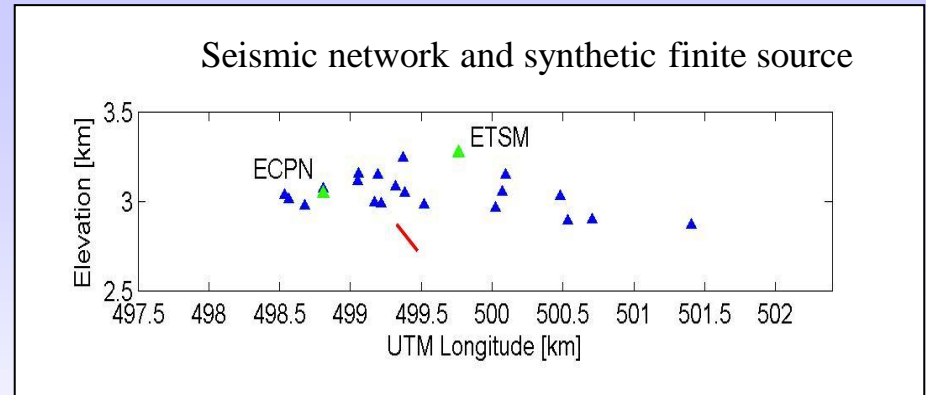
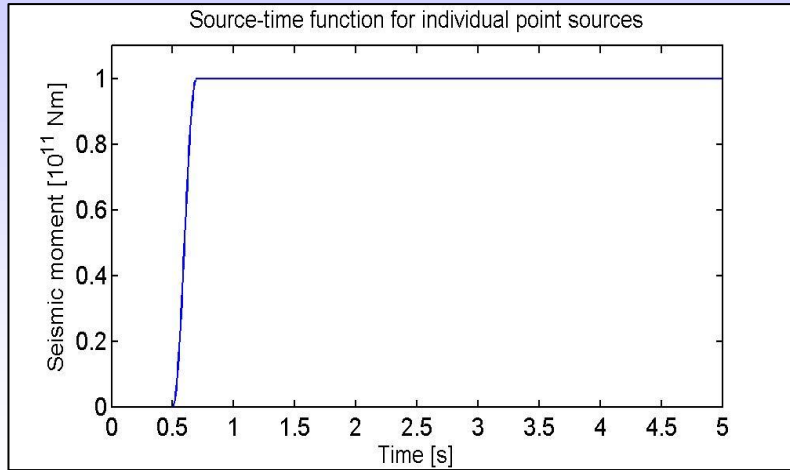
- NF term intertwined with both P and S waves
- NF, IP and IS have different polarisation to far-field P and S waves

→ Necessary to include into GF calculation

Displacement at a distance of 4 km ( $v_p = 2000$  m/s,  $v_s = 1150$  m/s) from a horizontal tensile crack (from Lokmer and Bean, 2011)

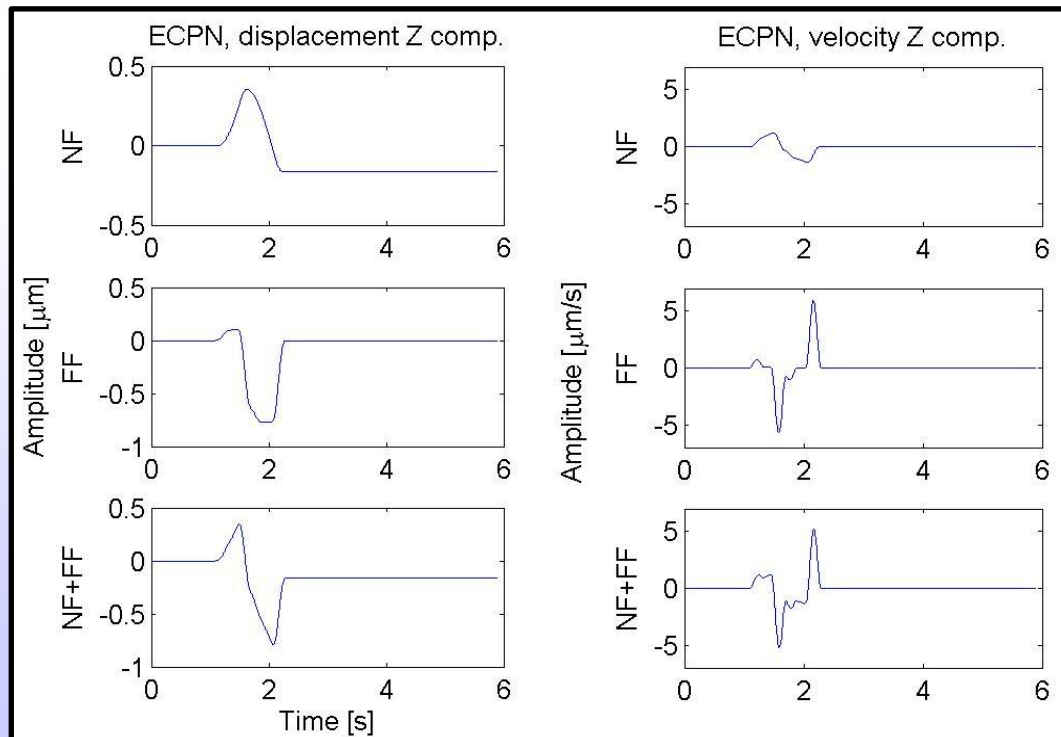


# Near-field effect II



← Source-time function

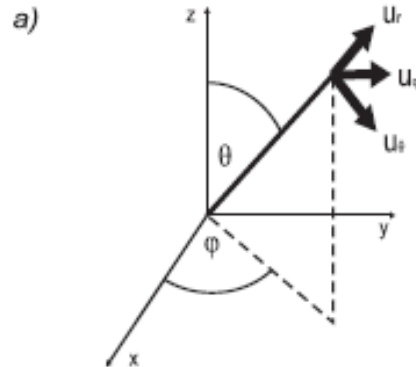
NF + IF terms →



200 x 100 m  
tensile fracture,  
 $v_{\text{rupture}}=600$  m/s

# Near-field effect III

## Radiation pattern for a vertical force source



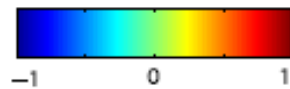
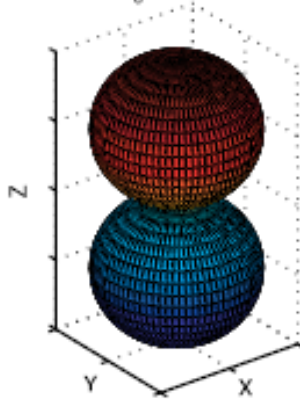
Lokmer and Bean, 2011

b)

P-wave

$$u_r = \cos(\theta)$$

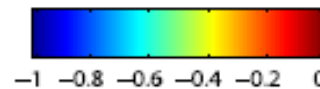
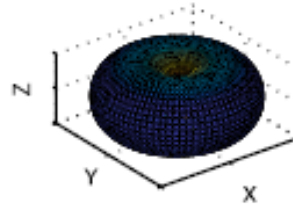
$$u_\theta = 0$$



S-wave

$$u_r = 0$$

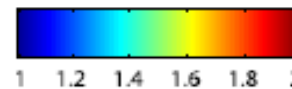
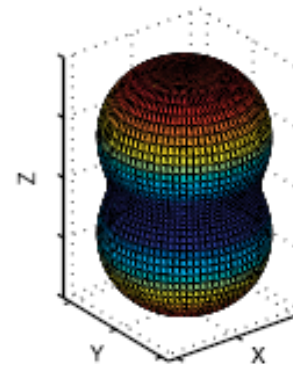
$$u_\theta = -\sin(\theta)$$



Near-field term

$$u_r = 2\cos(\theta)$$

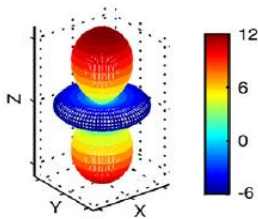
$$u_\theta = \sin(\theta)$$



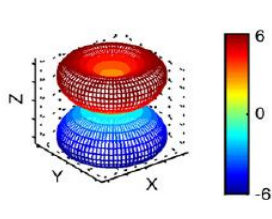
# Near-field effect IV

## Radiation pattern of a horizontal tensile crack

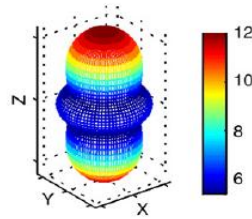
Near-field,  $u_r$



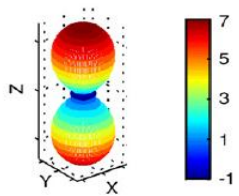
Near-field,  $u_\theta$



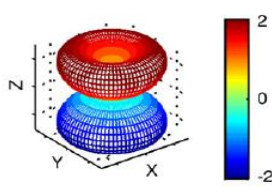
|Near-field|



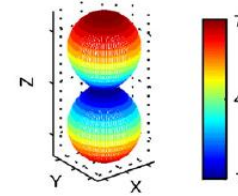
Intermediate-field P,  $u_r$



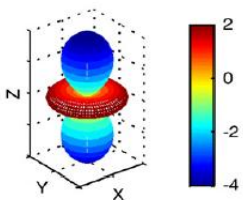
Intermediate-field P,  $u_\theta$



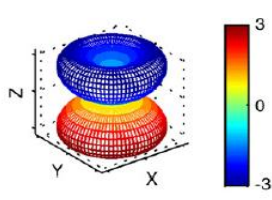
|Intermediate-field P|



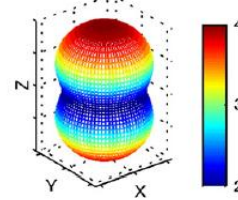
Intermediate-field S,  $u_r$



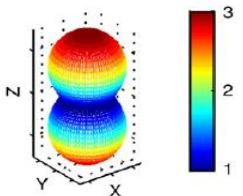
Intermediate-field S,  $u_\theta$



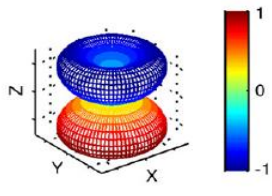
|Intermediate-field S|



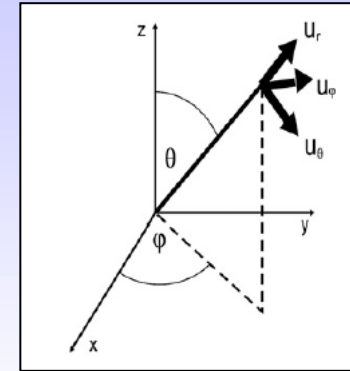
Far-field P



Far-field S



Lokmer and Bean, 2011

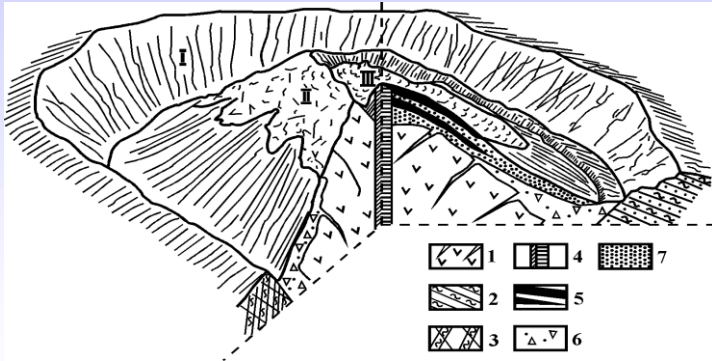


Benefit: Different radiation patterns of near, intermediate and far field terms introduce additional information in inversion

Symmetry!

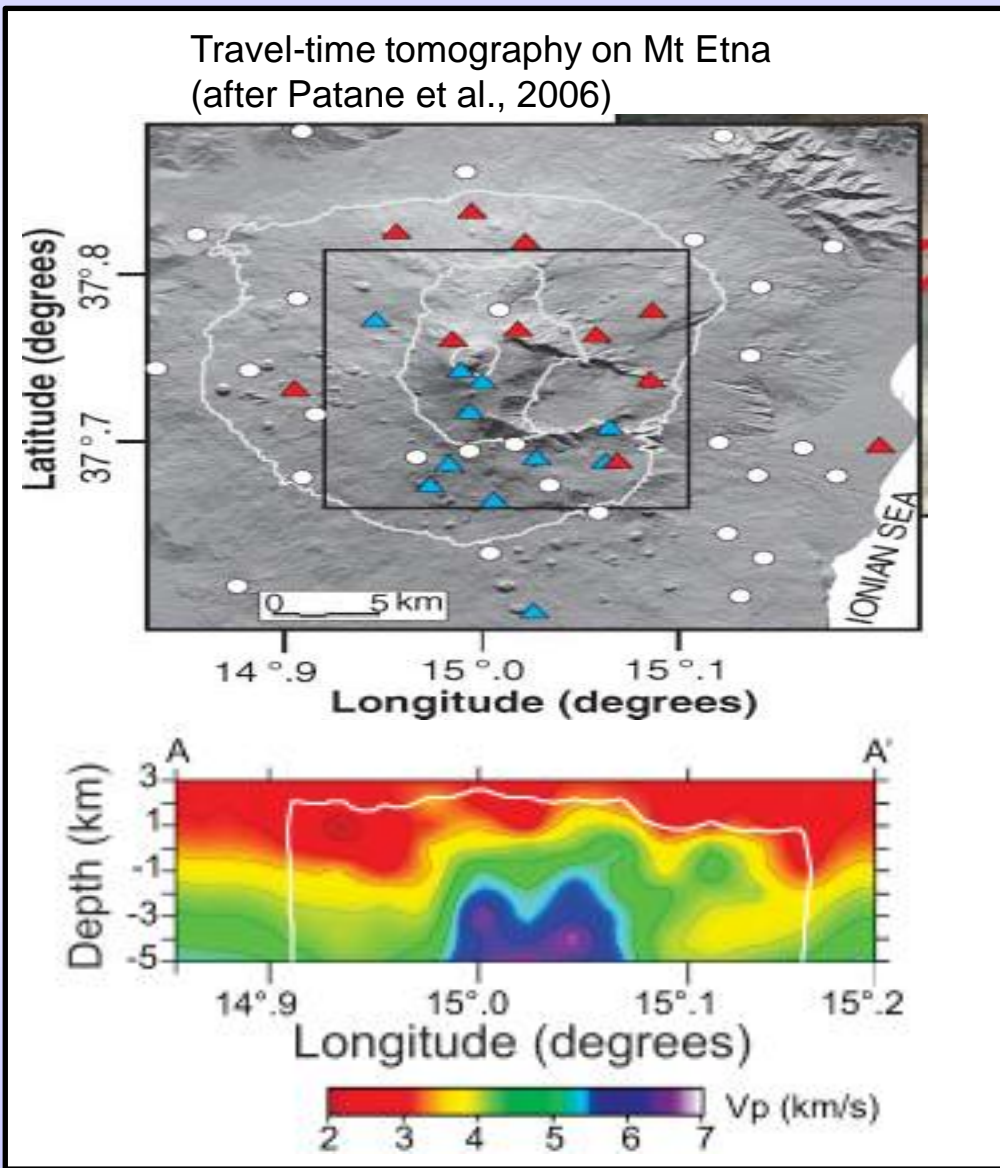
# Problem 1: Poorly resolved shallow velocity models on volcanoes

## 1. Travel-time tomography



- Extremely heterogeneous volcano structure (eruptions from different craters and fissures, solidified magma, new magma, gas, dykes, lava, pyroclastic flows)
- First 1-2 km not constrained by tomography (unfavourable earthquakes-stations distribution)
- LP events cannot be used for tomography due to their usually clustered hypocentres and undetectable onsets

**REMEMBER, WE ARE INTERESTED IN THE FIRST FEW HUNDRED METRES!**



# Problem 1: Poorly resolved shallow velocity models on volcanoes

## 2. Surface-waves dispersion (f-k analysis)

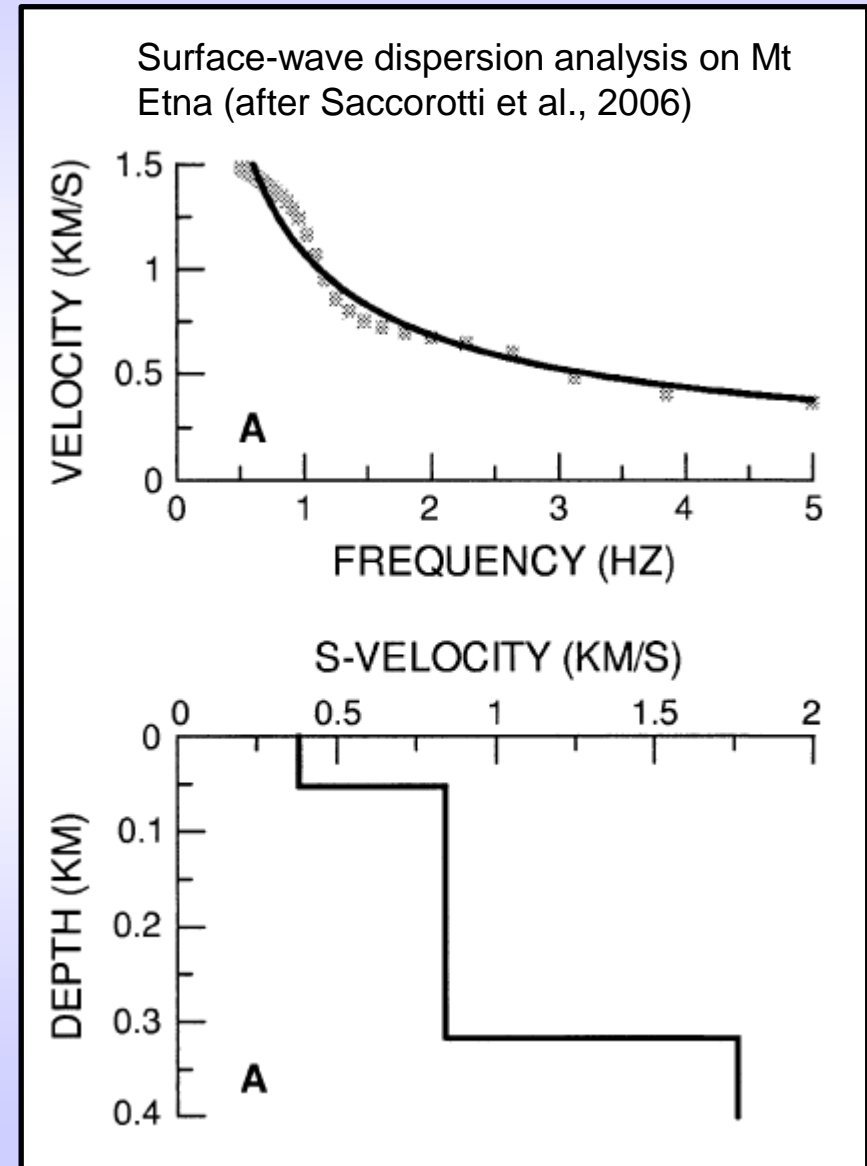
- Only S-wave structure (rather insensitive to the P-wave velocity),  $v_p/v_s$  unknown
- 1-D structure at the array location
- Trade-off between the layer thicknesses and velocities (non-unique); mode skipping

## 3. Full waveform tomography

- Very good starting model required (slightly perturbed with regard to the true model → unsatisfied)
- Extremely computationally demanding in 3D (see e.g. Tromp et al., 2004)

## 4. Active seismic surveys

- not recommended on active volcanoes

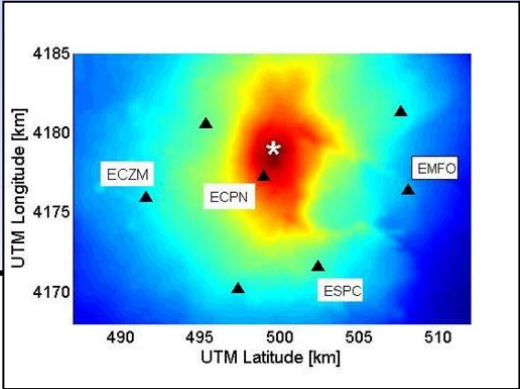


# Joint topography-heterogeneity effect: synthetics

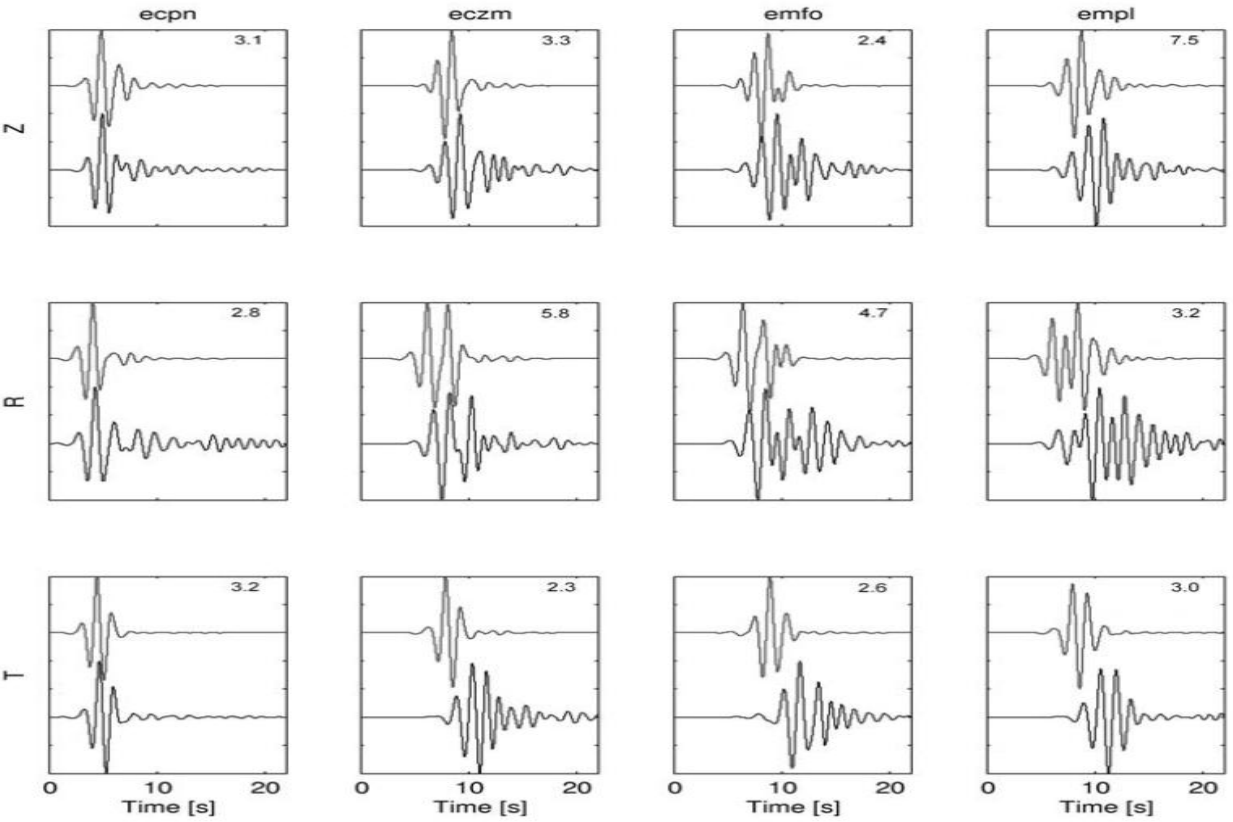
Model 1: homogeneous,  $v_p = 3000$  m/s,  $v_s = 1730$  m/s

Model 2: 400 m thick layer on top  $v_p=2000$  m/s,  $v_s=1150$  m/s

600 m deep source, vertical tensile crack



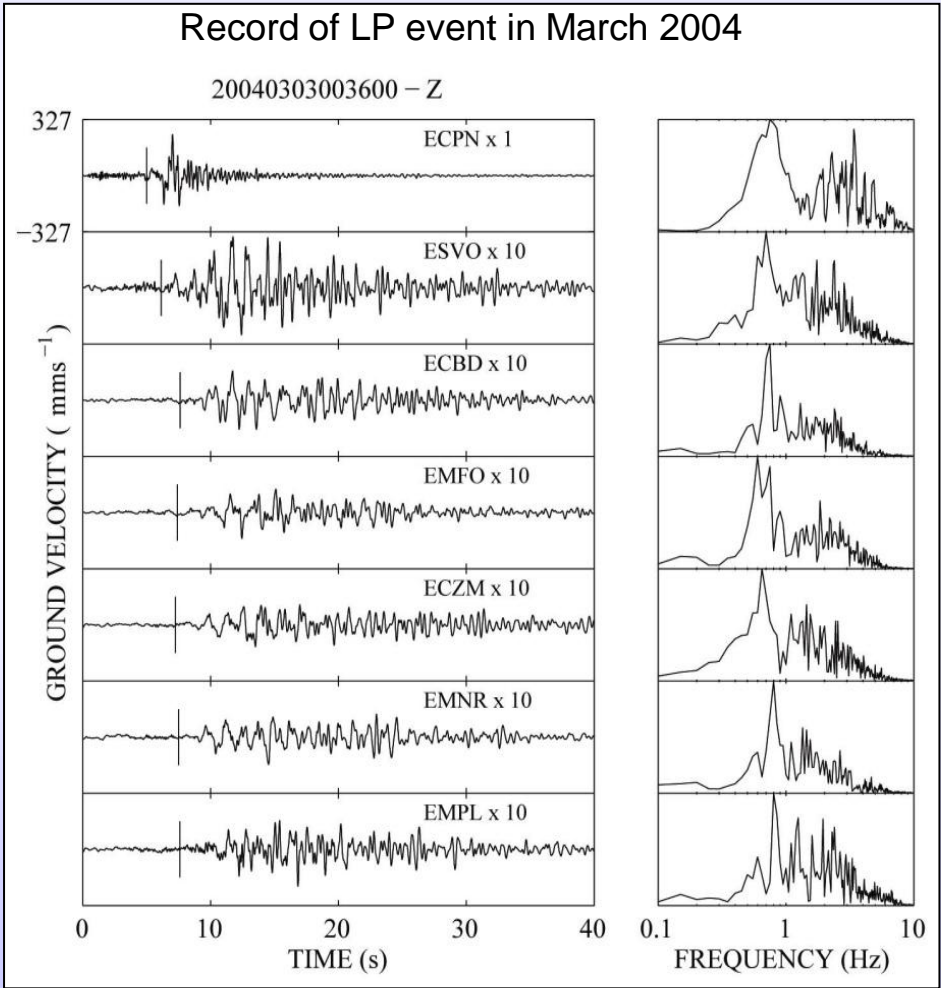
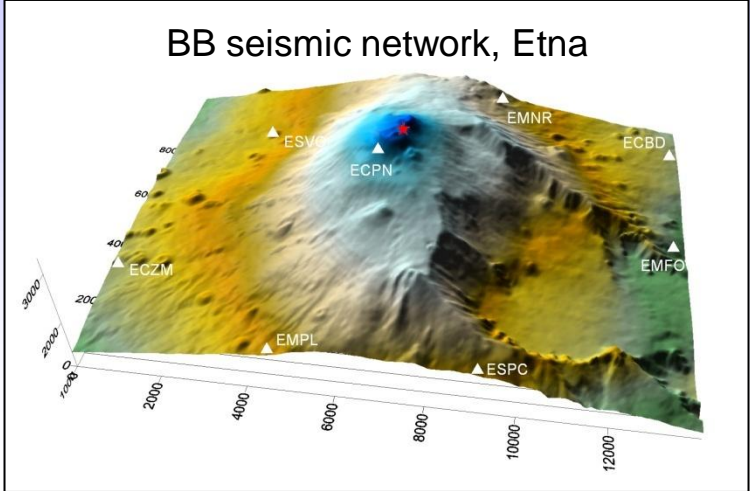
Synthetic seismograms for the homogeneous and layered models



Effect on both amplitudes and duration

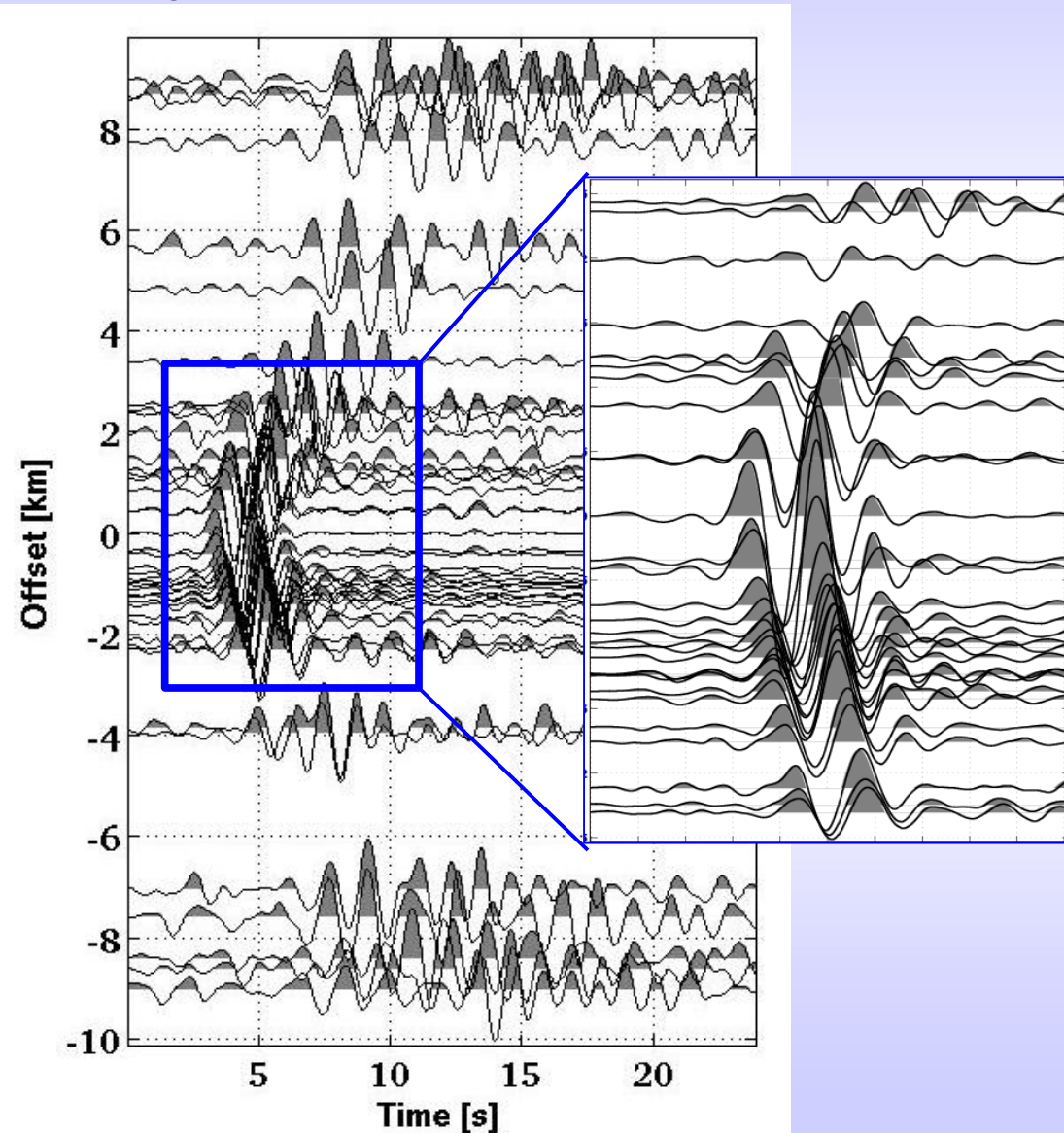
Let's see some real data examples

# Joint topography-heterogeneity effect: Etna 2004



# Joint topography-heterogeneity effect: Etna 2008

LP signals vs. distance from summit (Etna, 2008)

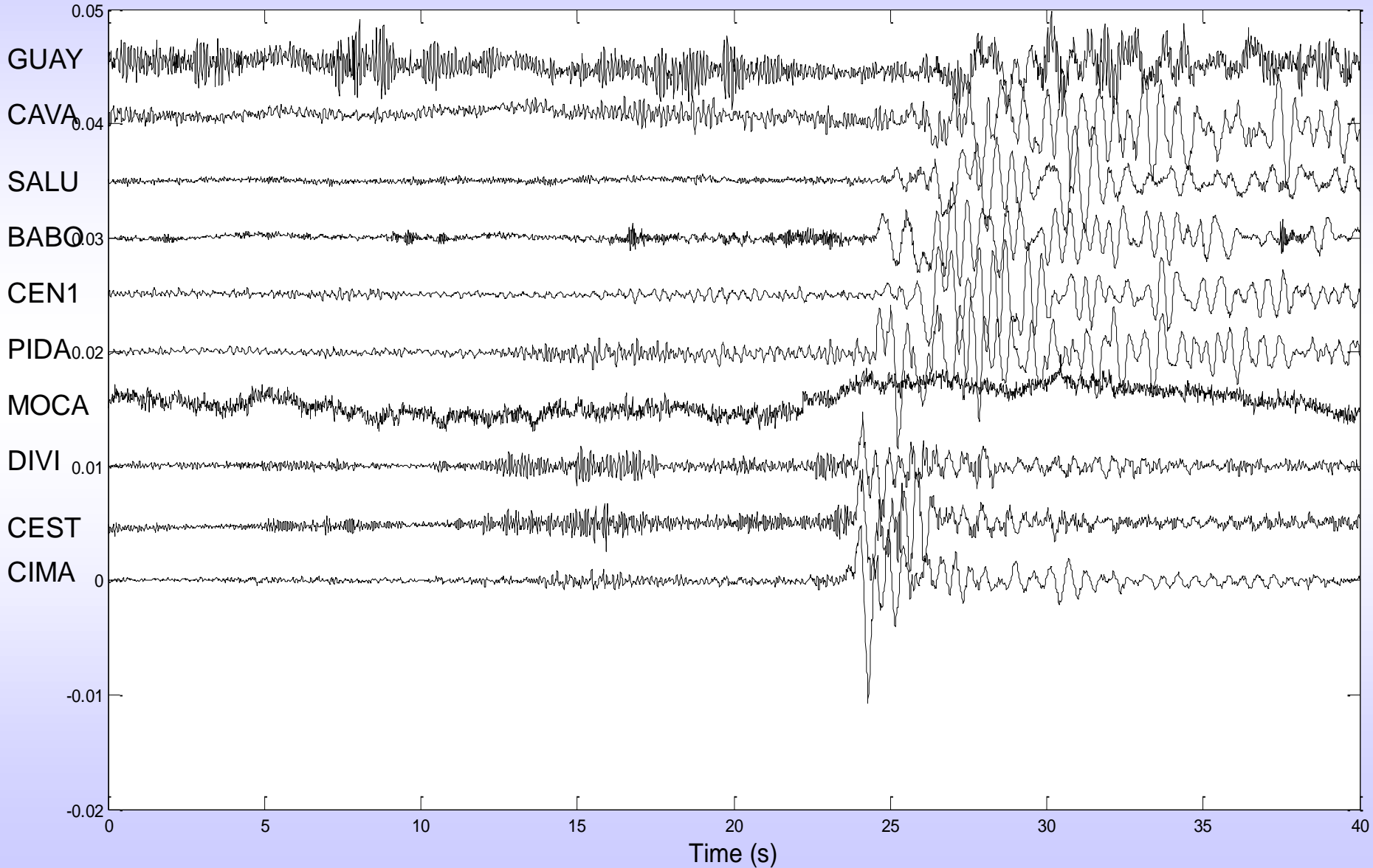


- Resonating waveforms only for stations furthest from the summit
- Waveforms are very similar for stations close to the summit and are of short duration
- Excellent match with the prediction from the numerical experiments
- There is no resonance of the source

# Joint topography-heterogeneity effect: Turrialba 2004

LP events at Turrialba, Costa Rica: GUAY ~ 7km dist; CIMA ~ 1km dist

CIMA, CEST and DIVI are in the summit area



# Joint topography-heterogeneity effect: Turrialba 2011

LP recorded in Turrialba experiment 2011 a few hundred metres from the summit

Files = E:\Data\11-TUR\WC1\Z\20110309\_1800.sac

Number of samples in the analyzed window = 5176 Filter: Fmin = 0.50 Fmax = 2.00 Hz

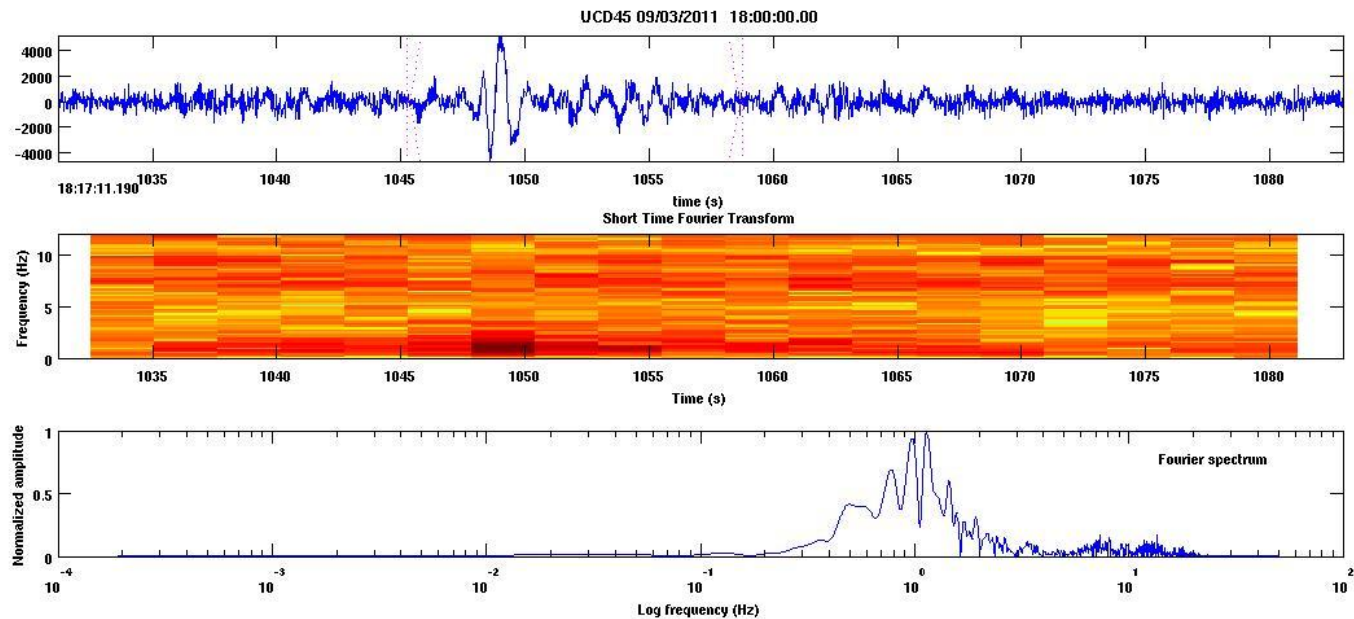
Sampling frequency = 100.0 Hz after resampling with factor 1

Time-Freq. Analysis : window = 512 nfft = 512 overlap = 256

Spectral Analysis :

Fourier spectrum with nfft = 524288

Maximum value of spectrum = 4.69e+005 Taper: Tukey cosine with taper ratio = 0.1



## Problem 2: Source locations

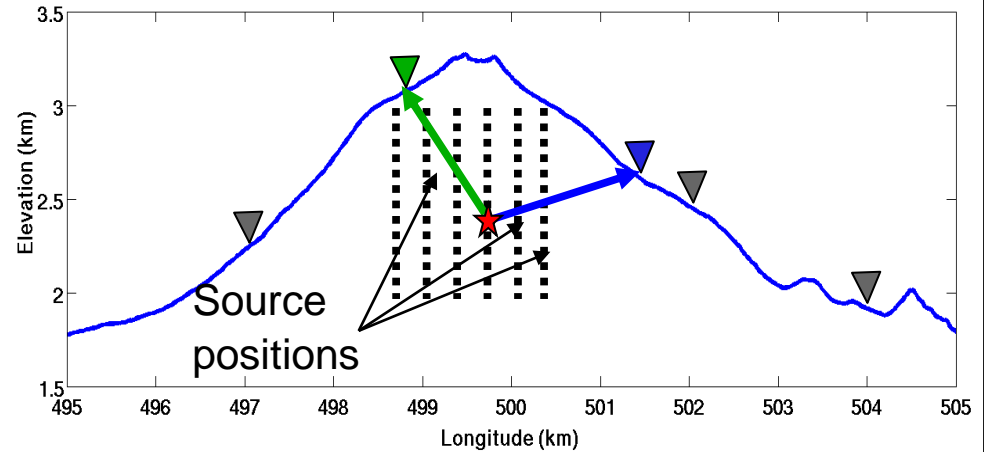
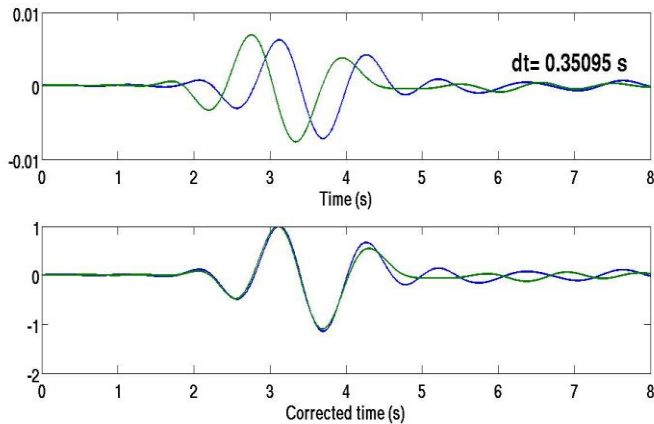
Locating events challenging due to:

- poorly resolved shallow structure (especially P-wave velocity)
- no clear onsets on seismograms
- no separate phases
- particle motion often compromised due to the near-field effect and topography

Location methods:

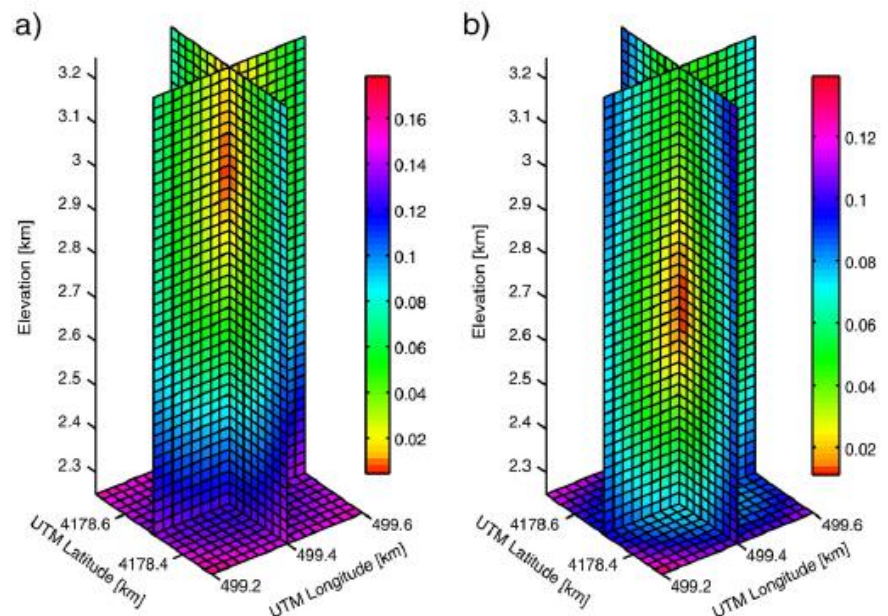
- Semblance, cross-correlation - these methods assume a purely isotropic source and far-field observation
- Amplitude decay – assumes purely isotropic source
- First arrivals travel-time location is rarely possible (swarms)
- Array methods – determining the slowness vector (direction and velocity) of the coherent waves crossing the array (much better)
- Time-reversal
- Moment- tensor inversion (for example, grid search over many sources and comparing residuals)

# Problem 2: example of mislocation due to the near-field effect



- Cross-correlation location method
- Method assumes identical waveform at all stations
- It gives incorrect location even if an isotropic source is used (due to the near-field effect)
- Error decreases with the increasing source depth (~ constant FF/NF ratio)
- Method may still work well for the relative location of close sources

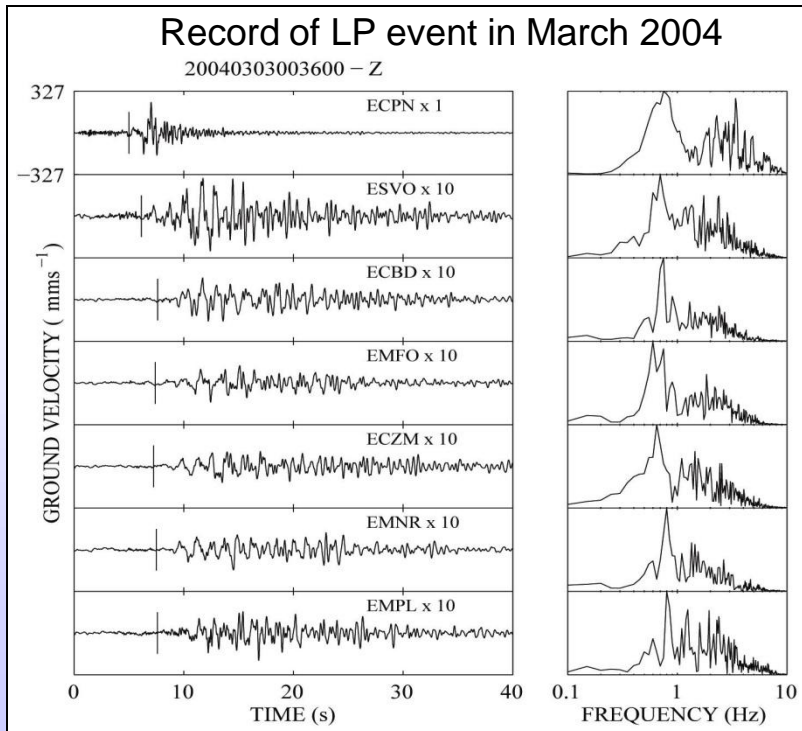
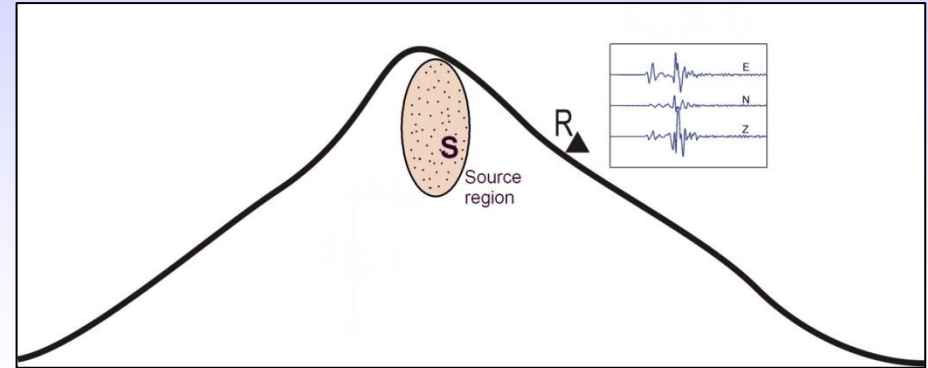
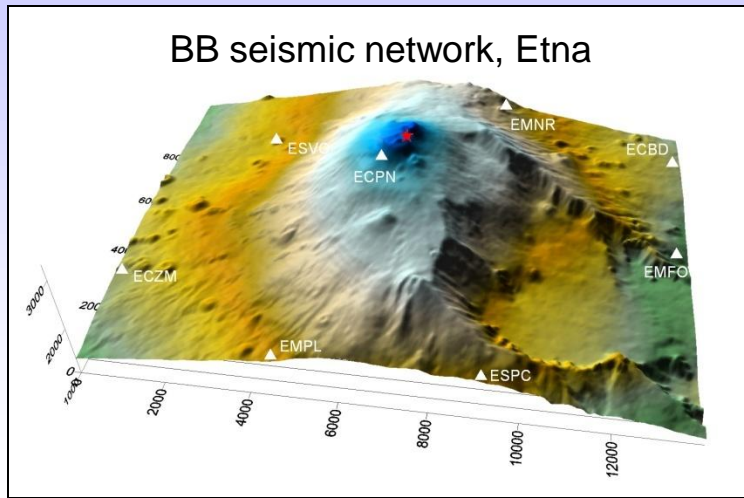
Locating a) far-field waveforms and b) complete seismograms (25 near-field stations)



from Lokmer and Bean (2010)

Moment tensor inversion on Etna in 2004

# MT inversion on Etna (2004)



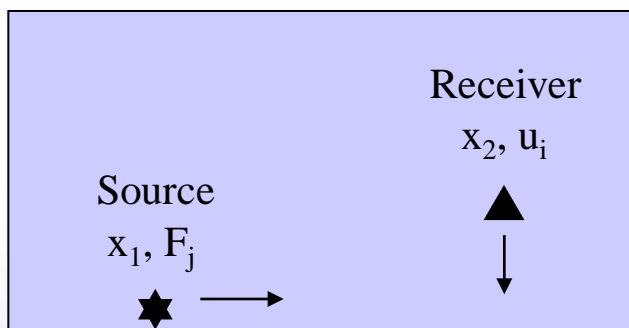
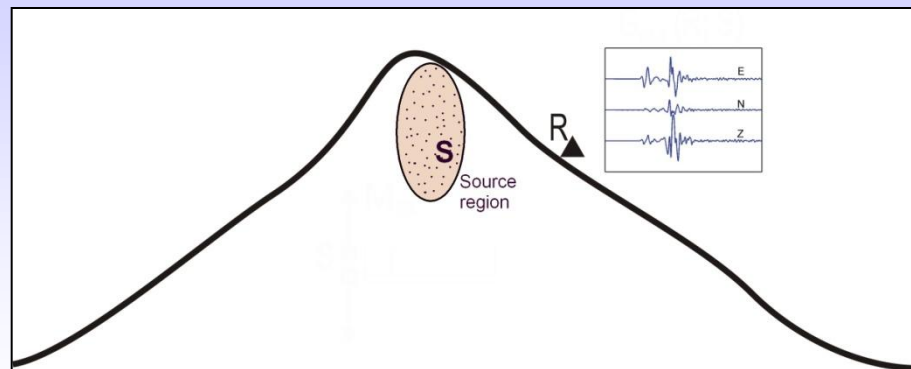
- Green's function were calculated using tomography model of Patane et al. (2002) and DEM topography of Etna, for 3240 source locations within the source region
- Computations up to 2 Hz
- Data were corrected for the instrument response, filtered 0.3 – 1.5 Hz and converted to displacement

# Reciprocity

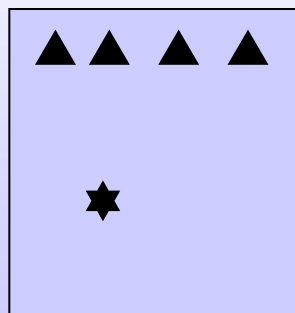
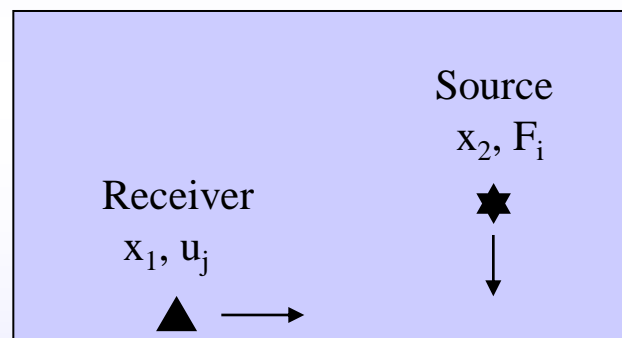
- Even for a relatively small source volume (e.g. 10 x 10 x 10 sources), it is not possible to calculate Green's functions directly (min 6000 calculations)

- Reciprocity approach can be used instead

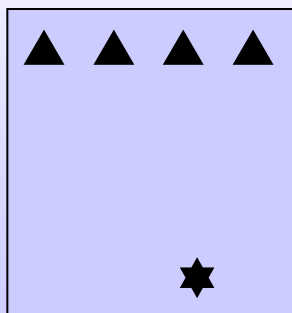
$$G_{np}(R;S) = G_{pn}(S;R)$$



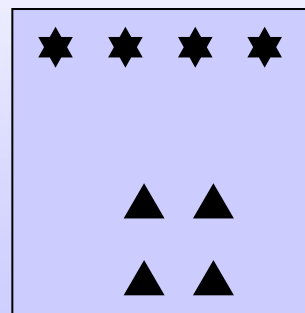
=



+ ... +

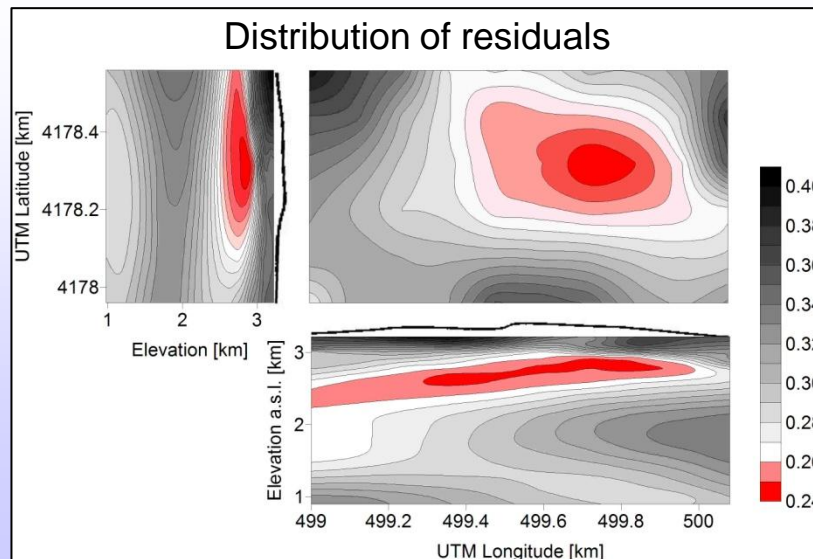
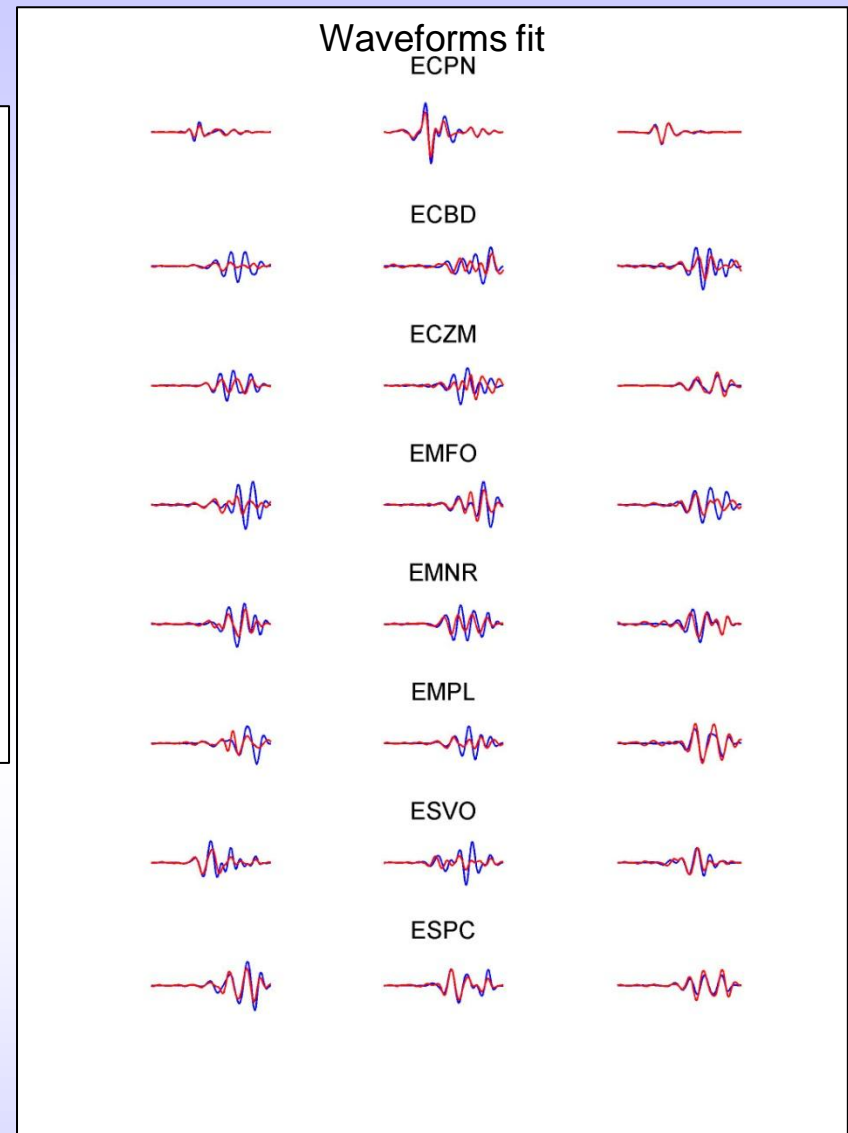
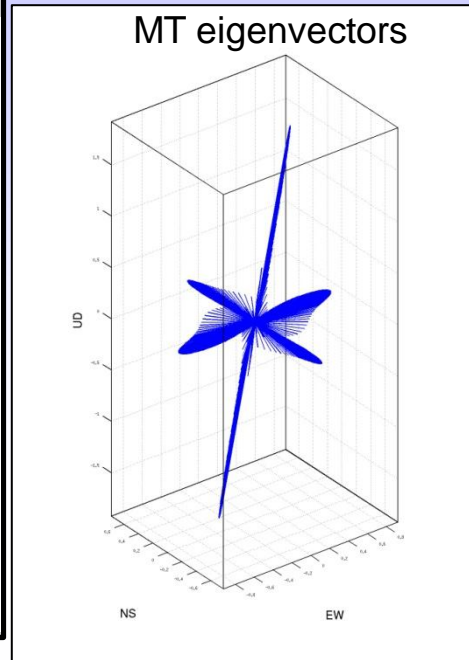
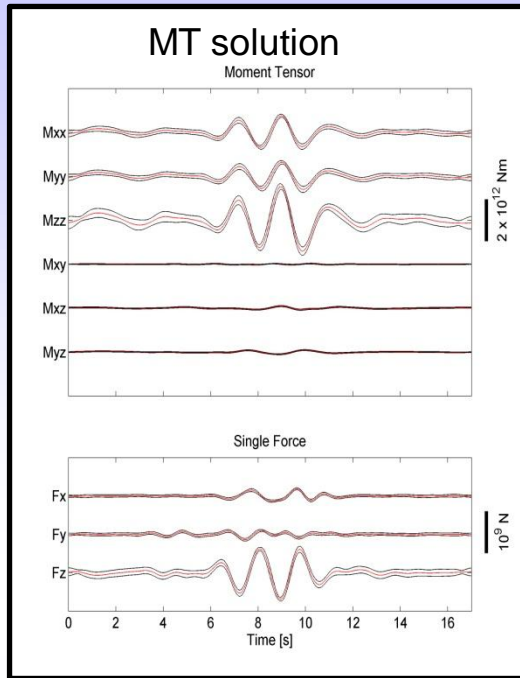


=



3 x the number of receivers computations needed → considerably reduced computational cost

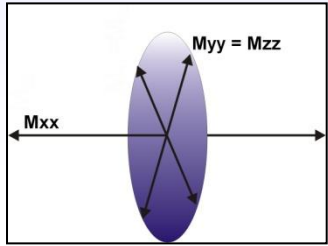
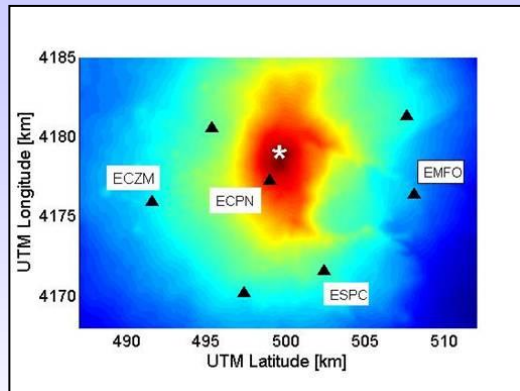
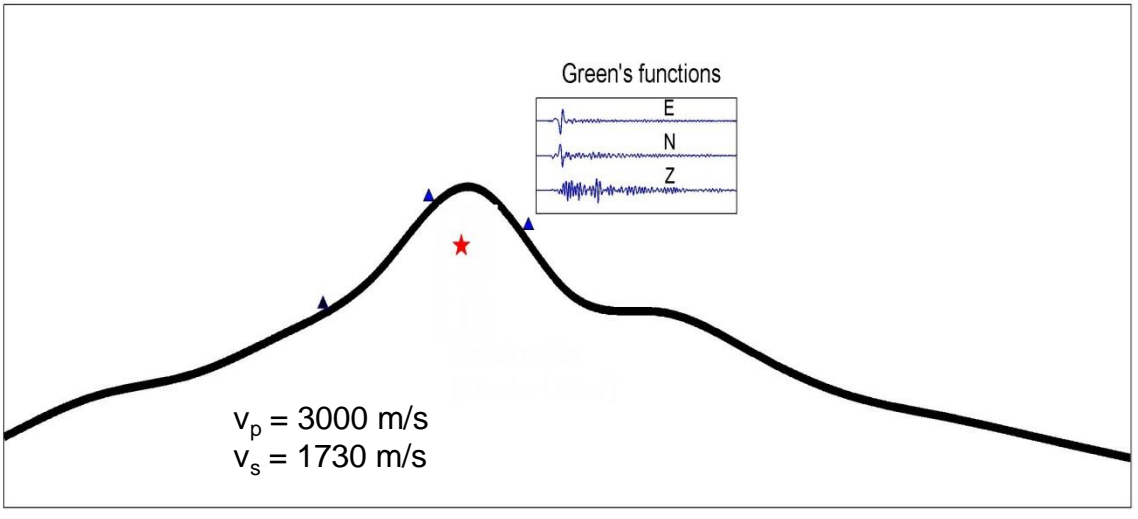
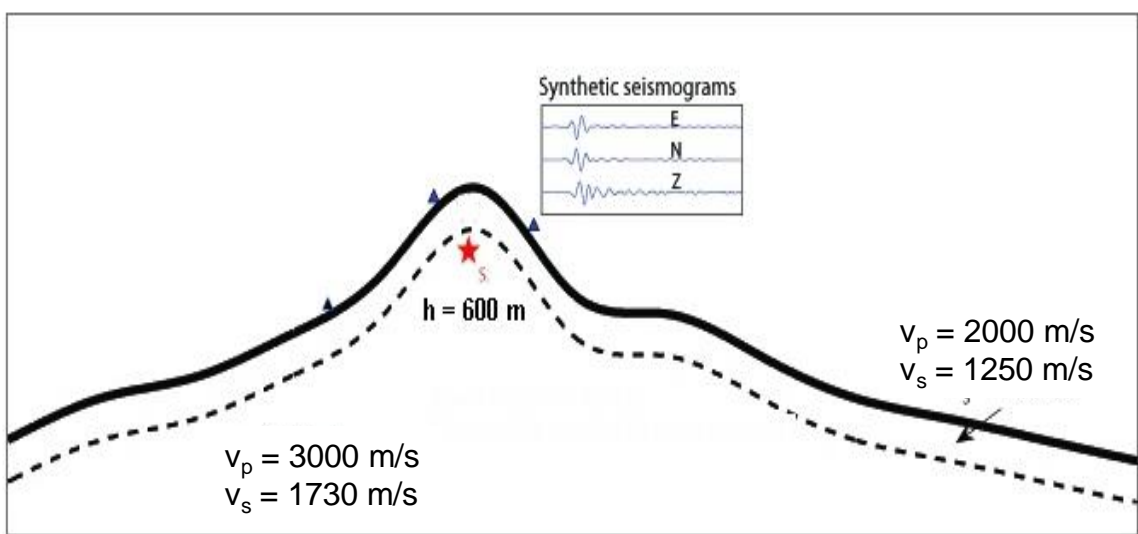
# MT solution on Etna (2004)



• Horizontal crack + strong vertical force → force direction incompatible with mass transport

→ Let's test the sensitivity of the solution to velocity model

# Synthetic test: sensitivity of MT to velocity model (setup)

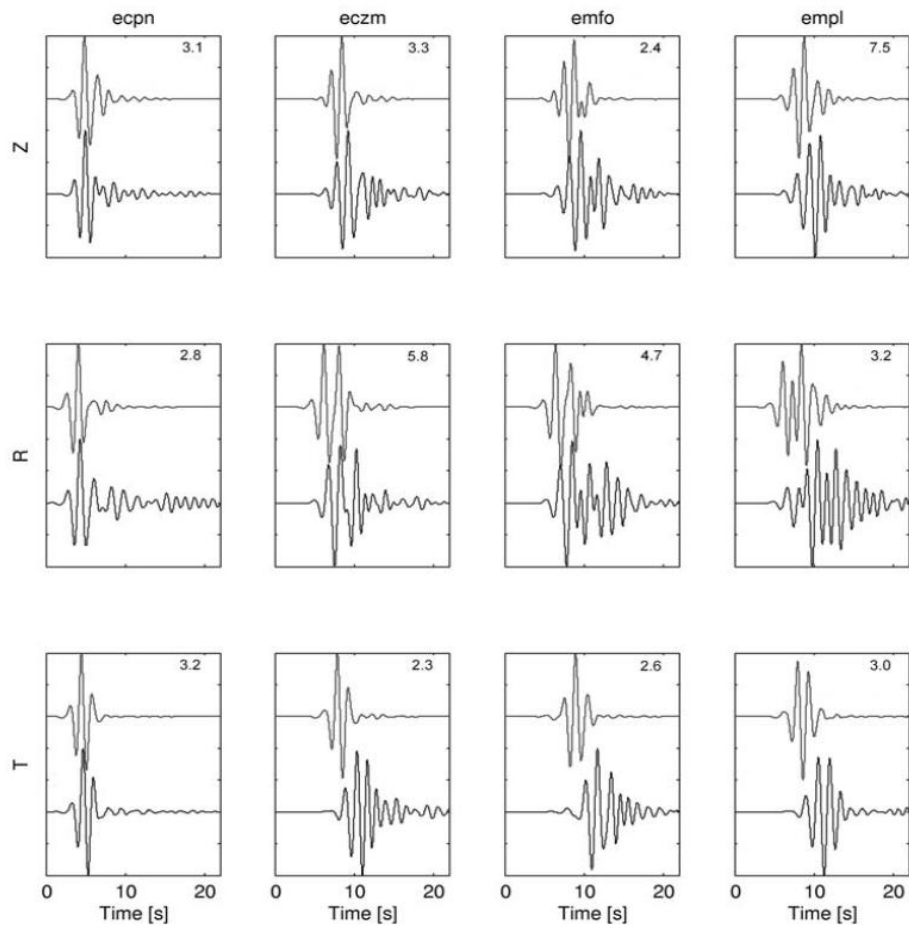


- We simulate a scenario where we do not know the uppermost part of the velocity structure
- The source mechanism is a vertical tensile crack
- Shallow structure is usually poorly constrained (or not constrained at all) by tomography

Having a limited knowledge about the medium, are we still able to retrieve the correct source mechanism from observations?

# MT solution for unconstrained inversion

Synthetic seismograms for the homogeneous and layered models

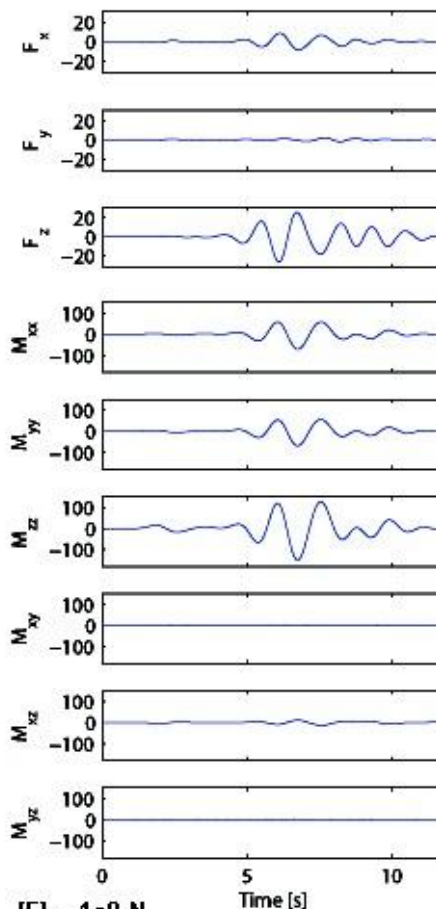


True mechanism

$$M_0 \begin{bmatrix} 3 & 0 & 0 \\ 0 & 1 & 0 \\ 0 & 0 & 1 \end{bmatrix}$$

MT solution

$$10M_0 \begin{bmatrix} 1 & 0 & 0 \\ 0 & 1.2 & 0 \\ 0 & 0 & 2.3 \end{bmatrix} + F_z$$

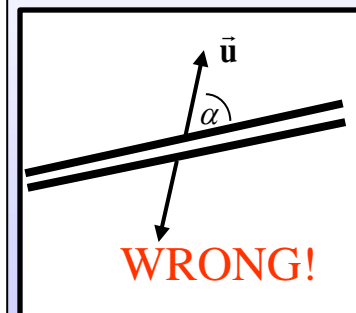


$[F] = 1e9 \text{ N}$   
 $[M] = 1e12 \text{ Nm}$

A horizontal instead of a vertical crack + strong vertical force

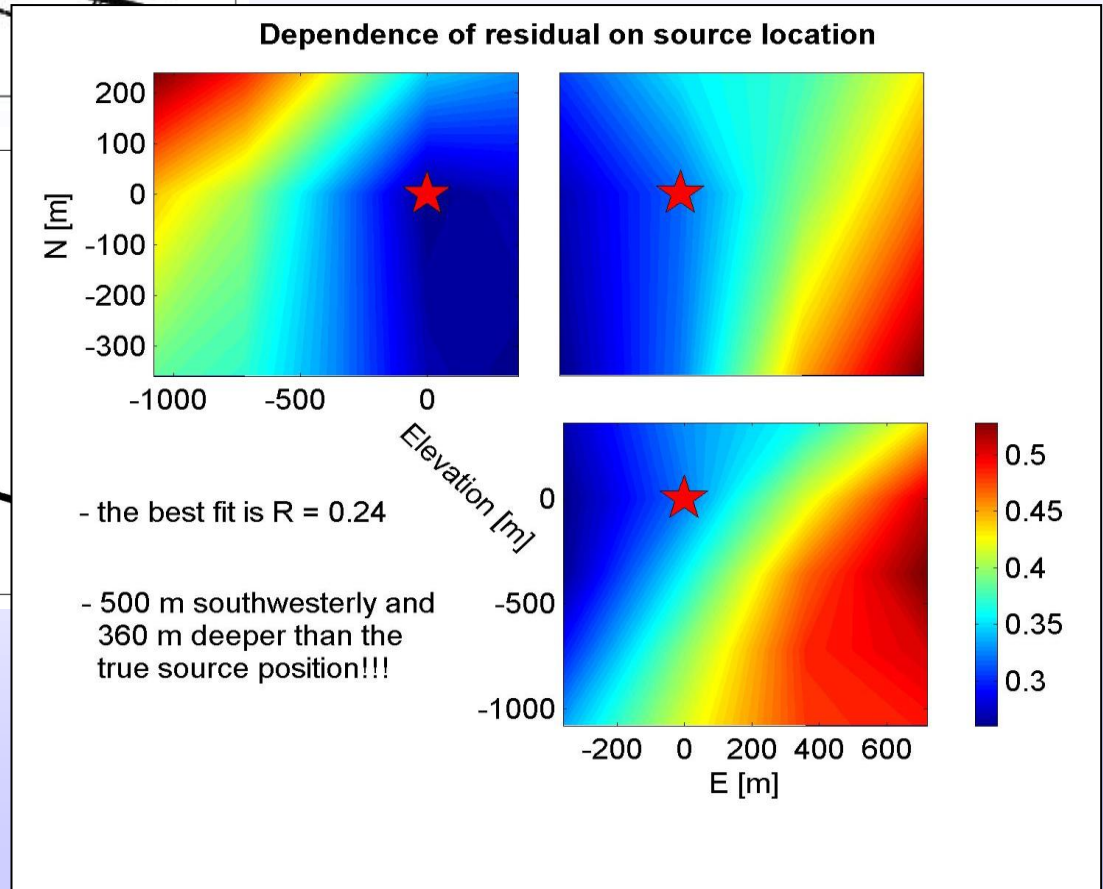
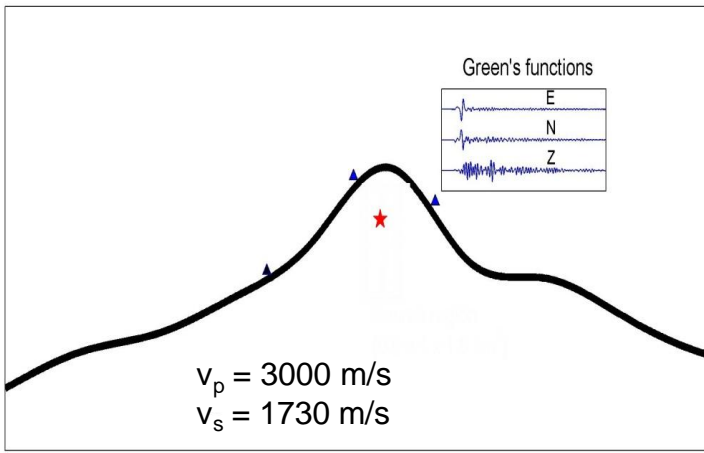
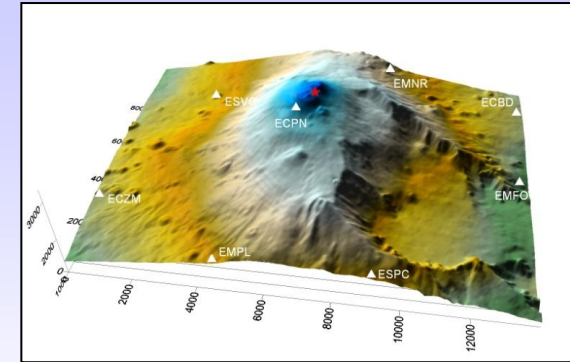
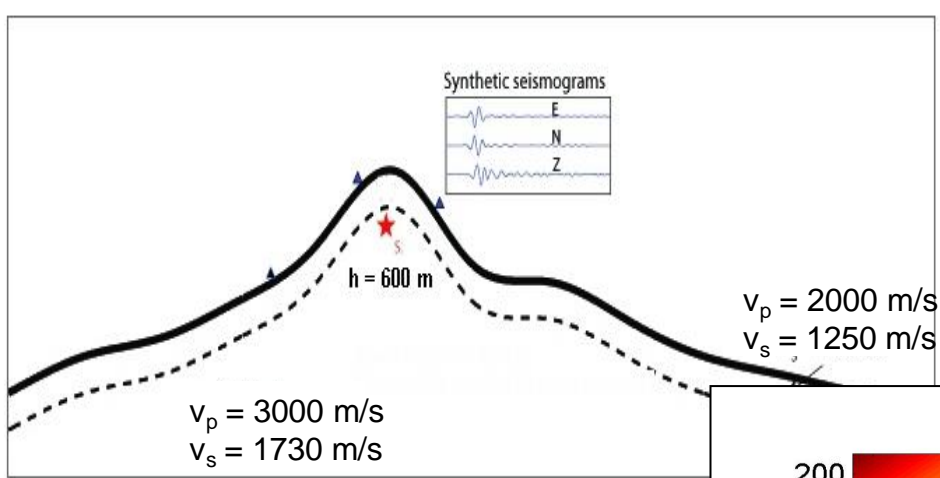
Incorrect magnitude of moment tensor

Misfit R = 0.24 (relatively small misfit)



- Information about the radiation pattern lost
- Waves propagate along the flanks, trapped in the low velocity layer (near-field stations needed)

# Synthetic test – sensitivity of MT to velocity model (source location)



For this particular network configuration, travel time inversion as well as cross-correlation method gave more accurate location of the epicenter (synthetic tests!)

# Unconstrained and constrained MT inversions on volcanoes

$$u_n^s(\omega, r) = \sum_{p,q} M_{pq}(\omega) \cdot G_{np,q}^s(\omega, r; s) \quad \leftarrow 6 \text{ parameters}$$

$$u_n^s(\omega, r) = \sum_{p,q} M_{pq}(\omega) \cdot G_{np,q}^s(\omega, r; s) + F_p(\omega) \cdot G_{np}^s(\omega, r; s) \quad \leftarrow 9 \text{ parameters}$$

Cartesian MT components for an arbitrary oriented crack

$$M_{xx} = M_0(\lambda/\mu + 2 \sin^2 \theta \cos^2 \varphi),$$

$$M_{yy} = M_0(\lambda/\mu + 2 \sin^2 \theta \sin^2 \varphi),$$

$$M_{zz} = M_0(\lambda/\mu + 2 \cos^2 \theta),$$

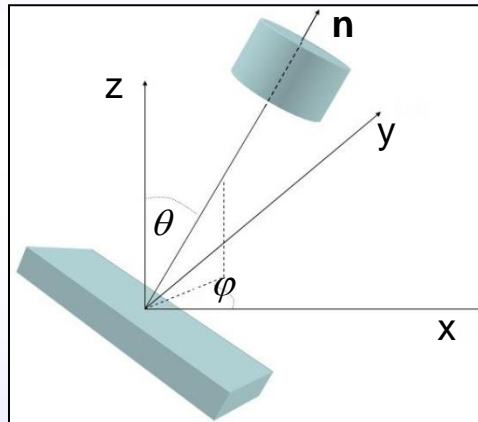
$$M_{xy} = M_0 \sin^2 \theta \sin 2\varphi,$$

$$M_{xz} = M_0 \sin 2\theta \cos \varphi,$$

$$M_{yz} = M_0 \sin 2\theta \sin \varphi,$$

where  $M_0 = \mu \Delta V$ .

$$u_n^s(\omega, r) = \sum_{p,q} M_0(\omega) \cdot f_{pq}(\theta, \varphi) \cdot G_{np,q}^s(\omega, r; s) \quad \leftarrow 1 \text{ parameter + grid search in } (\theta, \varphi) \text{ space}$$



$\leftarrow$  We can also perform constrained inversions for an arbitrarily oriented cylindrical pipe and a purely isotropic source (simplified most likely conduit geometries; Nakano and Kumagai, 2005)

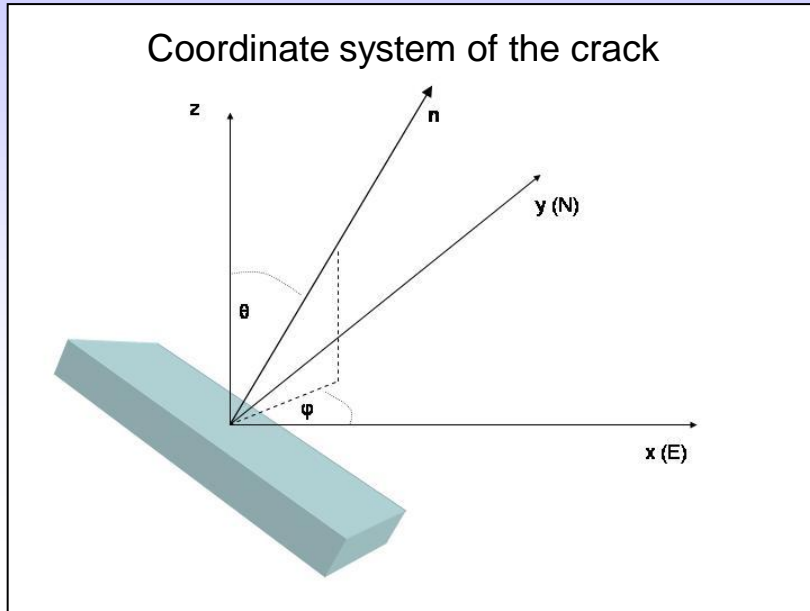
$$R = \|\mathbf{u} - \mathbf{G}\mathbf{m}\|^2 \equiv \text{min}, \quad \leftarrow \text{residual (misfit)}$$

$$AIC = N_{\text{data}} \ln(R) + 2N_{\text{parameters}} \quad \leftarrow \text{Akaike criterion}$$

AIC - model selection criterion (examined in O'Brien et al, 2010)  
 - it does not work if our estimated model is far from the true model

References: Nakano and Kumagai, 2005; Lokmer et al., 2007; Lokmer, 2008; Bean et al., 2008

# MT solution for constrained inversion (pre-assumed geometry)



Cartesian MT components for an arbitrary oriented crack

$$M_{xx} = M_0 \left( \frac{\lambda}{\mu} + 2 \sin^2 \theta \cos^2 \varphi \right),$$

$$M_{yy} = M_0 \left( \frac{\lambda}{\mu} + 2 \sin^2 \theta \sin^2 \varphi \right),$$

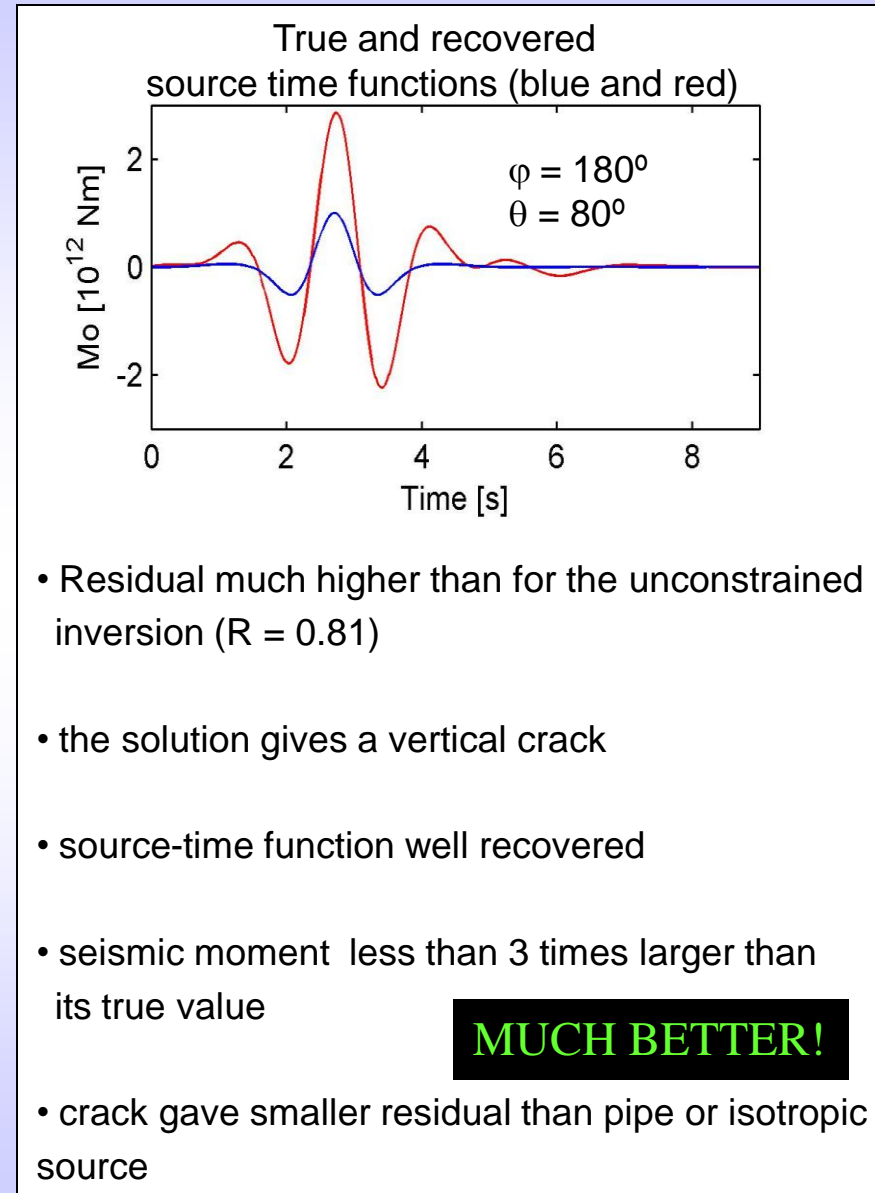
$$M_{zz} = M_0 \left( \frac{\lambda}{\mu} + 2 \cos^2 \theta \right),$$

$$M_{xy} = M_0 \sin^2 \theta \sin 2\varphi,$$

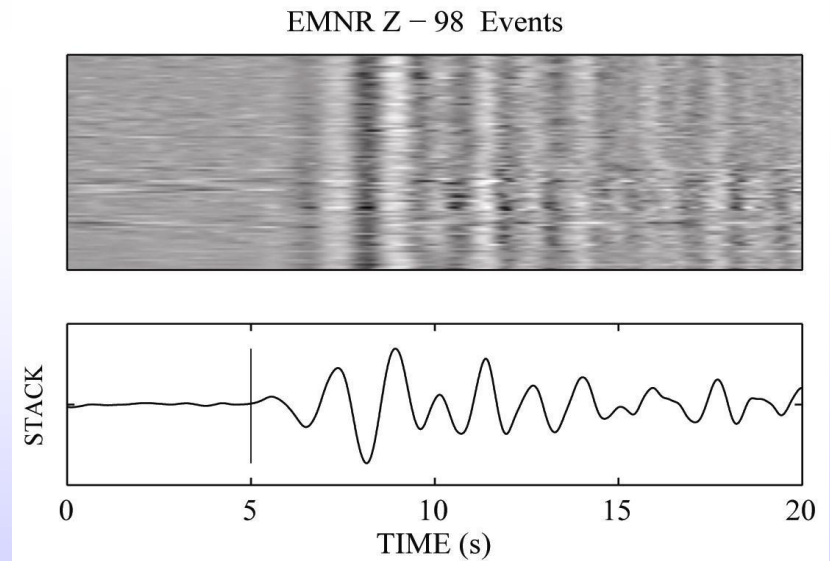
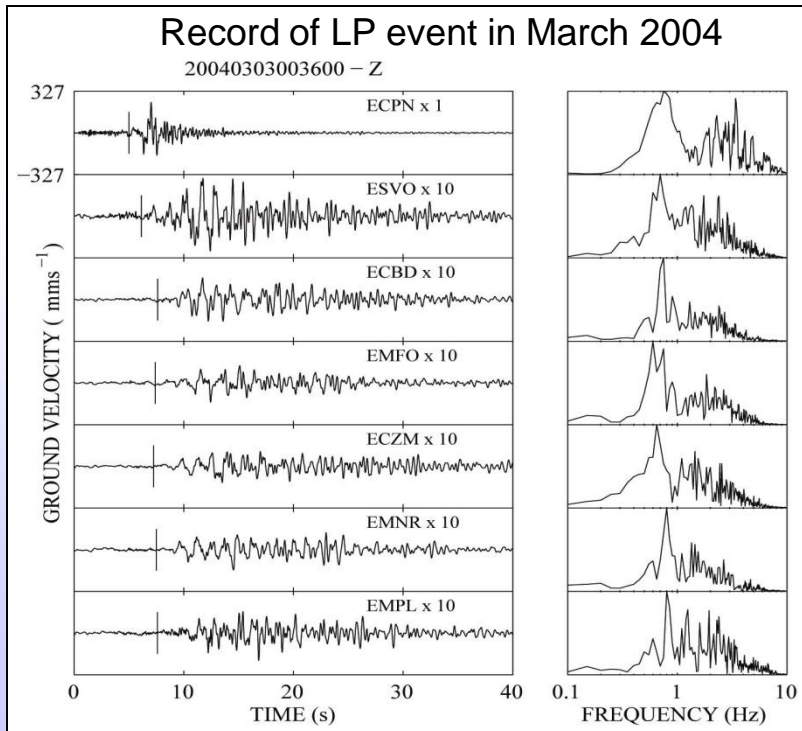
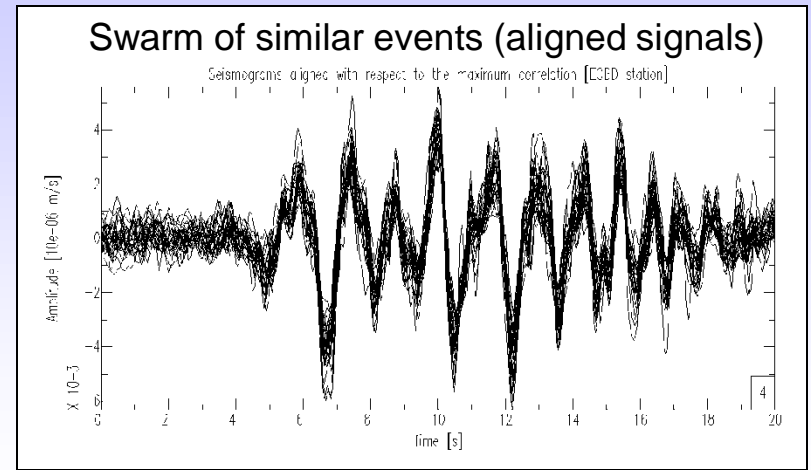
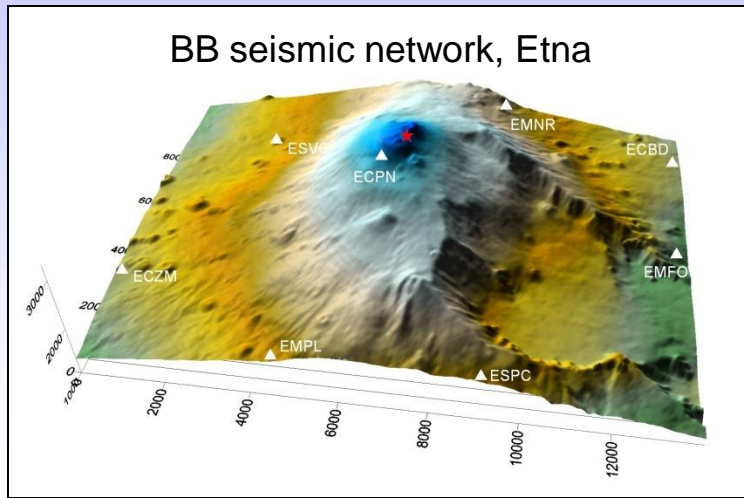
$$M_{xz} = M_0 \sin 2\theta \cos \varphi,$$

$$M_{yz} = M_0 \sin 2\theta \sin \varphi,$$

← for each pair  $(\theta, \varphi)$ , we invert for a single parameter  $M_0$



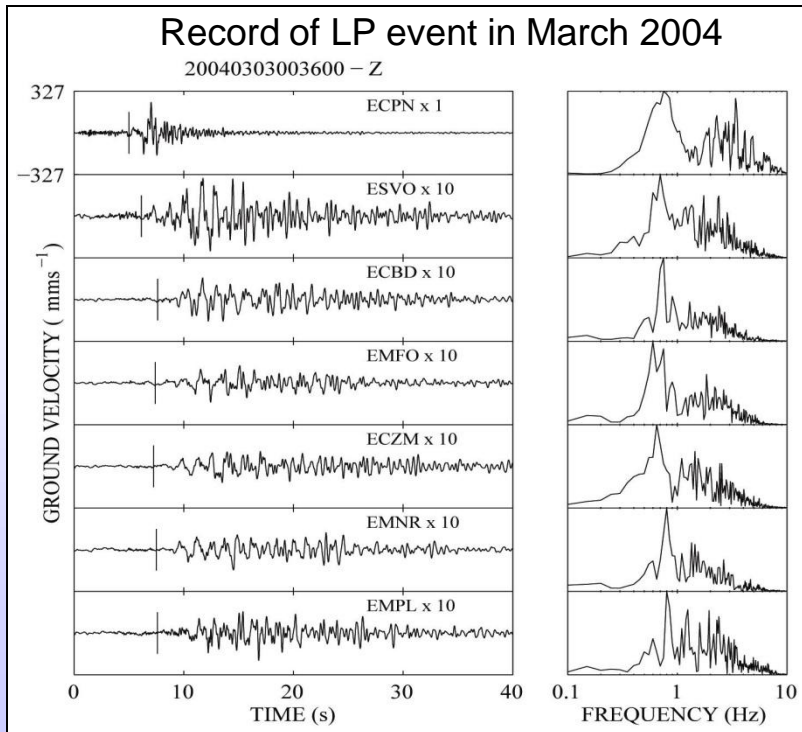
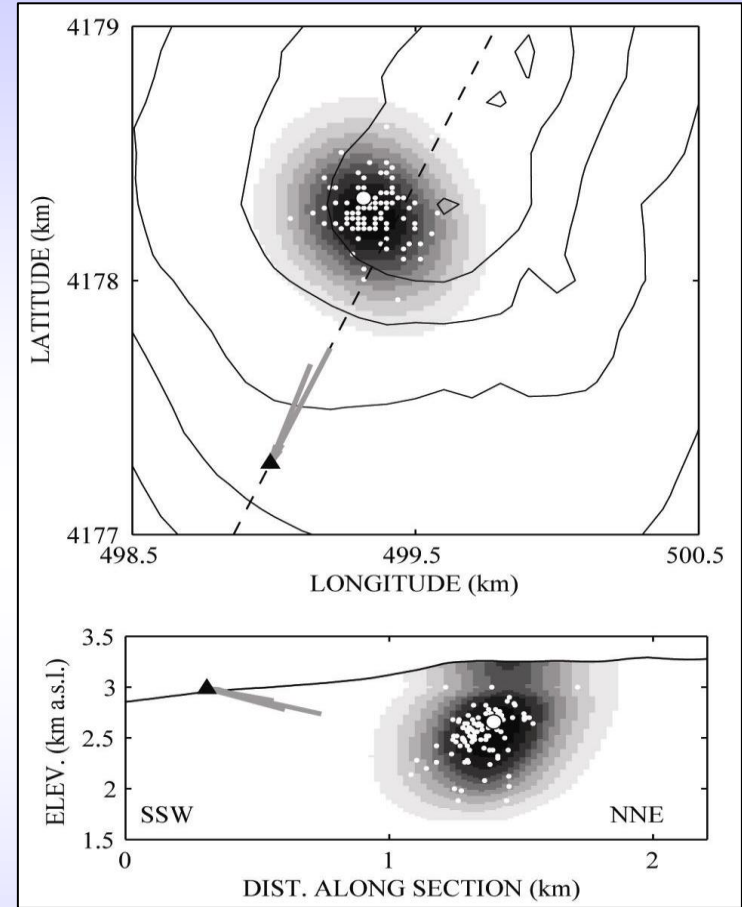
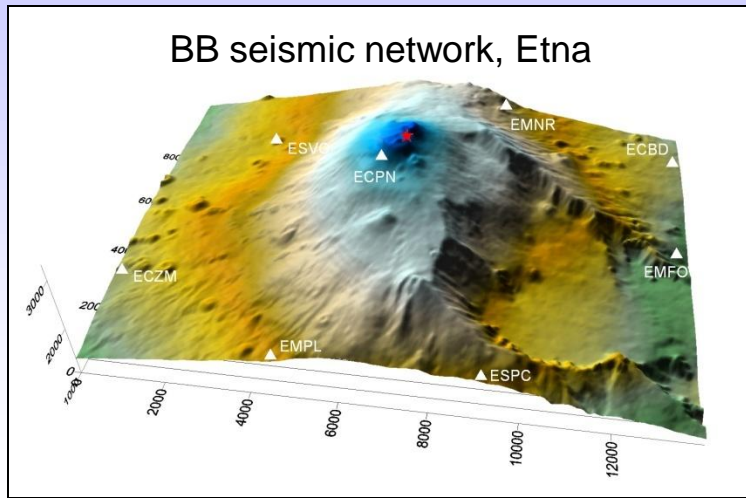
# LP source location methods: stack of similar events (LP swarm)



- improved SNR by stacking similar events
- location by using travel times
- uncertainties in location due to velocity model

(Saccorotti et al., 2007)

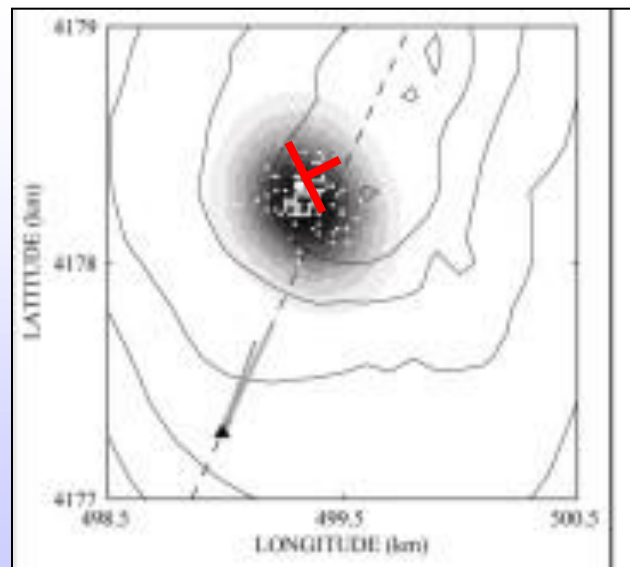
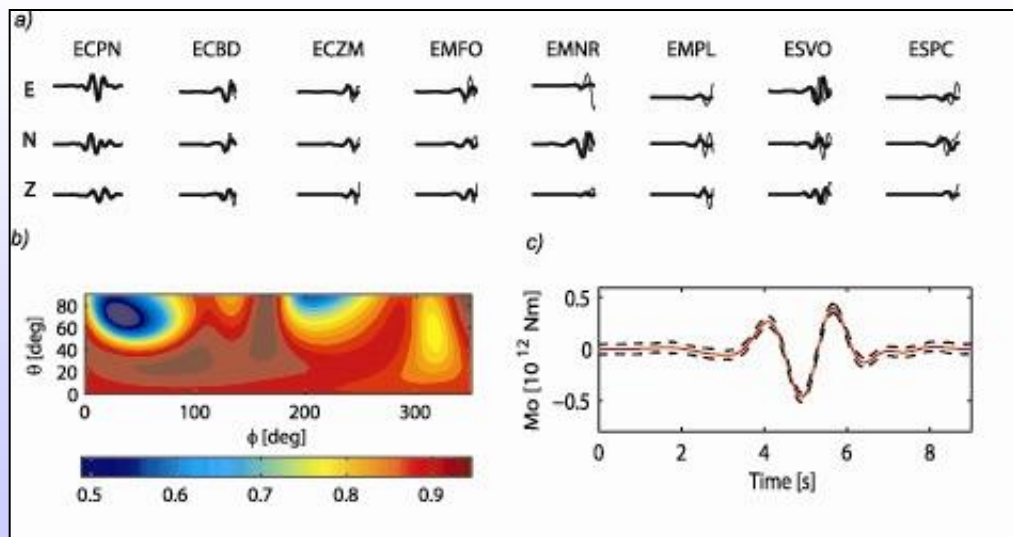
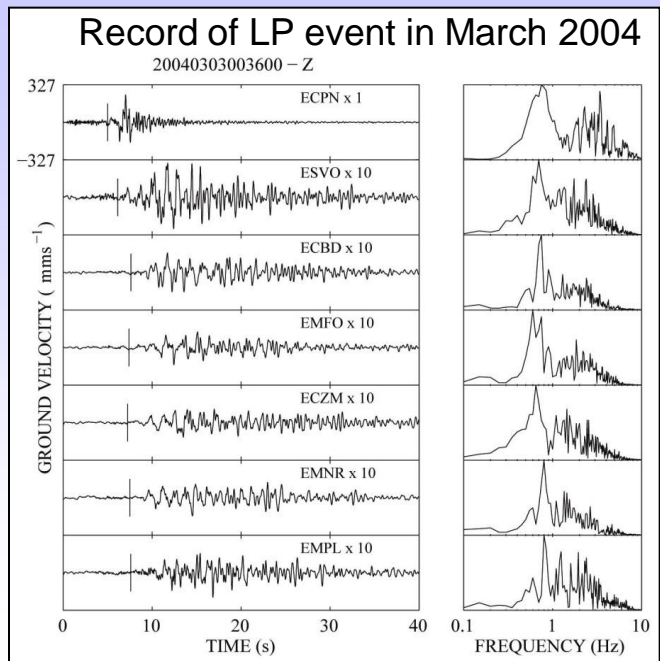
.... continued



- Events are located in a shallow cluster under the summit crater

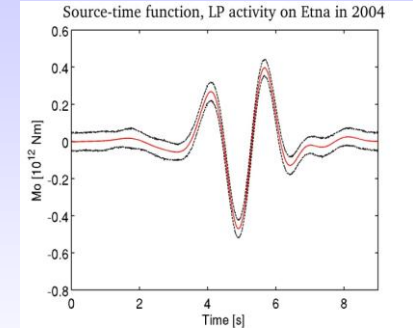
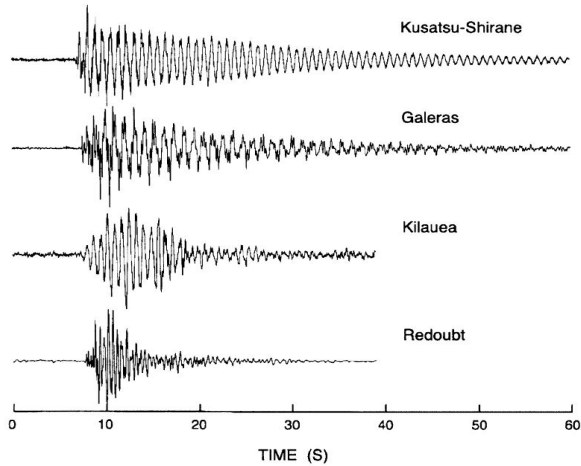
# Constrained MT inversion on Etna

- MT inversion performed for the three most probable LP source geometries: a crack, a pipe and a pure volumetric source (details of the source hidden by this approach)
- The source location was fixed to one obtained by the travel time inversion from stacked seismograms
- ECPN station determined source-time function, the other stations just helped to fix the mechanism
- Subvertical NNW-SSE crack in agreement with the trend of dyke propagation obtained from deformation studies



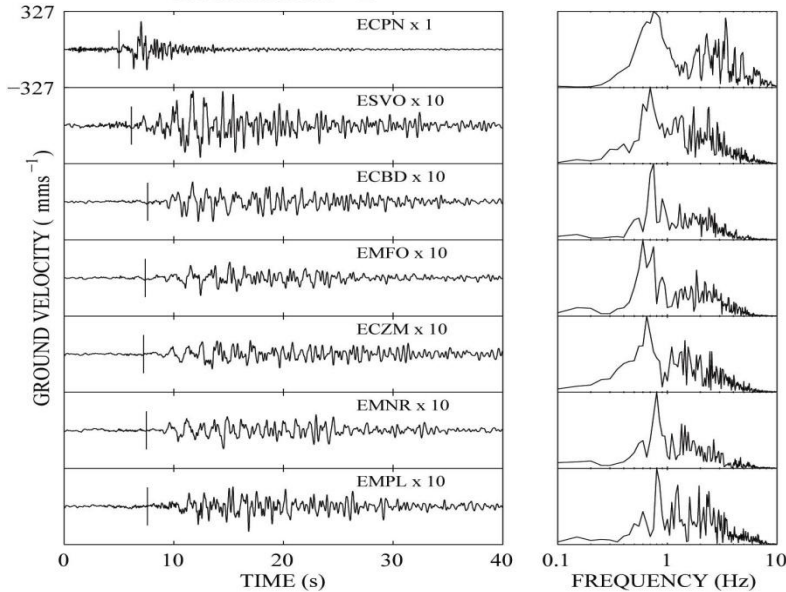
# What would source-time function look like if there is no summit station?

Long period (LP) signals (Chouet, 1996)

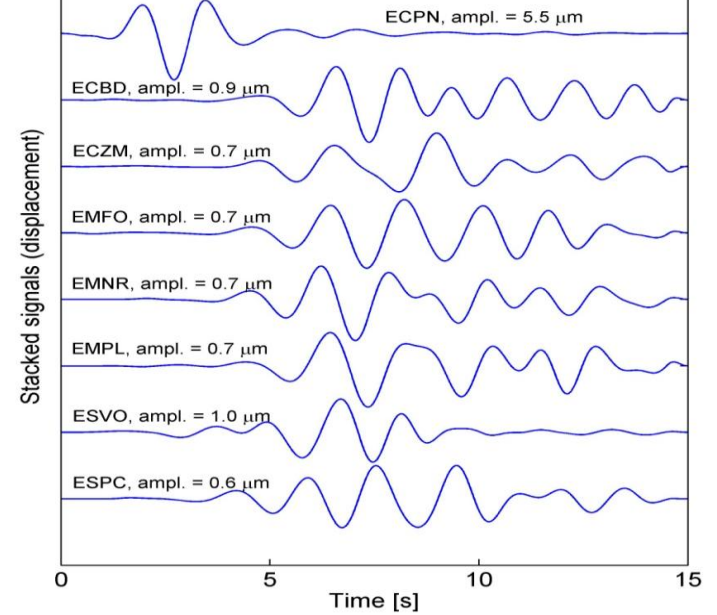


Record of LP event in March 2004

20040303003600 - Z



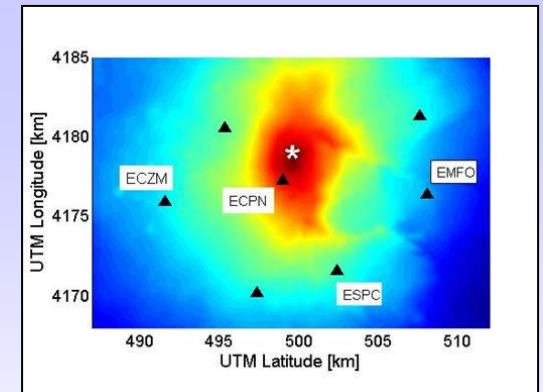
Filtered displacement ( $f = 0.3 - 1.5$  Hz)



More stations around summit needed in the summit area!

## What have we learnt so far?

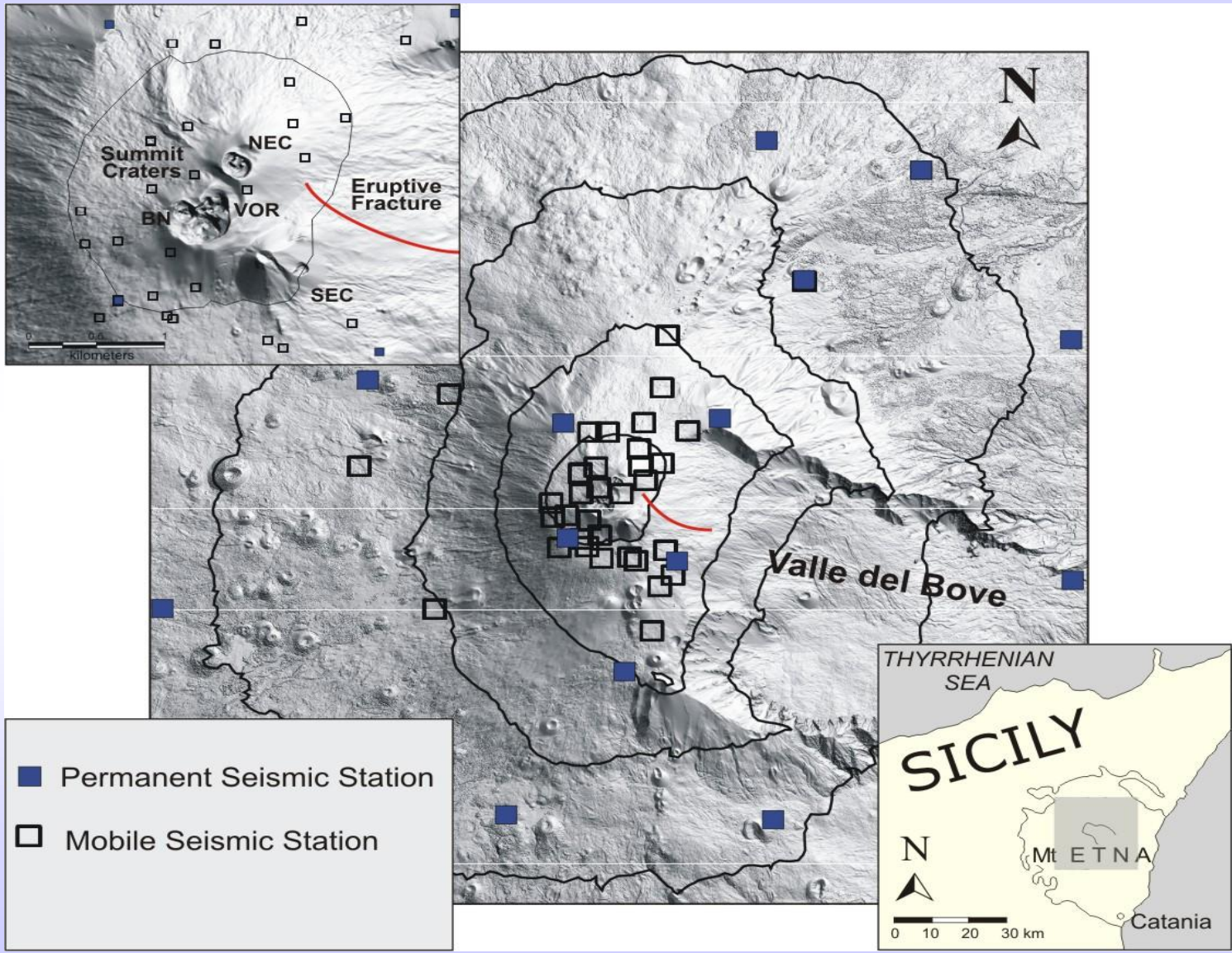
- Extremely strong joint effect of topography and shallow heterogeneity at the stations located more than a few km from the source (~ 2-3 km)
- Synthetic tests necessary!!!
- The unconstrained source inversion with a sparse network and poorly resolved shallow structure can produce stable, but incorrect moment tensor solution with spurious single forces (wrong orientation, magnitude and the source-time history)
- In case of such a sparse network, as much *a priori* information as possible should be used to constrain the inversion and decrease the number of parameters we invert for



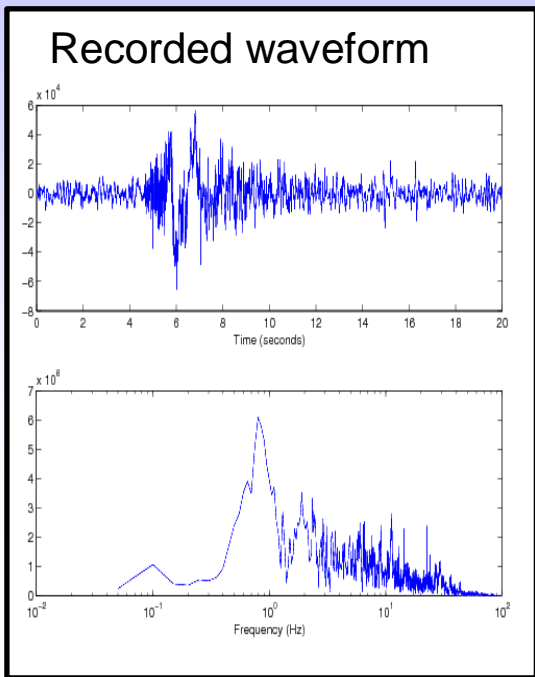
→ We need more near-field stations (preferably at different altitudes)!

Moment tensor inversion on Etna in 2008  
Experiment with lots of near-field stations

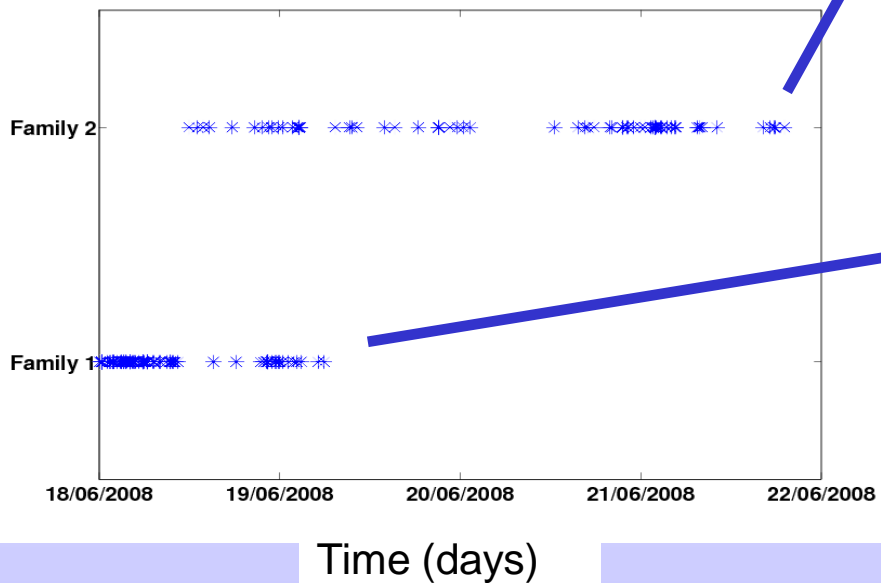
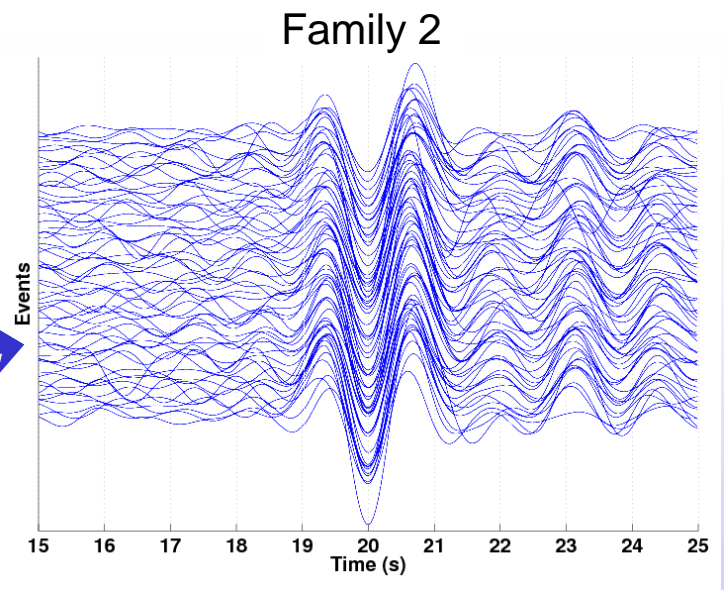
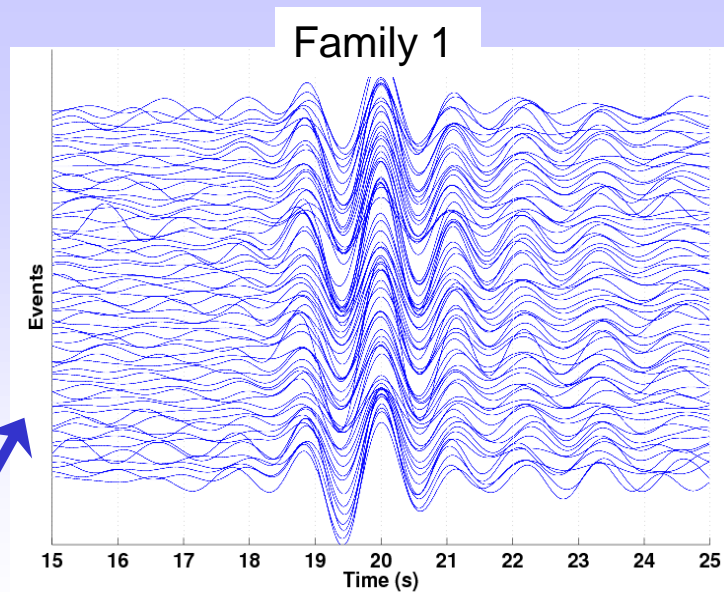
# Experiment: 50 seismological stations (18<sup>th</sup> june – 3<sup>rd</sup> july)



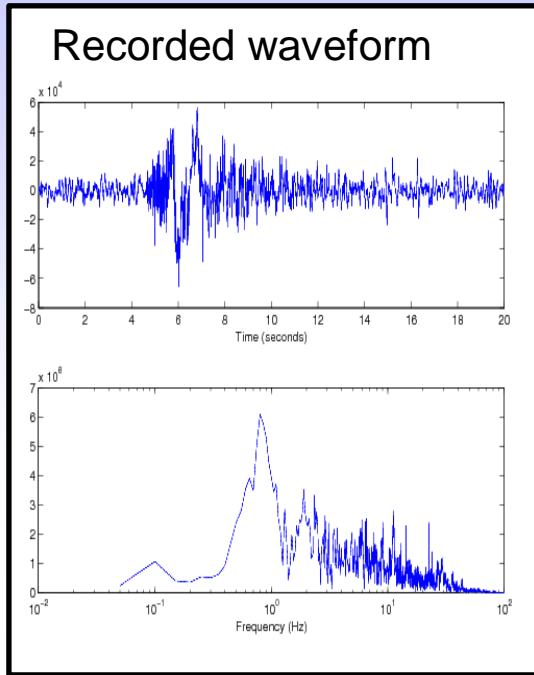
# Recorded LP seismicity



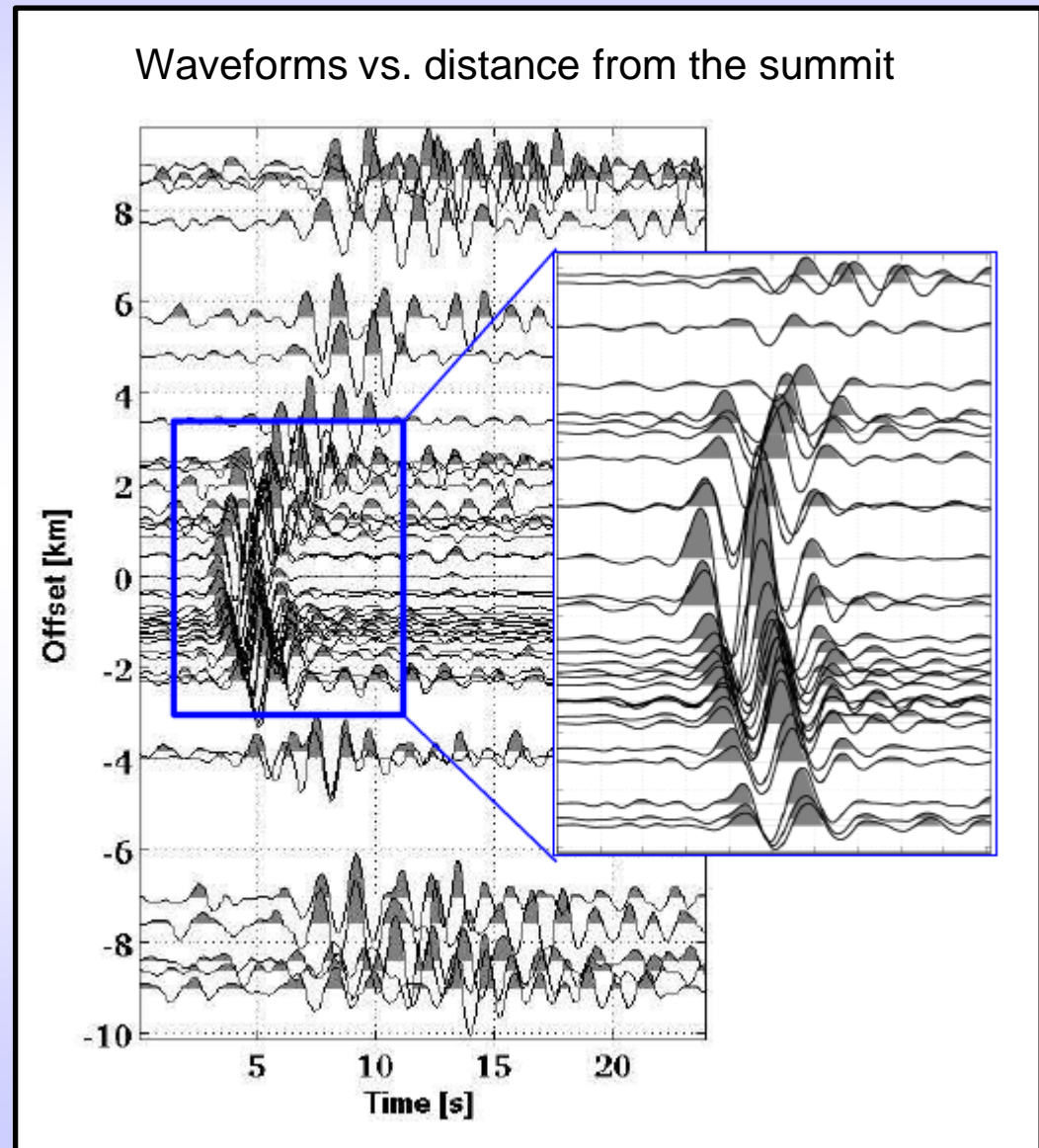
130 selected events



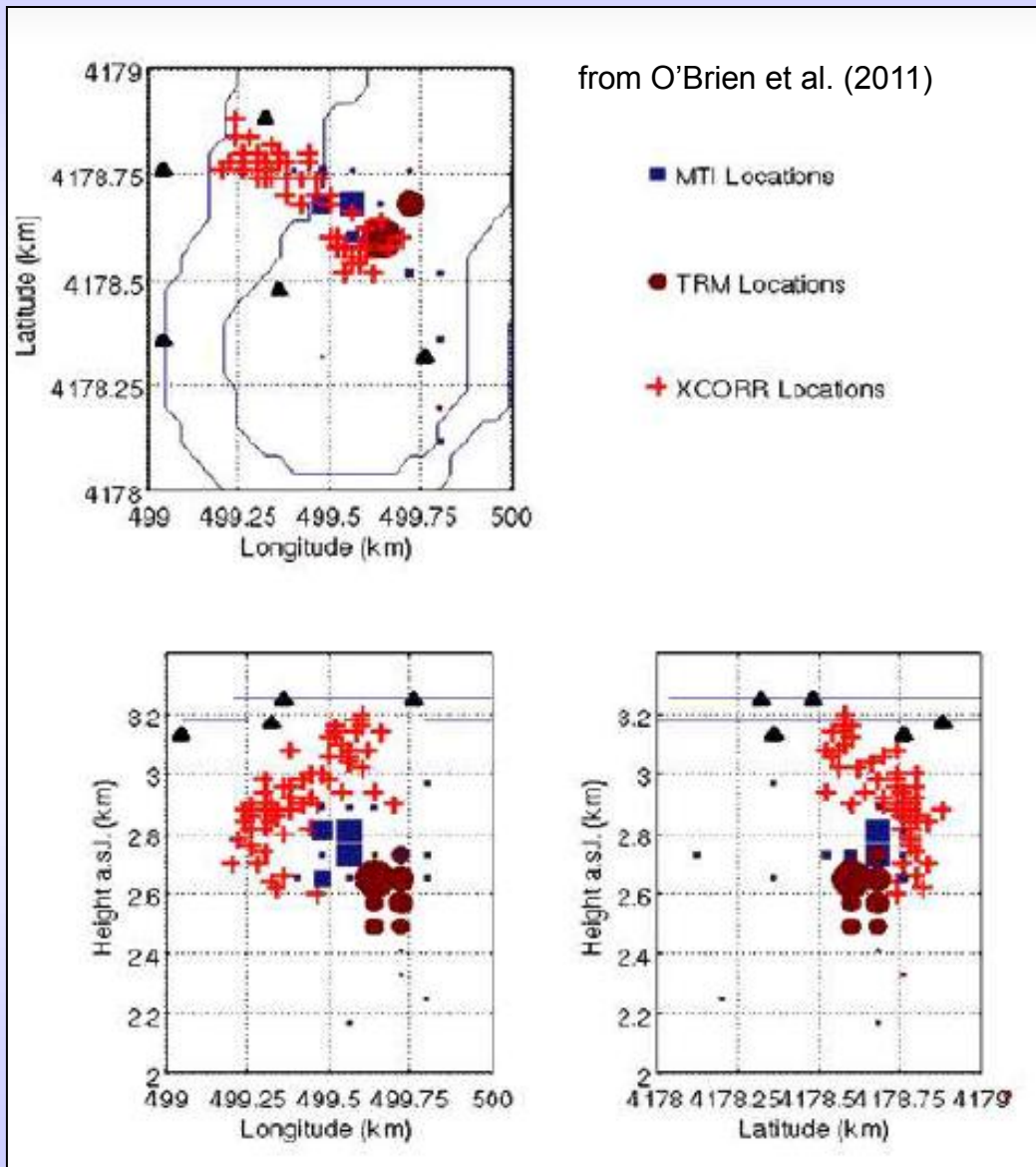
# Recorded LP seismicity



Only near station used for inversion  
( $< 2.5$  km)



# Source locations (3 different methods)



Good agreement between the 3 methods

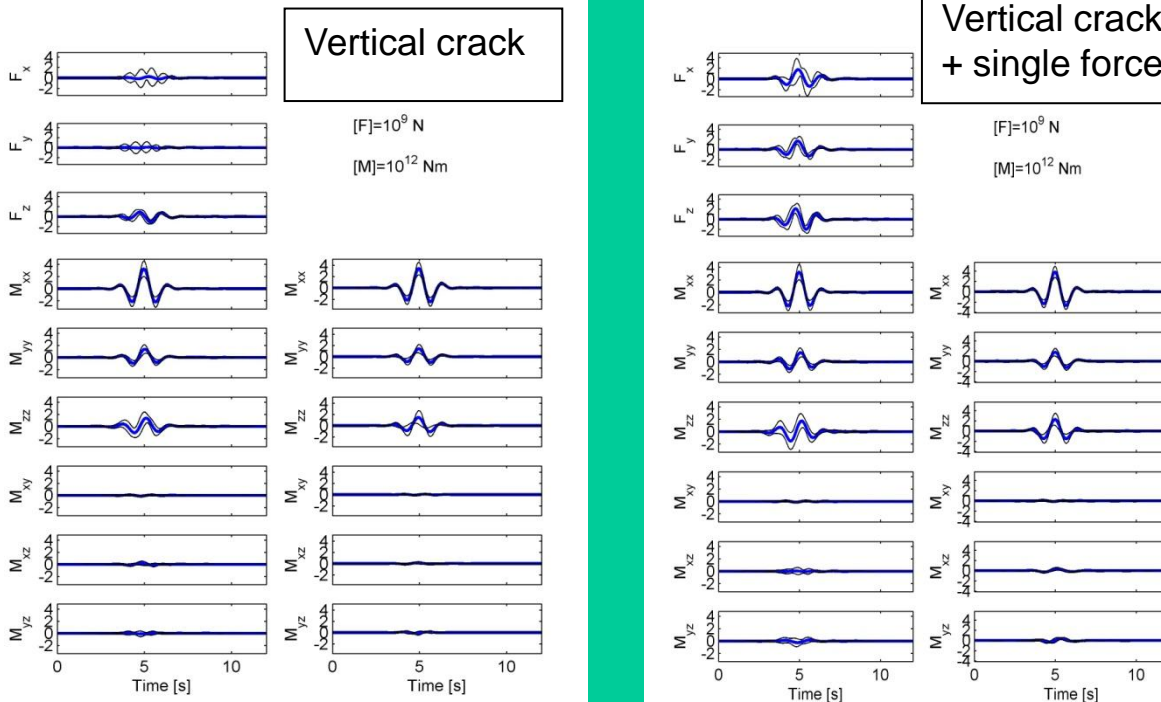
Velocity model: tomography with a gradient on top (1600-2400 m/s within the first 500 m)

Cross-correlation (double differences) assumes the same waveform at all stations → this is fulfilled only for the wavefield recorded in the far-field of a purely isotropic source

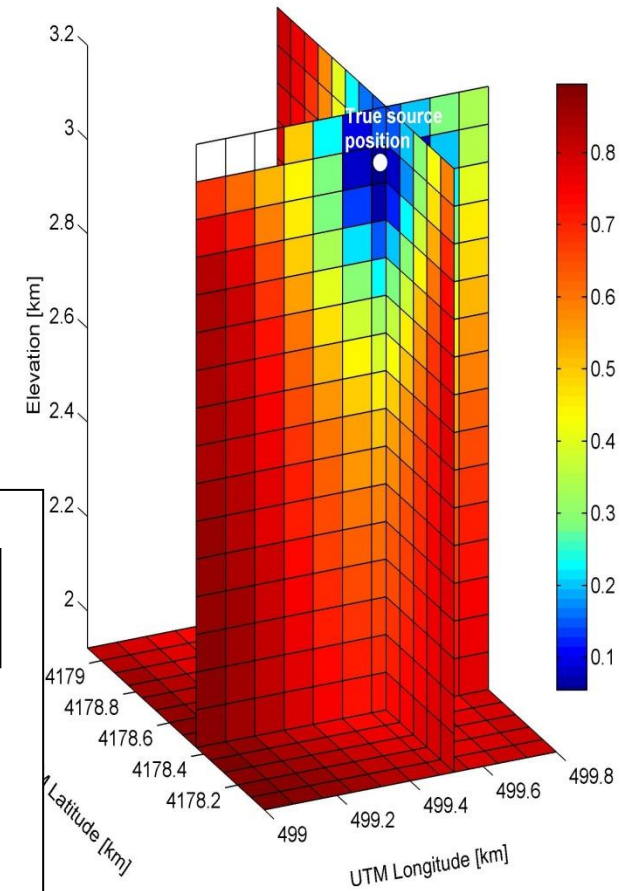
# Synthetic test: MT solution + location

- Gradient velocity model  $v_p = 1600 - 2400$  m/s within the first 500 m
- Larger standard deviation of  $M_{zz}$  than  $F_z \rightarrow$  due to incorrect velocity model  $M_{zz}$  leaks to  $F_z$  (what to do with spurious forces)
- Both source mechanism and source location well retrieved

## MT solutions and their standard deviations

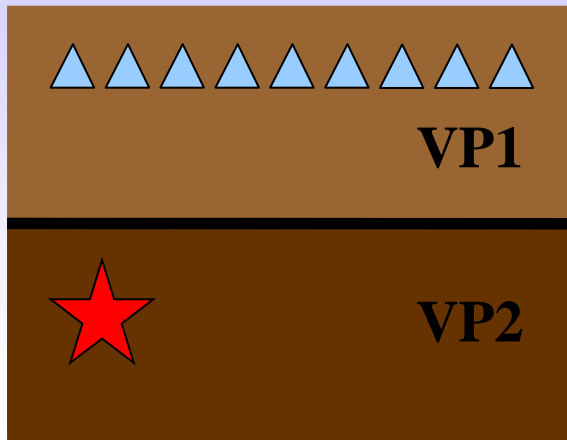


## Grid-search residuals

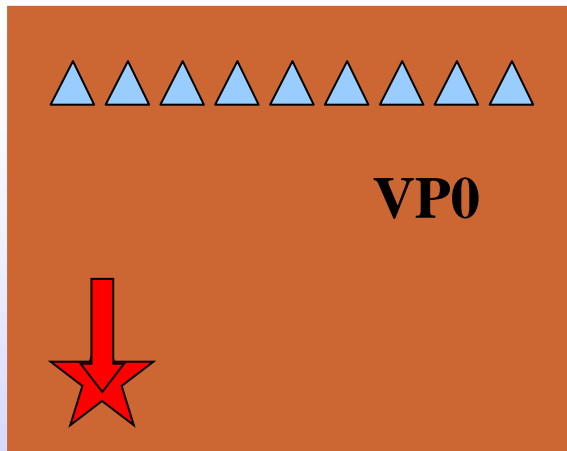
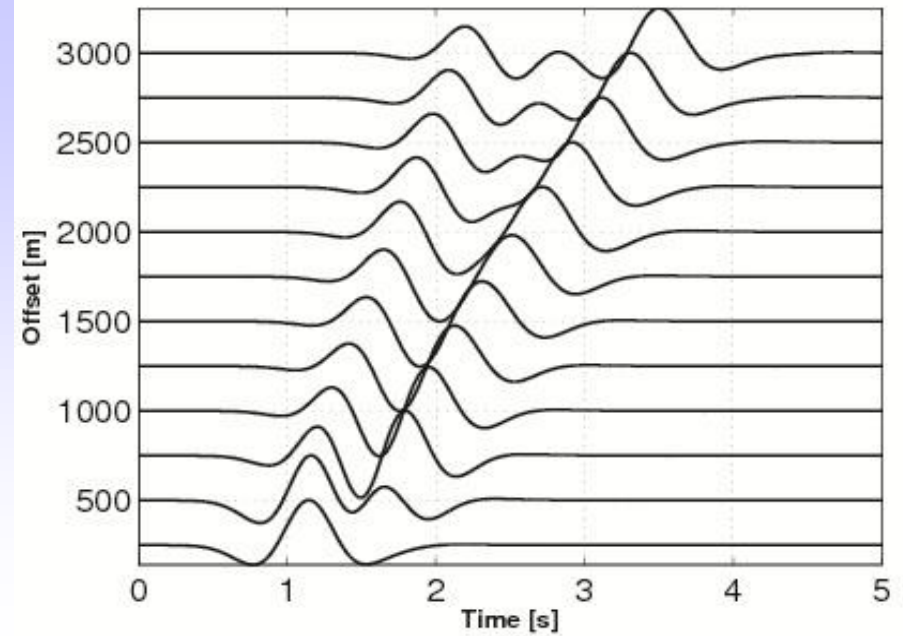
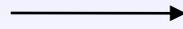


- Inversion for MT only does not perform well if we increase the input force twice

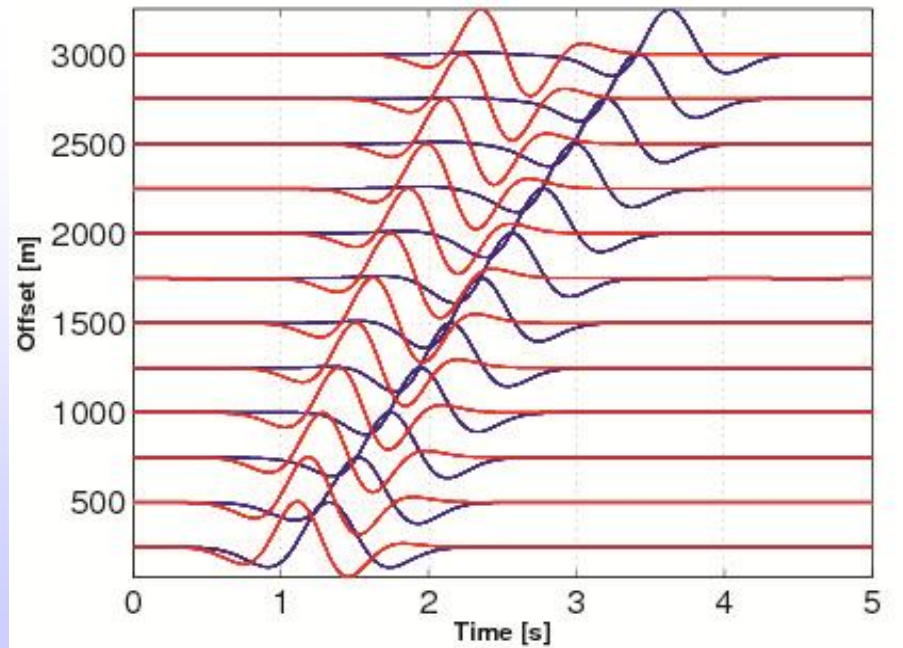
# Single forces and velocity mismodelling



Data



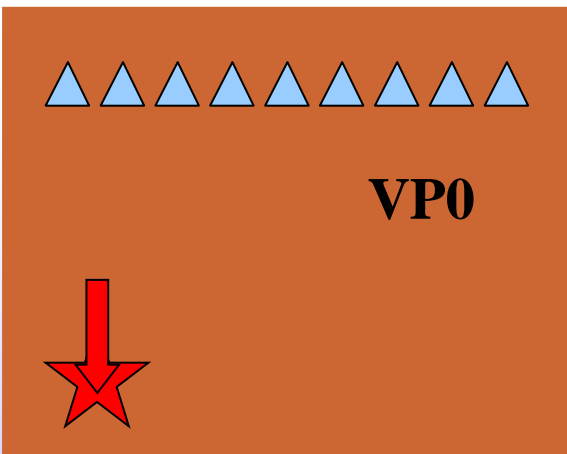
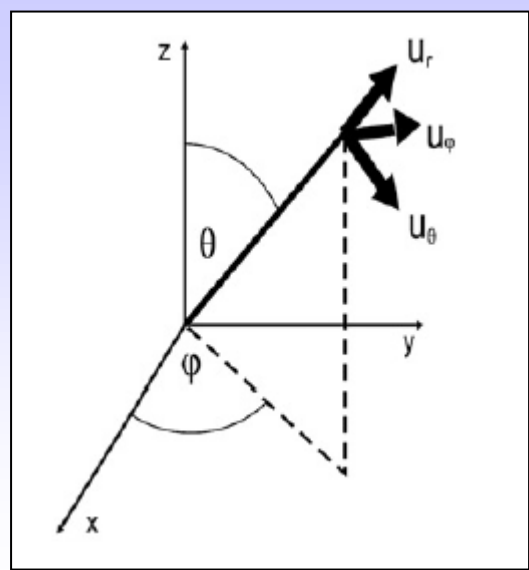
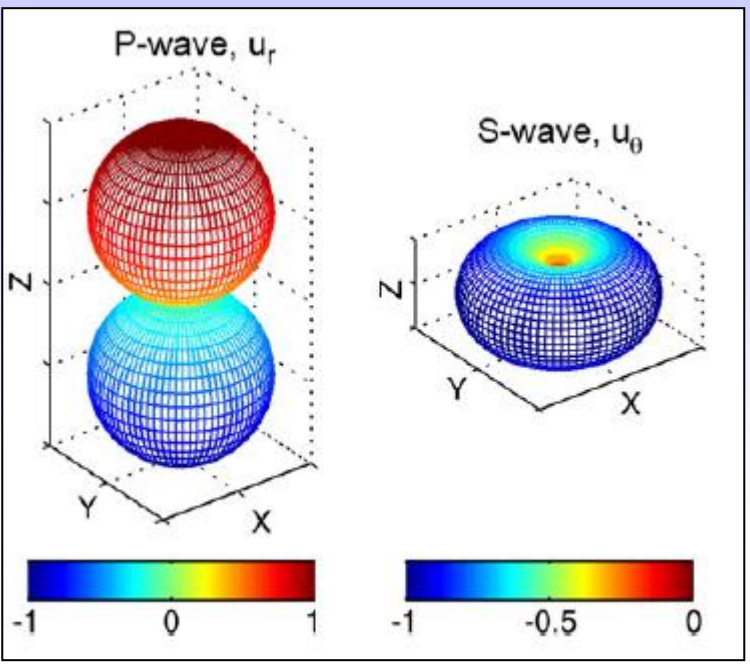
GF



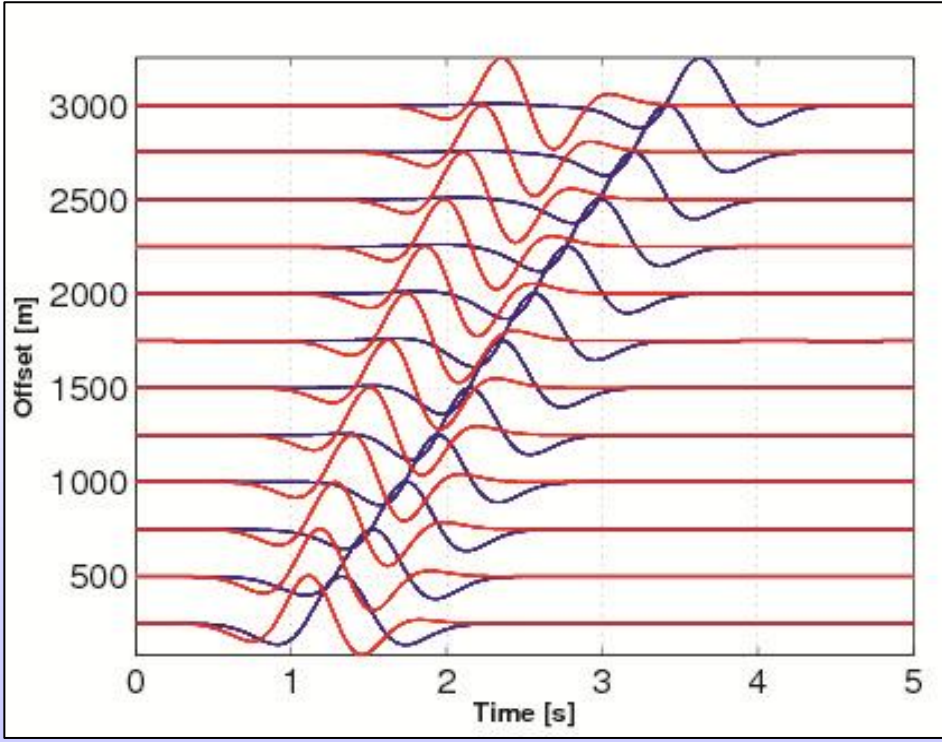
 = explosion

 = vert. force

# Radiation pattern of vertical single force

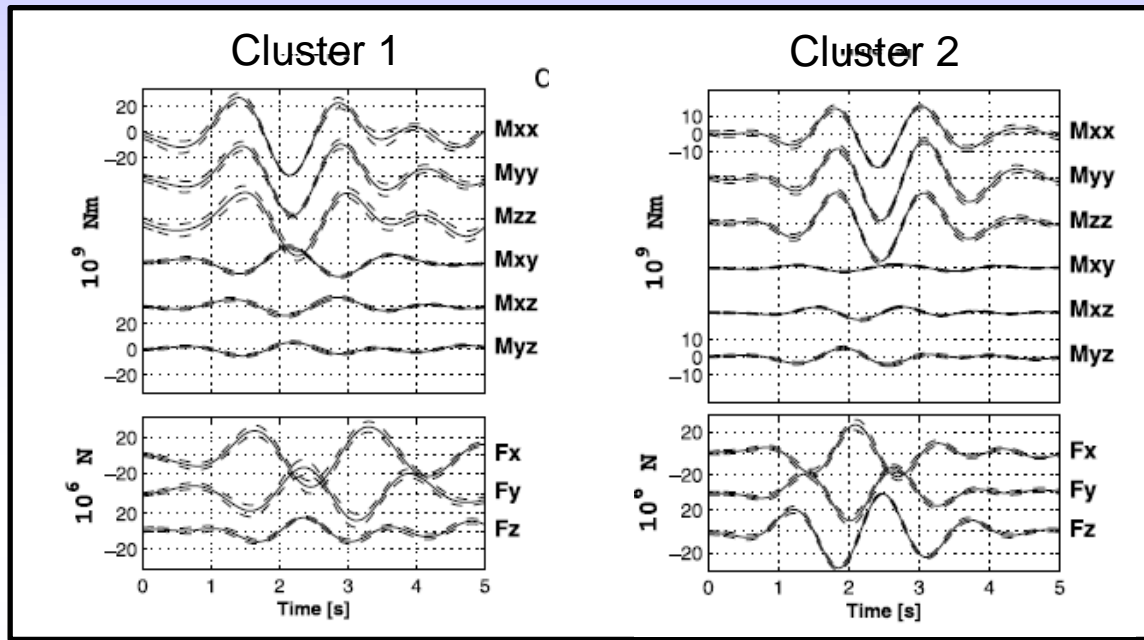


★ = explosion      ↓ = vert. force

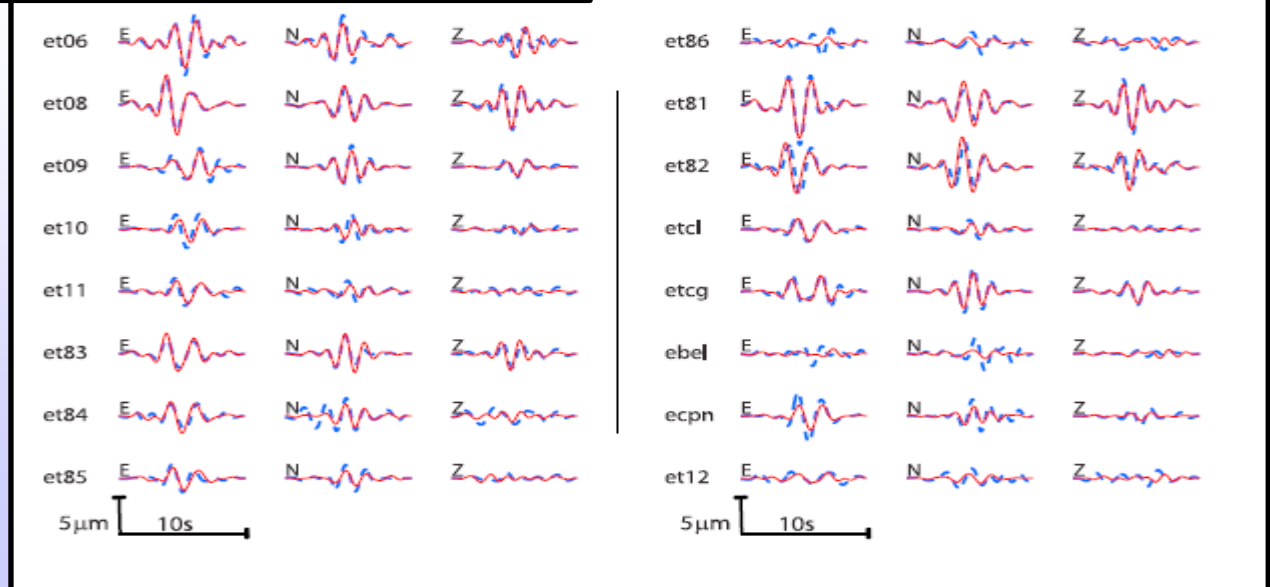


# MT solution and waveform fit

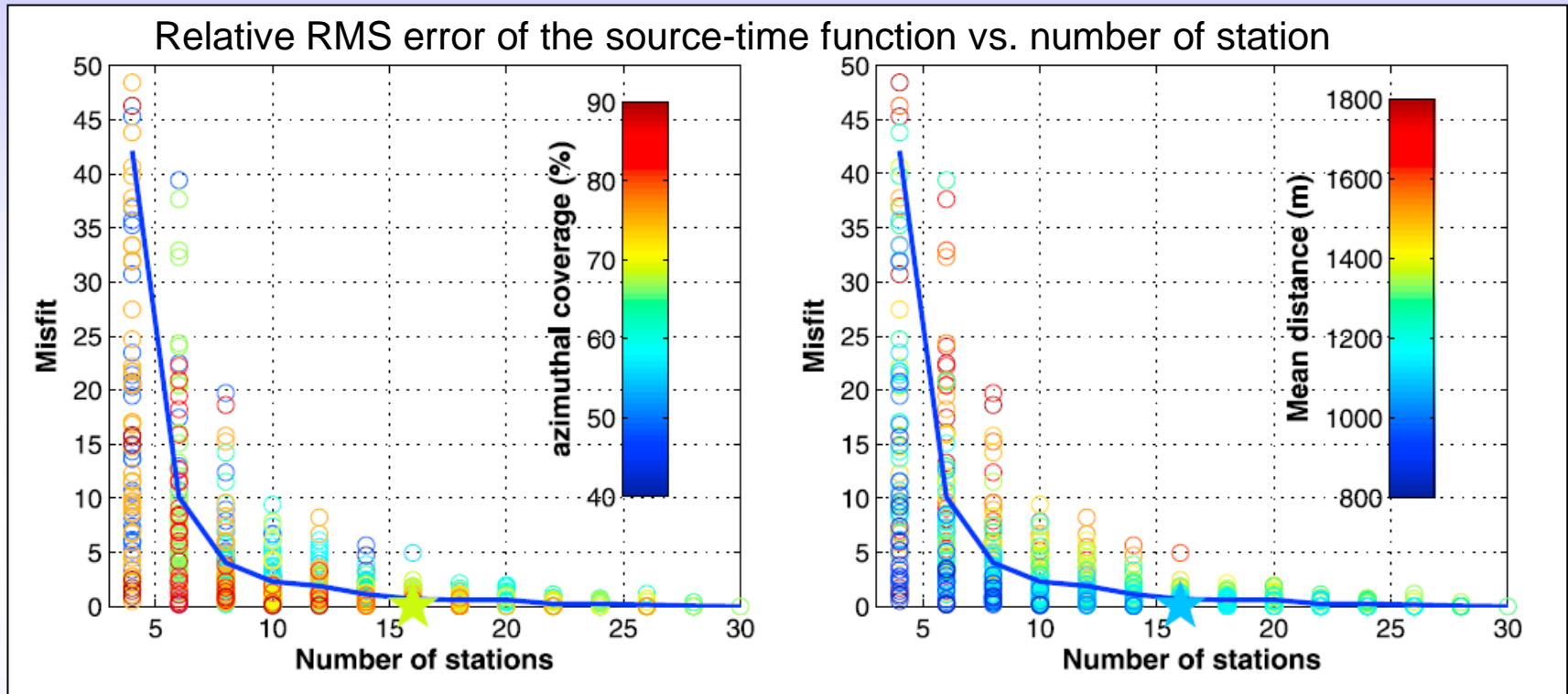
- Much worse quality of the dataset than in 2004, but more refined solution



Waveforms misfit ( $R=0.27$ )



# Stations distribution and density of the network

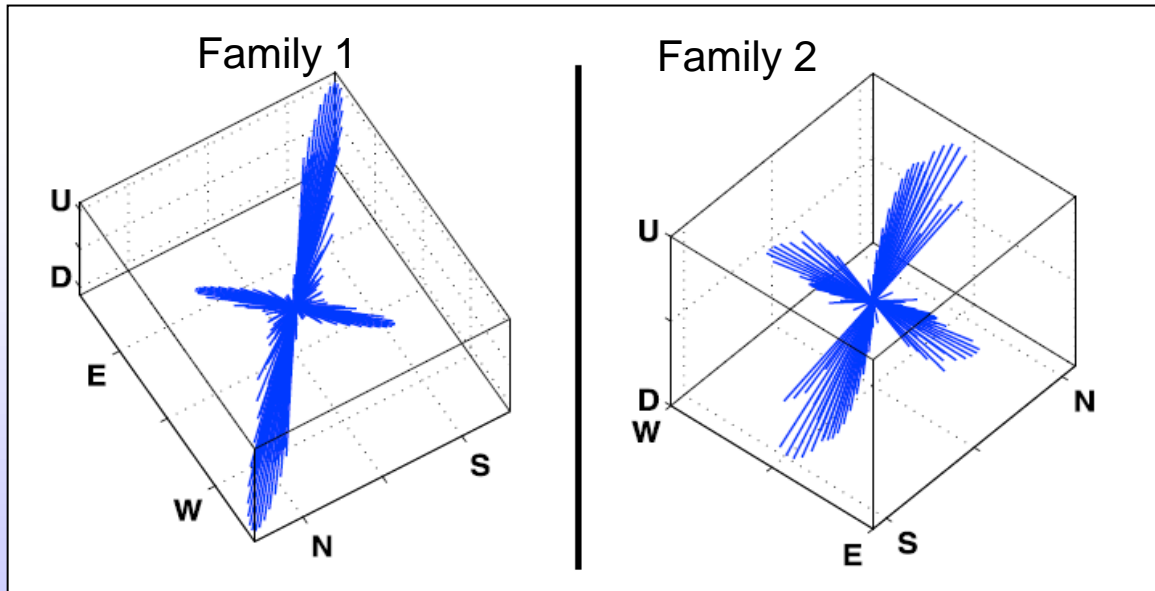


- 30 stations is taken as the reference
- The misfit is systematically increasing with the increase of the mean distance and decrease of azimuthal coverage
- No major improvement of the solution for more than 16 stations

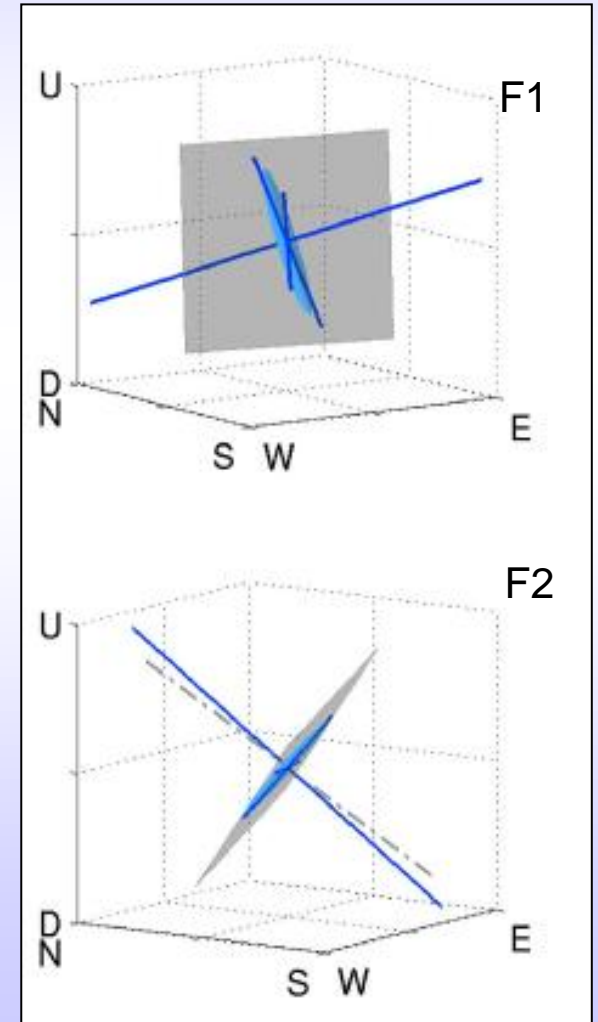
# MT principal axes (eigenvectors and eigenvalues)

- Family 1 – tensile crack dipping SE
- Family 2 – large amount of isotropic component; either non-planar source or a planar source with large Poisson's ratio ( $\sigma > 0.4$ ), e.g. fluid-saturated cracked medium
- similar unconstrained and constrained solutions (always check!)

Unconstrained solution MT+SF

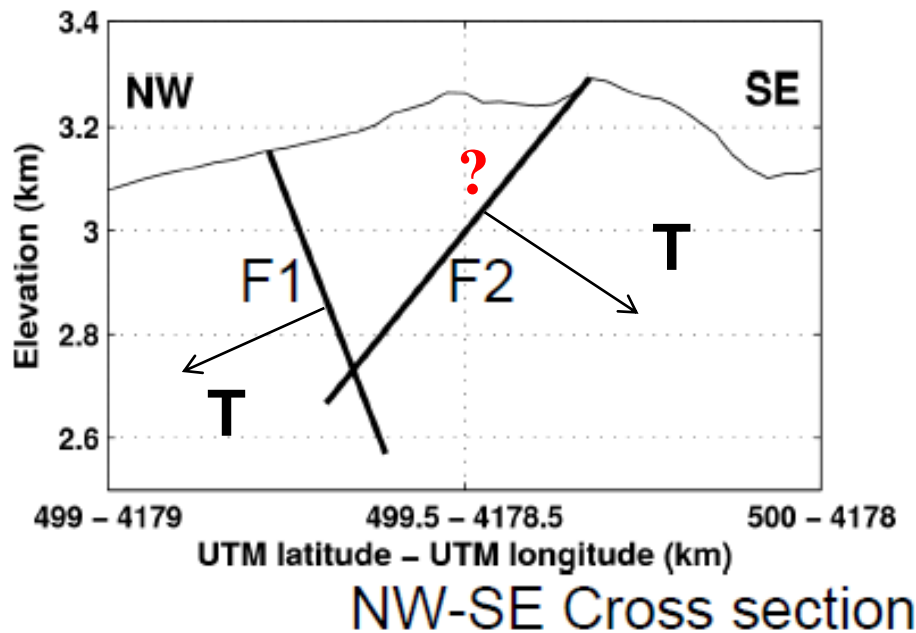
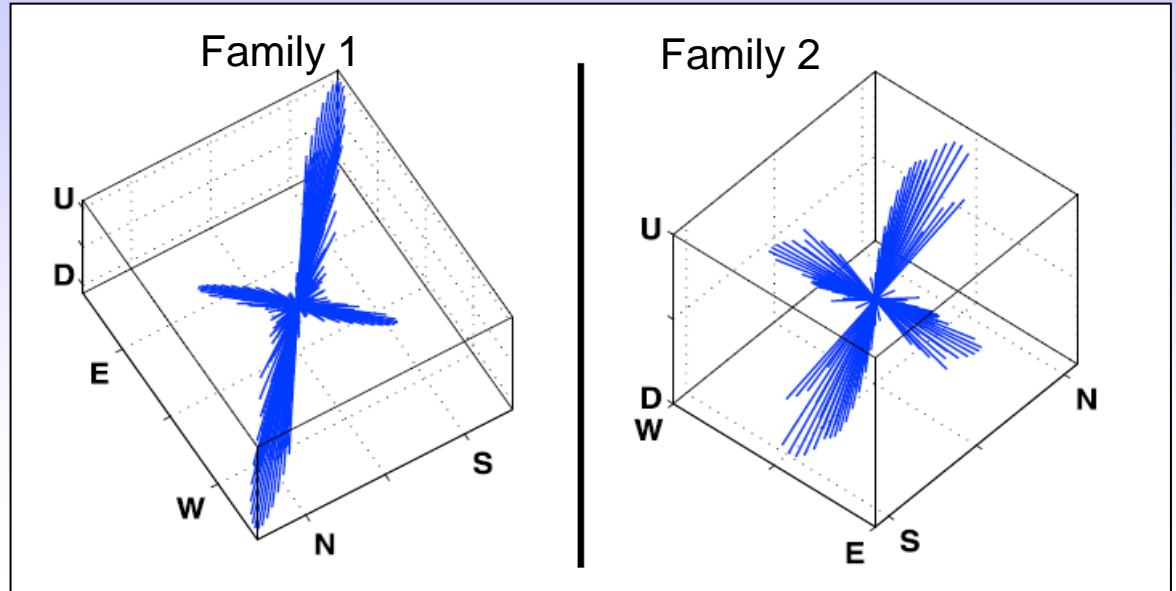


Solution constrained to a crack



# Interpretation

- Magma and gas inside a shallow conduit (decompression)?
- tensile fracturing of the edifice due to instability of the Eastern flank of Etna?
- crater collapse?



MT solution for VT → useful information about internal volcano dynamics (e.g., Dahm and Brandsdottir, 2007)

MT solution for LP → it does not give us yet definite answers, but helping in introducing new ideas about volcano dynamics

→ Are LPs generated by the fluid-solid interaction inside conduits or they are directly related to deformation/stress field on volcanoes?

## Recommendations for inversion on volcanoes:

- 3D simulations with topography necessary for calculating Green's functions
- Test the influence of velocity mismodelling and source mislocation (tests tests tests!)
- Decrease the number of model parameters for sparse networks (constrain the inversion)
- Compare constrained vs. unconstrained inversion
- If you are designing an experiment, try to deploy at least 10 stations (better 15) close to the source at different altitudes for good sampling of radiation pattern
- Remove site effects when possible (they were pronounced on Etna 2008 experiment)
- Remember, every volcano is different, so do not take these recommendations as "holy grail"